

بِسْمِ اللَّهِ الرَّحْمَنِ الرَّحِيمِ



Department of Mechanical & Chemical

Engineering (MCE)



Organisation of Islamic Cooperation

ISLAMIC UNIVERSITY OF TECHNOLOGY

(IUT)

**IMPROVEMENT OF MACHINABILITY RESPONSES
OF MILD STEEL DURING ELECTROMAGNET
ASSISTED TURNING PROCESS**

BY

SHAFI NOOR (081401)

ZIAUL HAQUE SHOYON (081422)

SUPERVISED BY

DR. ANAYET ULLAH PATWARI

Associate Professor

Department of Mechanical & Chemical Engineering (MCE)

ISLAMIC UNIVERSITY OF TECHNOLOGY (IUT)

**IMPROVEMENT OF MACHINABILITY RESPONSES
OF MILD STEEL DURING ELECTROMAGNET
ASSISTED TURNING PROCESS**

BY

SHAFI NOOR (081401)

ZIAUL HAQUE SHOYON (081422)

SUPERVISED BY

DR. ANAYET ULLAH PATWARI

**A thesis submitted to the Department of Mechanical & Chemical Engineering
(MCE) in partial fulfillment of the requirement for the degree of
Bachelor of Science in Mechanical Engineering**

بِسْمِ اللَّهِ الرَّحْمَنِ الرَّحِيمِ



**Department of Mechanical & Chemical Engineering (MCE)
ISLAMIC UNIVERSITY OF TECHNOLOGY (IUT)
October, 2012**

CANDIDATES' DECLARATION

It is hereby declared that this thesis or any part of it has not been submitted elsewhere
for the award of any degree or diploma

Signature of the candidate

Shafi Noor

Student Number: 081401

Department: MCE

IUT, OIC

Board Bazar, Gazipur

Signature of the candidate

Ziaul Haque Shovon

Student Number: 081422

Department: MCE

IUT, OIC

Board Bazar, Gazipur

Signature of the Supervisor

Dr. Md. Anayet Ullah Patwari

Associate Professor

Department of Mechanical & Chemical Engineering

Islamic University of Technology (IUT), OIC

Board Bazar, Gazipur

ACKNOWLEDGEMENT

We are grateful to Almighty Allah who made it possible for us to finish this project successfully on time and without any trouble.

It could never be possible for the authors to complete this thesis without the help of some people throughout these two semesters of final year. At first we want to give thanks and express our sincere gratitude to Dr. Md. Anayet Ullah Patwari, Associate Professor, Department of Mechanical and Chemical Engineering, IUT. We are deeply indebted to him for giving us moral support throughout the whole year. His patient guidance and constant supervision made us work in definite direction towards the completion of the project. His care and concern for all the students are appreciated and provided continuous encouragement for us.

We are grateful to Md. Nauzef Mahmood, Lecturer, IUT (on leave) for his continuous help throughout the project. Special thanks to Md. Shakhawat Hossain, senior operator (CAM lab), Md. Matiar Rahman, senior operator, Md. Rajaul Karim, operator (Machine shop), for their useful suggestion and cooperation which made it easier for us to carry out our experiments.

We extend our sincere thanks to all other faculty members of the Department for their valuable advice in every stage for successful completion of this project.

We would like to give thanks to all who helped us in many ways during performing the project work. Thanks to all our family members for their valuable support and prayers.

Although we have given our best effort to complete this thesis paper, we seek excuses if there is any mistake found in this report.

ABSTRACT

This project aims to investigate the effects of magnetic field applied in different orientation on the machinability responses of mild steel during turning operation. The machinability responses include tool wear, surface roughness, cutting force, temperature, chip morphology. A control experiment was also done where no magnetic field is applied at all.

The result showed significant reduction in the tool wear of the inserts with the application of magnetic fields. Not only non magnetic cutting shows the trend of increasing tool wear with the increase in cutting speed or depth of cut, trends can also be seen in case of magnetic cutting. It was also observed that the trends in the change in tool wear due to the application of magnetic field changes with different designs of electromagnets used to change the orientation of magnetic field lines. And explanation for this phenomenon is that there are several factors responsible for the tool wear during machining operation and these can be affected by different orientation of magnetic field lines. These include cutting force reduction due to e.m.f. induced as a result of magnetic flux lines intersecting with the work piece, reduction of vibration of the tool, high temperature resulting in softening of the work piece, building up a lubricating layer on the cutting edge of the tool insert.

All the electromagnets do not result in the improvement of machinability responses in the similar way. They vary with the change in cutting parameters.

The project is successful in establishing an improvement in tool life with the application of magnetic field on the tool insert during turning.

The quality of the finished product along with the productivity play a significant role in today's manufacturing market. From customers' viewpoint quality is very important because the extent of quality of the produced item influences the degree of satisfaction of the consumers during usage of the product. Every manufacturing industry aims at producing a large number of products within relatively lesser time. But it is felt that reduction in manufacturing time may cause severe quality loss. However application of magnetic field can result in the surface

quality of the product conditioned by the cutting parameter. The surface quality during magnetic cutting is significantly improved than that obtained from non magnetic cutting. The orientation of field lines also has some impact on the surface quality which is mainly because of the chip adhering to the tool during cutting operation.

Behavior of chips indicate the vibration nature of the machine and the tool. Chips produced during cutting operation have some teeth in its cross section which have been viewed with microscope to find out the effect of these electromagnets on the serration behavior. Here also it is clearly shown that the teeth produced during magnetic cutting are smaller in size whereas they are much bigger for non magnetic cutting. This phenomenon indicates that application of external electromagnetic force reduces the vibration of the machine tool.

Temperature and cutting force are related with each other. Reduction of cutting force during magnetic cutting occurs due to the induced emf by the magnetic field lines intersecting with the work piece. Since an emf is induced there will be an eddy current over the surface of the work piece. This increases the temperature of the work piece and the tool insert. Having difficulties in measuring the temperature of the work piece, we have measured the temperature of the insert near the cutting junction with the aid of a thermocouple.

When the emf is induced, according to Lenz's law there will be a back emf which will oppose the change in the flux that produces it. This has the result of inducing a force on the work piece that has a damping effect, as can be seen from the reduction of cutting forces.

TABLE OF CONTENTS

	<u>Page Number</u>
CHAPTER 1: INTRODUCTION	15 - 60
1.1 : Overview of Turning Process	17 - 39
1.1.1 : Adjustable Cutting parameters	18
1.1.2 : Different Turning Operation	19
1.1.3 : Turning machine	20
1.1.4 : Components of a lathe machine	22
1.1.5 : The specification of the lathe machine used in this study	27
1.1.6 : Brief description of the cutting tool geometry	28
1.1.7 : Cutting tool materials	30
1.1.8 : Inserts	35
1.1.9 : Material removal rate	36
1.1.10 : Work holding methods	37
1.2 : Tool wear	39
1.2.1 : Types of tool wear	41
1.2.2 : Tool wear evolution	49
1.2.3 : Effect of tool wear on performance measures	51
1.2.4 : Tool life	53
1.2.5 : Expanded Taylor's tool life formula	54
1.2.6 : Recent trends in tool life evolution	55
1.3 : Surface roughness	56
1.3.1 : Surface structure of metals	56
1.3.2 : Factors affecting the surface roughness	57
1.4 : Magnetic field	58
1.4.1 : Calculation of magnetic field	58
1.4.2 : Eddy current and magnetic force	59

CHAPTER 2: LITERATURE REVIEW AND PRESENT WORK	61-73
CHAPTER 3: DETAILS OF EXPERIMENTATION	74-94
3.1 : Introduction	75
3.2 : Experimental Set up	75
3.2.1 : Design 1 Electromagnet	75
3.2.2 : Design 2 Electromagnet	76
3.2.3 : Design 3 Electromagnet	76
3.3 : Machining Parameters	78
3.4 : Experimental details	79
3.5 : Process variable and their values	81
3.6 : Equipment used	81
3.6.1 : Center lathe	81
3.6.2 : Optical microscope	82
3.6.3 : Work piece used	83
3.6.4 : Cutting tool used	84
3.6.5 : Mechanisms used for electromagnets	84
3.7 : Measurement technique used in this study	85
3.7.1 : Measurement of tool wear	85
3.7.2 : Measurement of surface roughness	88
3.7.3 : Observation of chip behavior	90
3.7.4 : Measurement of temperature	92
3.7.5 : Measurement of cutting force	92
CHAPTER 4: RESULTS AND DISCUSSION	95-120
4.1 : Tool wear	96
4.2 : Surface roughness	110

4.3 : Temperature	113
4.4 : Chip Morphology	115
4.4.1 : Continuity of chips	115
4.4.2 : Tooth formation of the chips	116
4.4.3 : Color of chips	117
4.5 : Cutting force	117
CHAPTER 5 : CONCLUSIONS & RECOMMENDATION FOR FURTHER STUDY	121-123
5.1 : Conclusions	122
5.2 : Recommendations for further study	123
REFERENCE	124-129
APPENDIX	130-140

LIST OF FIGURES

Page number

CHAPTER 1

Fig 1.1 : Adjustable parameters in turning operation	18
Fig 1.2 : Centre lathe used for turning	21
Fig 1.3 : Geometry of a single point turning tool	28
Fig 1.4 : Carbide tool inserts	36
Fig 1.5 : MRR in turning	37
Fig 1.6 : Different Modes of Wear	40
Fig 1.7 : Tool wear phenomenon	41
Fig 1.8 : Crater Wear	42
Fig 1.9 : Effects of cutting speed V and cutting time T on crater wear depth KT	42
Fig 1.10 : Flank Wear	43
Fig 1.11 : Different regions of wear	44
Fig 1.12 : Notch Wear	44
Fig 1.13 : Chipping Wear	45
Fig 1.14 : Attrition Wear	45
Fig 1.15 : Abrasive Wear	46
Fig 1.16 : Fracture	46
Fig 1.17 : Spalling	47
Fig 1.18 : Built up edge	47
Fig 1.19 : Thermal Cracking	48

Fig 1.20 : Plastic Deformation	48
Fig 1.21 : Wear curves: (a) normal wear curve, (b) evolution of flank wear land V_B as a function of cutting time for different cutting speeds	50
Fig 1.22 : Evolution of the flank wear land V_B as a function of cutting time for different cutting speeds	51
Fig 1.23 : (a) Wear curves for several cutting speeds (1, 2 & 3) and (b) tool life curve	53
Fig 1.24 : Cross section of surface structure of metals	56

CHAPTER 3

Fig 3.1 : Experimental set up with the first design of electromagnet	75
Fig 3.2 : Experimental setup of the second design of electromagnet	76
Fig 3.3 : Experimental setup of the third design of electromagnet	77
Fig 3.4 : CAD Model of the core of electromagnet	77
Fig 3.5 : Flow sequence of the experimentation	80
Fig 3.6 : Photograph and details of the optical microscope	82
Fig 3.7 : Optical microscope connected with laptop for taking image.	83
Fig 3.8 : Work piece	83
Fig 3.9 : Insert with dimension	84
Fig 3.10 : Electrical Circuit to produce electromagnetic field	85
Fig 3.11 : Process logic sequence flowchart for measuring tool wear	86
Fig 3.12 : Image processing result sample for measuring tool wear	88
Fig 3.13 : Flow diagram of image processing for surface roughness	90

Fig 3.14 : DIP results (work-piece surface roughness, without magnet)	90
(a) 10x zoom RGB microphotograph, (b) grayscale, (c) profile plot, (d) 2-D colored contour plot, (e) 3-D colored contour plot	
Fig 3.15 : Samples of mounted chip	91
Fig 3.16 : Instruments used for chip analysis. a) Polishing wheel, b) optical microscope	91
Fig 3.17 : Set up for measuring temperature	92
Fig 3.18 : Arrangement for measuring cutting force with half bridge circuit and strain meter	93
Fig 3.19 : SM 1010 Digital Strain Display	93
Fig 3.20 : Circuit used to connect strain gauges to the strain meter	94

CHAPTER 4

Fig 4.1 : Comparison of tool wear at 530 rpm and 0.5 mm depth of cut	99
Fig 4.2 : Comparison of tool wear at 530 rpm and 0.75 mm depth of cut	99
Fig 4.3 : Comparison of tool wear at 530 rpm and 1.0 mm depth of cut	100
Fig 4.4 : Comparison of tool wear at 860 rpm and 0.5 mm depth of cut	100
Fig 4.5 : Comparison of tool wear at 860 rpm and 0.75 mm depth of cut	101
Fig 4.6 : Comparison of tool wear at 860 rpm and 1.0 mm depth of cut	101
Fig 4.7 : Comparison of tool wear at 1400 rpm and 0.5 mm depth of cut	102
Fig 4.8 : Comparison of tool wear at 1400 rpm and 0.75 mm depth of cut	102
Fig 4.9 : Comparison of tool wear at 1400 rpm and 1.0 mm depth of cut	103
Fig 4.10 : Non magnetic cutting at 0.5 mm depth of cut	104
Fig 4.11 : Cutting with Design 1 Electromagnet at 0.5 mm depth of cut	104
Fig 4.12 : Cutting with Design 2 Electromagnet at 0.75 mm depth of cut	105

Fig 4.13 : Cutting with Design 3 Electromagnet at 1.0 mm depth of cut	105
Fig 4.14 : Non magnetic cutting at a cutting speed of 530 rpm	106
Fig 4.15 : Cutting with design 1 electromagnet at 860 rpm	107
Fig 4.16 : Cutting with design 2 electromagnet at 1400 rpm	107
Fig 4.17 : Cutting with design 3 electromagnet at 860 rpm	108
Fig 4.18 : Images of the surface of the work piece and corresponding contour plot for the cutting under different condition	110
Fig 4.19 : Comparison of surface roughness at 530 rpm and 0.5 mm depth of cut	111
Fig 4.20 : Comparison of surface roughness at 530 rpm and 1.0 mm depth of cut	111
Fig 4.21 : Comparison of surface roughness at 1400 rpm and 1.0 mm depth of cut	112
Fig 4.22 : Variation of temperature with depth of cut at 530 rpm and 860 rpm	114
Fig 4.23 : (a) Discontinuous chips during non magnetic cutting (b) continuous chips during magnetic cutting	115
Fig 4.24 : Cross section of chips	116
Fig 4.25 : Microscopic view of the chip cross section at 860 rpm and 0.75 mm depth of cut	116
Fig 4.26 : (a) chips produced during non magnetic cutting condition (b) chips produced during magnetic cutting condition	117
Fig 4.27 : Strain and Cutting force with respect to cutting speed	118
Fig 4.28 : Strain and Cutting speed with respect to depth of cut (mm)	119

LIST OF TABLES

Page number

CHAPTER 3

Table: 3.1 : Process variables and their values	81
Table: 3.2 : Detail specification of the microscope	82
Table: 3.3 : Technical details of SM1010 digital strain display	94

CHAPTER 4

Table: 4.1 : Accuracy and repeatability of the automated tool wear analysis technique	96
--	----

CHAPTER 1

INTRODUCTION

OBJECTIVE OF THE STUDY:

- ❖ To develop a set up for magnetic cutting during turning operation of mild steel
- ❖ Investigation of machinability parameters in terms of tool wear, surface roughness, chip morphology, cutting temperature and cutting force.
- ❖ To find out the effect of magnetic field on these machinabilities by changing the orientation of the magnetic flux lines using three different designs of electromagnets
- ❖ To develop an in depth comparison in the change in machinability parameters in case of all three designs for different cutting condition.
- ❖ To find out a suitable design of electromagnet for a certain cutting condition.

BACKGROUND:

The useful life of cutting tool is limited by the progressive and frequently rapid deterioration of its active edges, a phenomenon commonly called “tool wear”. Tool wear affects productivity, dimensional accuracy and thereby product quality in most machining processes. This results in poor surface quality. The length of effective tool life is a matter of great concern in establishing the economic performance of machining processes, for which means are constantly searched for its enhancement by minimizing the wear susceptibility of the tool insert. To reduce the tool wear the effect of external electromagnetic force is studied by many contemporary researchers most of which involve the study of the tool life improvement at a particular cutting condition and changing the strength of the magnetic field. This is why in this experiment the study has been extended further to a wide range of cutting conditions. The surface roughness of the finished product has been measured using digital image processing technique. Thus this study analyzes the extent to which improvement in all these machinability factors is obtained and the interrelation among them by the application of magnetic field with different orientation of the magnetic flux lines.

1.1 OVERVIEW OF TURNING PROCESS:

Machining is the term used to describe a variety of material removal processes in which a cutting tool removes unwanted material from a work piece to produce the desired geometric shape and surface finish. The work piece is typically cut from a larger piece of stock, which is available in a variety of standard shapes, such as flat sheets, solid bars, hollow tubes, and shaped beams. Machining can also be performed on an existing part, such as a casting or forging. Out of these machining processes, turning still remains most important operation used to shape metal, because in turning the condition of operation are most varied. Turning is a form of machining, a material removal process, which is used create rotational parts by cutting away unwanted material. The turning process requires a turning machine or lathe, work piece, fixture, and cutting tool. The work piece is a pre-shaped material that is secured to the fixture, which itself is attached to the turning machine, and allowed to rotate at high speeds. The cutter is typically a single-point cutting tool that is also secured in the machine, although some operations make use of multi-point tools. The cutting tool feeds into the rotating work piece and cuts away material in the form of small chips create the desired shape. Turning is used to produce rotational, typically axi-symmetric, parts that have many features, such as holes, grooves, threads, tapers, various diameter steps, and even contoured surfaces. Parts that are fabricated completely through turning often include components that are used in limited quantities, perhaps for prototypes, such as custom designed shafts and fasteners. Turning is also commonly used as a secondary process to add or refine features on parts that were manufactured using a different process. Due to the high tolerances and surface finishes that turning can offer, it is ideal for adding precision rotational features to a part whose basic shape has already been formed.

The cutting characteristics of most turning applications are similar. For a given surface only one cutting tool is used. This tool must overhang its holder to some extent to enable the holder to clear the rotating work piece. Once the cut starts, the tool and the work piece is usually in contact until the surface is completely generated. During this time the cutting speed and cut dimensions will be constant when a cylindrical surface is being turned. In the case of facing operations the cutting speed is proportional to the work piece diameter, the speed decreasing as the center of the piece is approached. Sometimes a spindle speed changing mechanism is provided to

increase the rotating speed of the work piece as the tool moves to the center of the part.

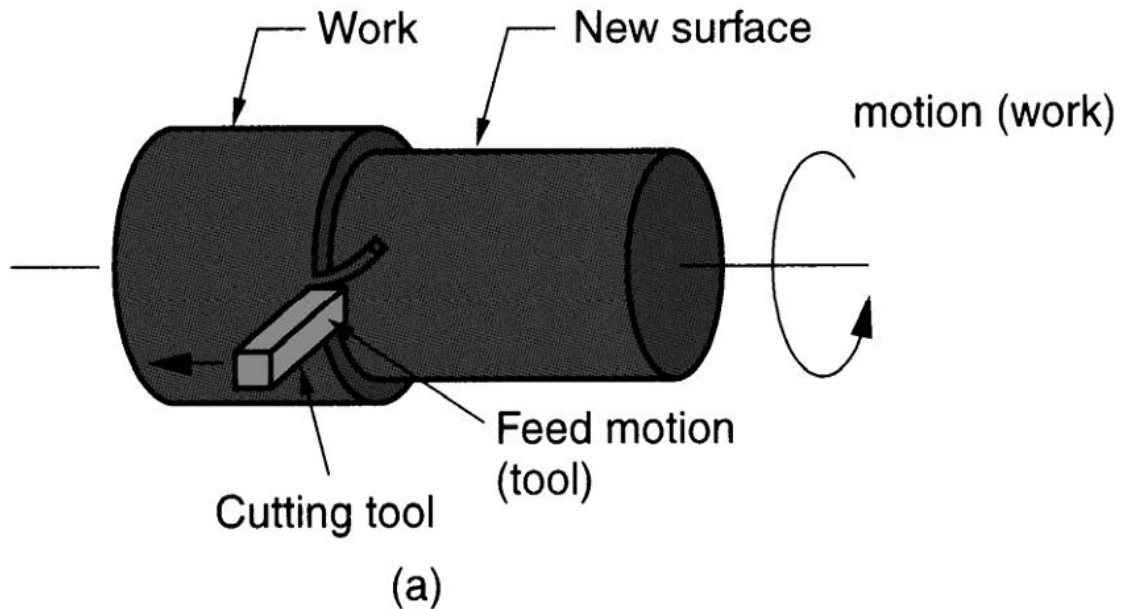


Fig 1.1 : Adjustable parameters in turning operation

1.1.1: ADJUSTABLE CUTTING PARAMETERS

The three primary factors in any basic turning operation are speed, feed, and depth of cut. Other factors such as kind of material and type of tool have a large influence, but these are the ones the operator can change by adjusting the controls, right at the machine.

SPEED:

Speed always refers to the spindle and the work piece. When it is stated in revolutions per minute (rpm) it tells their rotating speed. But the important feature for a particular turning operation is the surface speed, or the speed at which the work piece material is moving past the cutting tool. It is simply the product of the rotating speed times the circumference of the work piece before the cut is started. It is expressed in meter per minute (m/min), and it refers only to the work piece. Every

different diameter on a work piece will have a different cutting speed, even though the rotating speed remains the same.

$$v = \frac{\pi DN}{1000} \text{ m/min} \quad (1.1)$$

Here v is the cutting speed in turning, D is the initial diameter of the work piece in mm, and N is the spindle speed in rpm.

FEED:

Feed always refers to the cutting tool, and it is the rate at which the tool advances along its cutting path. On most power-fed lathes, the feed rate is directly related to the spindle speed and is expressed in mm of tool advance per revolution of the spindle or mm/rev.

Feed of the tool, $F_m = f \cdot N$ mm/min; where f is the feed in mm/rev and N is the spindle speed in rpm.

DEPTH OF CUT:

Depth of cut is practically self explanatory. It is the thickness of the layer being removed in a single pass from the work piece or the distance from the uncut surface of the work to the cut surface, expressed in mm. It is important to note that the diameter of the work piece is reduced by two times the depth of cut because this layer is being removed from both sides of the work piece.

$$d_{\text{cut}} = \frac{D-d}{2} \text{ mm ;} \quad (1.2)$$

Here D and d represent initial and final diameter (mm) of the job respectively.

1.1.2 : DIFFERENT TURNING OPERATION

Chamfering: The tool is used to cut an angle on the corner of a cylinder.

Parting: The tool is fed radially into rotating work at a specific location along its length to cut off the end of a part.

Threading: Feeding a pointed tool linearly across the outside or inside surface of rotating parts to produce external or internal threads.

Boring: Enlarging a hole made by a previous process. A single-point tool is fed linearly and parallel to the axis of rotation.

Drilling: Producing a hole by feeding the drill into the rotating work piece along its axis. Drilling can be followed by reaming or boring to improve accuracy and surface finish.

Knurling: Metal formation operation used to produce a regular cross-hatched pattern in work surfaces.

1.1.3 : TURNING MACHINE

The turning machines are every kind of lathes. Lathes used in manufacturing can be classified as engine, turret, automatics, and numerical control etc.

They are heavy duty machine tools and have power drive for all tool movements. They commonly range in size from 12 to 24 inches swing and from 24 to 48 inches center distance, but swings up to 50 inches and center distances up to 12 feet are not uncommon. Many engine lathes equipped with chip pans and built-in coolant circulating system.

Turret Lathe:

In a turret lathe, longitudinally feedable, hexagon turret replaces the tailstock. The turret, on which six tools can be mounted, can be rotated about a vertical axis to bring each tool into operating position, and the entire unit can be moved longitudinally, either manually or by power, to provide feed for the tools. When the turret assembly is backed away from spindle by means of a capstan wheel; the turret indexes automatically at the end of its movement, thus, bring each of the six tools into operating position. The square turret on the cross slide can be rotated manually about a vertical axis to bring each of the four tools into operating position.

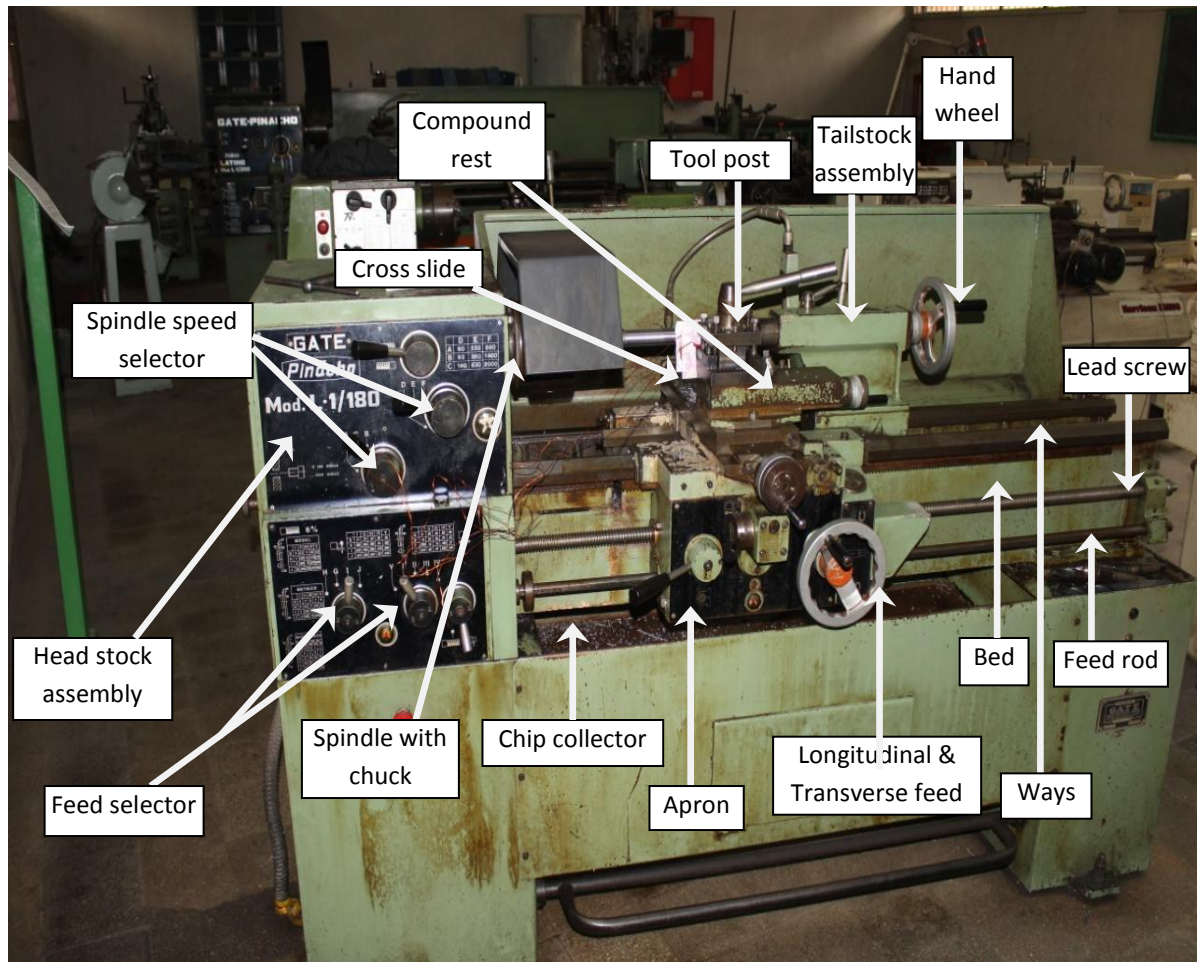


Fig 1.2: Centre lathe used for turning

On most machines, the turret can be moved transversely, either manually or by power, by means of the cross slide, and longitudinally through power or manual operation of the carriage. In most cases, a fixed tool holder also is added to the back end of the cross slide; this often carries a parting tool. Through these basic features of a turret lathe, a number of tools can be set on the machine and then quickly be brought successively into working position so that a complete part can be machined without the necessity for further adjusting, changing tools, or making measurements.

Single-Spindle Automatic Screw Machine:

There are two common types of single-spindle screw machines, one, an American development and common called the turret type (Brown & Sharp), is shown in the following figure. The other is of Swiss origin and is referred to as the Swiss type. The Brown & Sharp screw machine is essentially a small automatic turret, cross slide, spindle, chuck and stock-feed mechanism are controlled by cams. The turret

cam is essentially a program that defines the movement of the turret during a cycle. These machines usually are equipped with an automatic rod feeding magazine that feeds a new length of bar stock into the collect as soon as one rod is completely used.

CNC Machine:

Now-a-days more and more Computer Numerically Controlled (CNC) machines are being used in every kind of manufacturing processes. In a CNC machine, functions like program storage, tool offset and tool compensation, program-editing capability, various degree of computation, and the ability to send and receive data from a variety of sources, including remote locations can be easily realized through on board computer. The computer can store multiple-part programs, recalling them as needed for different parts.

1.1.4 : COMPONENTS OF A LATHE MACHINE

Bed:

The bed of the lathe provides the foundation for the whole machine and holds the headstock, tailstock and carriage in alignment. The surfaces of the bed that are finely machined – and upon which the carriage and tailstock slide – are known as “ways”.

Some beds have a gap near the headstock to allow extra-large diameters to be turned. Sometimes the gap is formed by the machined ways stopping short of the headstock, sometimes by a piece of bed that can be unbolted, removed – and lost.

Some very large lathes have a “sliding bed” where the upper part, on which the carriage and tailstock sit, can be slid along a separate lower part – and so make the gap correspondingly larger or smaller.

Saddle:

The casting that fits onto the top of the bed and slides along it is known, almost universally, as the “Saddle” – a self-explanatory and very suitable term.

Apron:

The vertical, often flat and rectangular “plate” fastened to the front of the “Saddle” is known as the “Apron” and carries a selection of gears and controls that allow the carriage to be driven (by hand or power) up and down the bed. The mechanism inside can also engage the screw cutting feed and various powered tool feeds, should they be fitted. The lead screw, and sometimes a power shaft as well, are often arranged to pass through the apron and provide it with a drive for the various functions. The sophistication of the apron-mounted controls, and their ease of use is a reliable indicator of the quality of a lathe. Virtually all screw-cutting lathes have what is commonly called a “half-nut” lever that closes down one and sometimes two halves of a split nut to grasp the lead screw and provide a drive for screw cutting.

Apron design can be roughly divided into “single-wall” and “double-wall” types. The “single-wall” apron has just one thickness of metal and, protruding from it (and unsupported on their outer ends) are studs that carry gears. The “double-wall” apron is a much more robust structure, rather like a narrow, open-topped box with the gear-carrying studs fitted between the two walls- and hence rigidly supported at both ends. This type of construction produces a very stiff structure – and one that is far less likely of deflect under heavy-duty work; another advantage is that the closed base of the “box” can be used to house an oil reservoir the lubricant ion which is either splashed around or, preferably, pumped to supply the spindles, gears and even, on some lathes, the sliding surfaces of the bed and cross slide as well.

Compound Slide Rest consisting of the Cross Slide and Top Slide:

Sitting on top of the “Saddle” is the “Cross Slide” – that, as its name implies, moves across the bed – and on top of that there is often a “Top Slide” or “Tool Slide” that is invariably arranged so that it can be swiveled and locked into a new position.

Very early lathes had a simple T-shaped piece of metal against which the turner “rested” its tool (all turning being done by hand) but when it became possible to move this “Rest” across the bed by a screw feed it became known, appropriately enough, as a “Slide-rest”.

When two slides are provided, the complete assembly is known as the “Compound” or “Compound Slide” or even “Compound Slide-rest”.

Carriage:

The whole assembly of Saddle, Apron, Top and Cross Slide is known as the “Carriage”.

Headstock:

The lathe headstock used, at one time, to be called the “Fixed Headstock” or “Fixed Head” , and the rotating within it the “Spindle”. The head stock is normally mounted rigidly to the bed (exceptions exist in some production, CNC, automatic and “Swiss-auto” types) and holds all the mechanisms, including various kinds and combinations of gears, so that the spindle can be made turn at different speed.

Headstock Spindle:

The end of the headstock spindle is usually machined so that it can carry a faceplate, chuck, drive-plate, internal or external collets – or even special attachments designed for particular jobs. In turn, these attachments hold the work piece that is going to be machined.

The “fitting” formed on the end of the spindle is normally one of the five types:

- (i) A simple flange through which threaded studs on a faceplate or chuck (for example) can pass and be tightened into place with nuts. This is secure method, and allows high-speed reverse, but is very inconvenient on a general purpose lathe.
- (ii) A threaded nose onto which fittings screw. This is perfectly acceptable for smaller lathes, but unsatisfactory on larger industrial machines where, for reasons of production economy, the spindle may need to be reversed at high speed.
- (iii) A “D-1 taper Cam lock” fitting a long used, standard system that employs three or more “ studs” that are turned to lock into the back of the chucks and faceplates, etc.
- (iv) A taper- either of the simple Harding type or, for bigger lathes, the “taper-nose, long-key drive” –an older but excellent American design where a large screwed ring was held captive on the end of the spindle and used to draw the chuck, or other fitting, onto a long, keyed taper formed on the spindle end.

- (v) Various fittings that became increasingly complex and apparently invented for the sake of being able to claim a National Standard. All these succeeded in doing was to raise manufacturing costs by preventing the interchange of spindle-nose tooling between machines and requiring firms to keep larger inventories of spares and numbers of duplicated firings.

Back gear:

As its name implies, “back gear” is a gear mounted at the back of the headstock that allows the chuck to rotate slowly with greatly increase torque. Back geared lathes are sometimes referred to a “Background for slow speeds” or “Background and screw cutting”. A large diameter casting, fastened to the faceplate and run at 200 rpm (about the slowest speed normally available on a lathe without back gear) would have a linear speed at its outer edge beyond the turning capacity of a small lathe. By engaging back gear, and so reducing the speed but increasing the torque, even the largest faceplate-mounted jobs can be turned successfully. Screw cutting also requires slow speeds, typically between 25 and 50 rpm – especially if the operator is a beginner, or the job tricky.

Lead Screw:

Originally termed a “master thread”, or described as the leading screw”, but now always referred to as the “lead screw”, this is a long threaded rod normally found running along the front of the bed or, on some early examples running between the bed ways down the bed’s center line. By using a train of gears to connect the lathe spindle to the lead crew- and the lead screw to the lathe carriage- the latter, together with its cutting tool, could be forced to move a set distance for every revolution of the spindle.

Tailstock:

The tailstock is arranged to slide along the bed and can be locked to it at any convenient point; the upper portion of the unit it fitted with what is variously called a “barrel”, “spindle”, “ram” or shoot that can be moved in and out of the main casting by hand, lever or screw feed and carries a “Dead Center” that supports the other end of the work piece held in the headstock.

Countershaft:

It is used to reduce the speed of the motor and provide to the lathe's spindle. In a typical arrangement, the motor is fastened to an upright, hinged, cast-iron plate and fitted with a small pulley on its spindle. On the same shaft as the very large pulley is a set of three smaller pulleys, arranged in the "reverse" order from those on the lathe. If the middle pulley on the countershaft is made to drive the identically-sized pulley on the lathe spindle that too, of course, will turn at 300 rpm. The pulleys each side of are normally arranged to halve and double that speed – hence the creation of a speed set covering a useful 150 rpm, 300 rpm and 600 rpm.

Change wheels and Tumble Reverse:

These are the gears that take the drive from the headstock spindle down to the lead screw. They are normally contained within a cover at the extreme left-hand side of the lathe. They are called "change wheels" because of the necessity to change them every time a different thread, or rate of tool feed, was required. The *gear train* is usually carried on a *quadrant arm* able to be adjusted by being swung on its mounting to allow the mesh of the topmost gear with the output gear on the spindle (or tumble reverse mechanism) to be set.

1.1.5 : THE SPECIFICATION OF THE LATHE MACHINE USED IN THIS STUDY

CAPACITY		SP/200
	mm	inches
center height	200	7 7/8"
center distance	750-1000	30"-40"
swing over bed	400	15 3/8"
swing over gap	560	22"
swing over carriage	375	14 3/4"
swing over cross slide	245	9 5/8"
bed width	250	10"
gap length in front of face plate	120	4 3/4"
HEAD STOCK		
main spindle bore	42	1 5/8"
main spindle nose	DIN 55027-5	cam lock no 5
main spindle morse taper	4	4
9 speed range	60-2000	60-2000
THREAD AND FEED BOX		
44 longitudinal feeds	0,05-0.75	0.0018-0,026"
44 cross feeds	0,025-0,375	0,0005-0,0076"
44 metric threads	0,5-7,5	0,5-0,7
44 withworth thread in T.P.1	60-4	60-4
44 modular threads	0,25-3,75	0,25-3,75
44 pitch diametral thread	120-8	120-8
thread of lead screw	6	4h/1h"
SLIDE AND CARRIAGE		
cross slide travel	245	9 5/8"
tool post slide travel	120	4 3/4"
maximum tool dimensions	20*20	3/4"-3/4"
TAILSTOCK		
tailstock barrel diameter	58	2 9/32"
tailstock barrel travel	200	7 7/8"
tailstock taper	4	4
MOTORS		
main motor power in kW	4	4
pump motor power in kW	0,06	0,06
STEALDIES		
max~min capacity of fixed steady	10-130	3/8"-5"
max~min capacity of traveling steady	Oct-80	3/8"-3" 3/16"

The lathe used in our experiment is GATE INC. (UK); Model: L-1/180.

The specification of the lathe machine used in this experiment is shown in the above figure.

1.1.6 : BRIEF DESCRIPTION OF THE CUTTING TOOL GEOMETRY

For cutting tools, geometry depends mainly on the properties of the tool material and the work material. The standard terminology is shown in the following figure. For single point tools, the most important angles are the rake angles and the end and side relief angles.

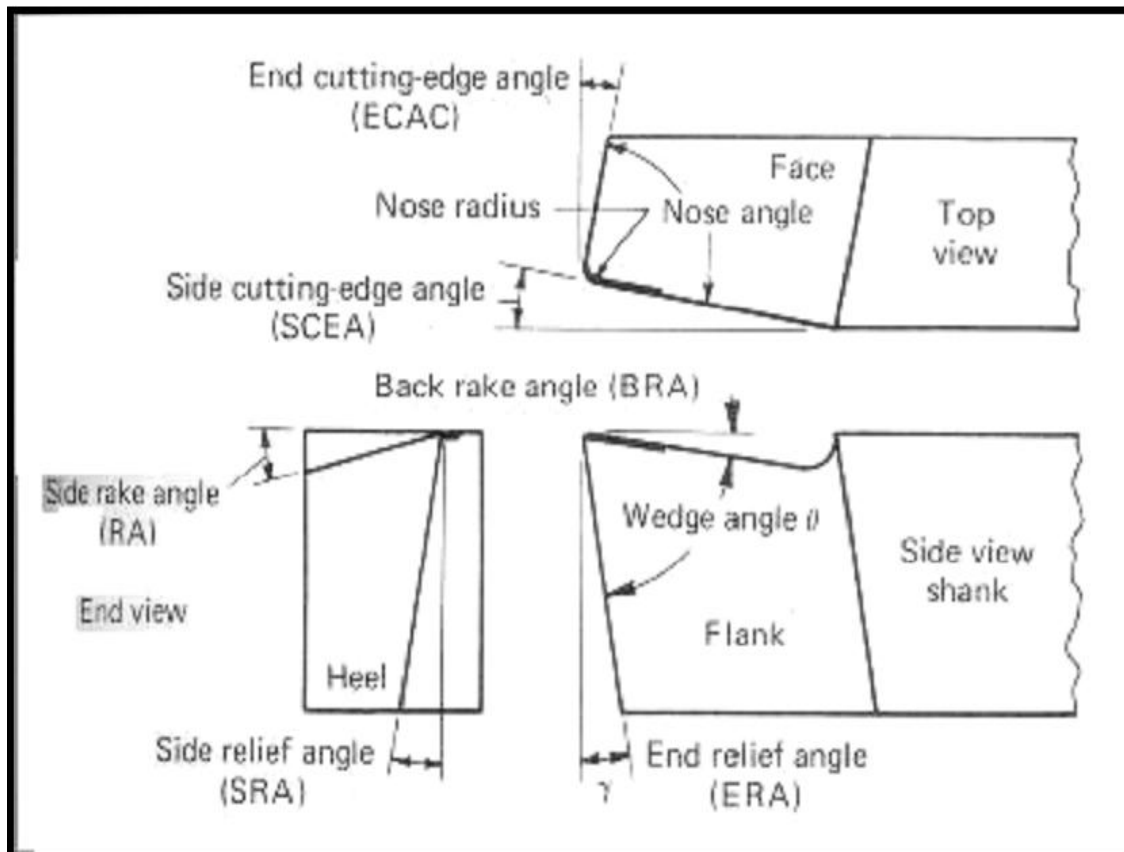


Fig 1.3 : Geometry of a single point turning tool

Flank:

A flat surface of a single-point tool that is adjacent to the face of the tool. During turning, the side flank faces the direction that the tool is fed into the work piece, and the end flank passes over the newly machined surface.

Face:

The flat surface of a single point tool through which, the work piece rotates during turning operation. On a typical turning setup, the face of the tool is positioned upwards.

Shank:

It is the main body of tool. The shank is used to attach with tool holder.

Back rake angle:

If viewed from the side facing the end of the work piece, it is the angle formed by the face of the tool and a line parallel to the floor. A positive back rake angle tilts the tool face back, and a negative angle tilts it forward and up.

Side rake angle:

If viewed behind the tool down the length of the tool holder, it is the angle formed by the face of the tool and the centerline of the work piece. A positive side rake angle tilts the tool face down toward the floor, and a negative angle tilts the face up and toward the work piece.

Side cutting edge angle:

If viewed from above looking down on the cutting tool, it is the angle formed by the side flank of the tool and a line perpendicular to the work piece centerline. A positive side cutting edge angle moves the side flank into the cut, and a negative angle moves the side flank out of the cut.

End cutting edge angle:

If viewed from above looking down on the cutting tool, it is the angle formed by the end flank of the tool and a line parallel to the work piece centerline. Increasing the end cutting edge angle tilts the far end of the cutting edge away from the work piece.

Side relief angle:

If viewed behind the tool down the length of the tool holder, it is the angle formed by the side flank of the tool and a vertical line down to the floor. Increasing the side relief angle tilts the side flank away from the work piece.

End relief angle:

If viewed from the side facing the end of the work piece, it is the angle formed by the end flank of the tool and a vertical line down to the floor. Increasing the end relief angle tilts the end flank away from the work piece.

Nose radius:

It is the rounded tip on the cutting edge of a single point tool. A zero degree nose radius creates a sharp point of the cutting tool.

Lead angle:

It is the common name for the side cutting edge angle. If a tool holder is built with dimensions that shift the angle of an insert, the lead angle takes this change into consideration. The back rake angle affects the ability of the tool to shear the work material and form the chip. It can be positive or negative. Positive rake angles reduce the cutting forces resulting in smaller deflections of the work piece, tool holder, and machine. If the back rake angle is too large, the strength of the tool is reduced as well as its capacity to conduct heat. In machining hard work materials, the back rake angle must be small, even negative for carbide and diamond tools. The higher the hardness, the smaller will be the back rake angle. For high-speed steels, back rake angle is normally chosen in the positive range.

1.1.7 CUTTING TOOL MATERIALS:

The classes of cutting tool materials currently in use for machining operation are high-speed tool steel, cobalt-base alloys, cemented carbides, ceramic, polycrystalline cubic boron nitride and polycrystalline diamond. Different machining applications require different cutting tool materials. The Ideal cutting tool material should have all of the following characteristics:

- Harder than the work it is cutting
- High temperature stability
- Resists wear and thermal shock
- Impact resistant

- Chemically inert to the work material and cutting fluid

To effectively select tools for machining, a machinist or engineer must have specific information about:

- The starting and finished part shape
- The work piece hardness
- The material's tensile strength
- The material's abrasiveness
- The type of chip generated
- The work holding setup
- The power and speed capacity of the machine tool

Some common cutting tool materials are described below:

Carbon steels:

Carbon steels have been used since the 1880s for cutting tools. However carbon steels start to soften at a temperature of about 180 °C. This limitation means that such tools are rarely used for metal cutting operations. Plain carbon steel tools, containing about 0.9% carbon and about 1% manganese, hardened to about 62 Rc, are widely used for woodworking and they can be used in a router to machine aluminium sheet up to about 3mm thick.

High speed steels (HSS):

HSS tools are so named because they were developed to cut at higher speeds. Developed around 1900 HSS are the most highly alloyed tool steels. The tungsten (T series) was developed first and typically contains 12 - 18% tungsten, plus about 4% chromium and 1 - 5% vanadium. Most grades contain about 0.5% molybdenum and most grades contain 4 - 12% cobalt. It was soon discovered that molybdenum (smaller proportions) could be substituted for most of the tungsten resulting in a more economical formulation which had better abrasion resistance than the T series and undergoes less distortion during heat treatment. Consequently about 95% of all HSS tools are made from M series grades. These contain 5 - 10% molybdenum, 1.5 - 10% tungsten, 1 - 4% vanadium, 4% Chromium and many grades contain 5 - 10% cobalt. HSS tools are tough and suitable for interrupted cutting and are used to manufacture

tools of complex shape such as drills, reamers, taps, dies and gear cutters. Tools may also be coated to improve wear resistance. HSS accounts for the largest tonnage of tool materials currently used. Typical cutting speeds: 10 - 60 m/min.

Cast Cobalt alloys:

Introduced in early 1900s these alloys have compositions of about 40 - 55% cobalt, 30% chromium and 10 - 20% tungsten and are not heat treatable. Maximum hardness values of 55 - 64 Rc. They have good wear resistance but are not as tough as HSS but can be used at somewhat higher speeds than HSS. Now only in limited use.

Carbides:

Also known as cemented carbides or sintered carbides were introduced in the 1930s and have high hardness over a wide range of temperatures, high thermal conductivity, high Young's modulus making them effective tool and die materials for a range of applications. The two groups used for machining are tungsten carbide and titanium carbide; both types may be coated or uncoated. Tungsten carbide particles (1 to 5 micrometer) are bonded together in a cobalt matrix using powder metallurgy. The powder is pressed and sintered to the required insert shape. Titanium and niobium carbides may also be included to impart special properties. A wide range of grades are available for different applications. Sintered carbide tips are the dominant type of material used in metal cutting. The proportion of cobalt (the usual matrix material) present has a significant effect on the properties of carbide tools. 3 - 6% matrix of cobalt gives greater hardness while 6 - 15% matrix of cobalt gives a greater toughness while decreasing the hardness, wear resistance and strength. Tungsten carbide tools are commonly used for machining steels, cast irons and abrasive non-ferrous materials. Titanium carbide has a higher wear resistance than tungsten but is not as tough. With a nickel-molybdenum alloy as the matrix, TiC is suitable for machining at higher speeds than those which can be used for tungsten carbide. Typical cutting speeds are: 30 - 150 m/min or 100 - 250 when coated.

Coatings:

Coatings are frequently applied to carbide tool tips to improve tool life or to enable higher cutting speeds. Coated tips typically have lives 10 times greater than uncoated tips. Common coating materials include titanium nitride, titanium carbide

and aluminium oxide, usually 2 - 15 micro-m thick. Often several different layers may be applied, one on top of another, depending upon the intended application of the tip. The techniques used for applying coatings include chemical vapor deposition (CVD) plasma assisted CVD and physical vapor deposition (PVD). Diamond coatings are also in use and being further developed.

Cermets:

Developed in the 1960s, these typically contain 70% aluminium oxide and 30% titanium carbide. Some formulation contains molybdenum carbide, niobium carbide and tantalum carbide. Their performance is between those of carbides and ceramics and coatings seem to offer few benefits. Typical cutting speeds: 150 - 350 m/min.

Ceramics:

Alumina introduced in the early 1950s, two classes are used for cutting tools: fine grained high purity aluminium oxide (Al_2O_3) and silicon nitride (Si_3N_4) are pressed into insert tip shapes and sintered at high temperatures. Additions of titanium carbide and zirconium oxide (ZrO_2) may be made to improve properties. But while ZrO_2 improves the fracture toughness, it reduces the hardness and thermal conductivity. Silicon carbide (SiC) whiskers may be added to give better toughness and improved thermal shock resistance. The tips have high abrasion resistance and hot hardness and their superior chemical stability compared to HSS and carbides means they are less likely to adhere to the metals during cutting and consequently have a lower tendency to form a built up edge. Their main weakness is low toughness and negative rake angles are often used to avoid chipping due to their low tensile strengths. Stiff machine tools and work set ups should be used when machining with ceramic tips as otherwise vibration is likely to lead to premature failure of the tip. Typical cutting speeds: 150-650 m/min.

Silicon Nitride:

In the 1970s a tool material based on silicon nitride was developed, these may also contain aluminium oxide, yttrium oxide and titanium carbide. SiN has an affinity for iron and is not suitable for machining steels. A specific type is 'Sialon', containing the elements: silicon, aluminium, oxygen and nitrogen. This has higher thermal shock

resistance than silicon nitride and is recommended for machining cast irons and nickel based super alloys at intermediate cutting speeds.

Cubic Boron Nitride (CBN):

Introduced in the early 1960s, this is the second hardest material available after diamond. CBN tools may be used either in the form of small solid tips or as a 0.5 to 1 mm thick layer of polycrystalline boron nitride sintered onto a carbide substrate under pressure. In the latter case the carbide provides shock resistance and the CBN layer provides very high wear resistance and cutting edge strength. Cubic boron nitride is the standard choice for machining alloy and tool steels with a hardness of 50 RC or higher. Typical cutting speeds: 30 - 310 m/min.

Diamond:

The hardest known substance is diamond. Although single crystal diamond has been used as a tool, they are brittle and need to be mounted at the correct crystal orientation to obtain optimal tool life. Single crystal diamond tools have been mainly replaced by polycrystalline diamond (PCD). This consists of very small synthetic crystals fused by a high temperature high pressure process to a thickness of between 0.5 and 1mm and bonded to a carbide substrate. The result is similar to CBN tools. The random orientation of the diamond crystals prevents the propagation of cracks, improving toughness. Because of its reactivity, PCD is not suitable for machining plain carbon steels or nickel, titanium and cobalt based alloys. PCD is most suited to light uninterrupted finishing cuts at almost any speed and is mainly used for very high speed machining of aluminium - silicon alloys, composites and other non - metallic materials. Typical cutting speeds: 200 - 2000 m/min.

To improve the toughness of tools, developments are being carried out with whisker reinforcement, such as silicon nitride reinforced with silicon carbide whiskers. As rates of metal removal have increased, so has the need for heat resistant cutting tools. The result has been a progression from high-speed steels to carbide, and on to ceramics and other super hard materials. High-speed steels cut four times faster than the carbon steels they replaced. There are over 30 grades of high-speed steel, in three main categories: tungsten, molybdenum, and molybdenum-cobalt based grades. In industry today, carbide tools have replaced high-speed steels in most applications.

These carbide and coated carbide tools cut about 3 to 5 times faster than high-speed steels. Cemented carbide is a powder metal product consisting of fine carbide particles cemented together with a binder of cobalt. The major categories of hard carbide include tungsten carbide, titanium carbide, tantalum carbide, and niobium carbide. Ceramic cutting tools are harder and more heat-resistant than carbides, but more brittle. They are well suited for machining cast iron, hard steels, and the super alloys. Two types of ceramic cutting tools are available: the alumina-based and the silicon nitride-based ceramics. The alumina-based ceramics are used for high speed semi- and final-finishing of ferrous and some non-ferrous materials. The silicon nitride-based ceramics are generally used for rougher and heavier machining of cast iron and the super alloys.

1.1.8 INSERTS:

A tipped tool generally refers to any cutting tool where the cutting edge consists of a separate piece of material, either brazed, welded or clamped on to a separate body. Common materials for tips include tungsten carbide, polycrystalline diamond, and cubic boron nitride. The advantage of tipped tools is only a small insert of the cutting material is needed to provide the cutting ability. The small size makes manufacturing of the insert easier than making a solid tool of the same material. This also reduces cost because the tool holder can be made of a less-expensive and tougher material. In some situations a tipped tool is better than its solid counterpart because it combines the toughness of the tool holder with the hardness of the insert. Inserts are removable cutting tips, which mean they are not brazed or welded to the tool body. They are usually indexable, meaning that they can be rotated or flipped without disturbing the overall geometry of the tool (effective diameter, tool length offset, etc.). This saves time in manufacturing by allowing fresh cutting edges to be presented periodically without the need for tool grinding and setup changes.

Indexable turning inserts are manufactured in a variety of shapes, sizes and thicknesses, with straight holes, with countersunk holes, without holes, with chip breakers on one side, with chip breakers on two sides or without chip breakers. The selection of the appropriate turning tool holder geometry, accompanied by the correct

insert shape and chip breaker geometry, will ultimately have a significant impact on the productivity and tool life of a specific turning operation.

Insert strength is one important factor in selecting the correct geometry for a work piece material or hardness range. Triangle inserts are the most popular shaped inserts primarily because of their wide application range. A triangular insert can be utilized in any of the seven basic turning holders mentioned earlier. Diamond-shaped inserts are used for profile turning operations while squares are often used on lead angle tools. The general rule for rating an insert's strength based on its shape is: The larger the included angle on the insert corner, the greater the insert strength.



Fig 1.4: Carbide tool inserts

1.1.9 : MATERIAL REMOVAL RATE

The material removal rate (MRR) in turning operations is the volume of material/metal that is removed per unit time in mm^3/min . For each revolution of the work piece, a ring-shaped layer of material is removed. $\text{MRR} = (v. f. d * 1000)$ in mm^3/min

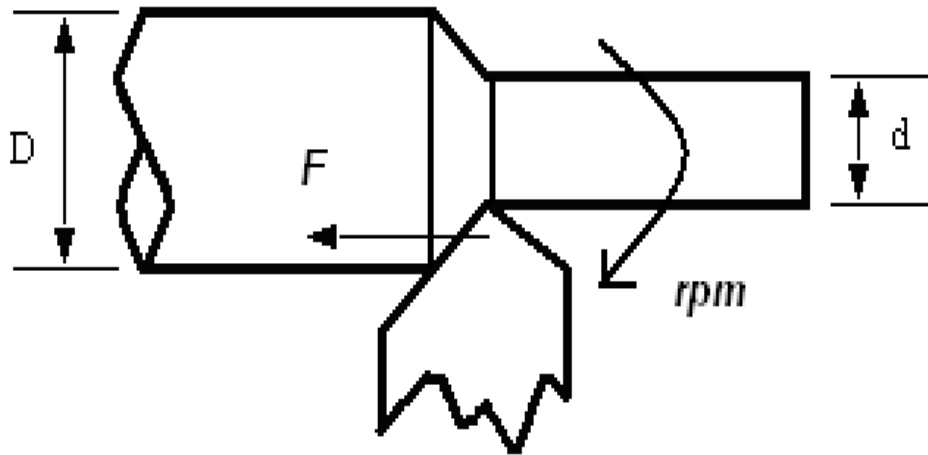


Fig 1.5: MRR in turning

$$mrr = \left(\frac{\pi D^2}{4} - \frac{\pi d^2}{4} \right) \times F \times rpm \quad (1.3)$$

Where

D = diameter of the work piece before cutting

d = diameter of the work piece after cutting

1.1.10: WORK HOLDING METHODS

In lathe work the three most common work holding methods are:

- Held in a chuck.
- Held between centers.
- Held in a collet.

Held in a Chuck:

The most common method of work holding, the chuck, has either three or four jaws and is mounted on the end of the main spindle. A three-jaw chuck is used for gripping cylindrical work pieces when the operations to be performed are such that the machined surface is concentric with the work surfaces.

With the four-jaw chuck, each jaw can be adjusted independently by rotation of the radially mounted threaded screws. Although accurate mounting of a work piece can be time consuming, a four jaw chuck is often necessary for non-cylindrical work pieces.

Held between Centers:

For accurate turning operations or in cases where the work surface is not truly cylindrical, the work piece can be turned between centers. Initially, the work piece has a conical center hole drilled at each end to provide location for the lathe centers. Before supporting the work piece between the centers (one in the headstock and one in the tailstock) a clamping device called a dog is secured to the work piece. The dog is arranged so that the tip is inserted into a slot in the drive plate mounted on the main spindle, ensuring that the work piece will rotate with the spindle.

Lathe centers support the work piece between the headstock and the tailstock. The center used in the headstock spindle is called the live center. It rotates with the headstock spindle. The dead center is located in the tailstock spindle. This center usually does not rotate and must be hardened and lubricated to withstand the wear of the revolving work.

The hole in the spindle into which the center fits is usually of a Morse standard taper. It is important that the hole in the spindle be kept free of dirt and also that the taper of the center be clean and free of chips or burrs. If the taper of the live center has particles of dirt or a burr on it, it will not run true. The centers play a very important part in lathe operation. Since they give support to the work piece, they must be properly ground and in perfect alignment with each other. The work piece must have perfectly drilled and countersunk holes to receive the centers. The center must have a 60-degree point.

Held in a Collet:

Collets are used when smooth bar stock, or work pieces that have been machined to a given diameter, must be held more accurately than normally can be achieved in a regular three or four jaw chuck. Collets are relatively thin tubular steel bushings that are split into three longitudinal segments over about two thirds of their

length. The smooth internal surface of the split end is shaped to fit the piece of stock that is to be held. The external surface at the split end is a taper that fits within an internal taper of a collet sleeve placed in the spindle hole. When the collet is pulled inward into the spindle, by means of the draw bar that engages threads on the inner end of the collet, the action of the two mating tapers squeezes the collet segments together, causing them to grip the work piece.

1.2 : TOOL WEAR

Tool wear in machining is defined as the amount of volume loss of tool material on the contact surface due to the interactions between the tool and work piece. Specifically, tool wear is described by wear rate (volume loss per unit area per unit time) and is strongly determined by temperature, stresses, and relative sliding velocity generated at the contact interface. Metal cutting tools are subjected to extremely arduous conditions, high surface loads, and high surface temperatures arise because the chip slides at high speed along the tool rake face while exerting very high normal pressures (and friction force) on this face. The forces may be fluctuating due to the presence of hard particles in the component micro-structure, or more extremely, when interrupted cutting is being carried out. Hence cutting tools need:

- Strength at elevated temperatures
- High toughness
- High wear resistance
- High hardness

During the past 100 years there has been extensive research and development which has provided continuous improvement in the capability of cutting tool. A key factor in the wear rate of virtually all tool materials is the temperature reached during operation; unfortunately it is difficult to establish the values of the parameters needed for such calculations. However, experimental measurements have provided the basis for empirical approaches. It is common to assume that all the energy used in cutting is converted to heat (a reasonable assumption) and that 80% of this is carried away in the chip (this will vary and depend upon several factors - particularly the cutting

speed). This leaves about 20% of the heat generated going into the cutting tool. Even when cutting mild steel tool temperatures can exceed 550°C, the maximum temperature high speed steel (HSS) can withstand without losing some hardness. Cutting hard steels with cubic boron nitride tools will result in tool and chip temperatures in excess of 1000 °C. During operation, one or more of the following wear modes may occur:

- Flank
- Notch
- Crater
- Edge rounding
- Edge chipping
- Edge cracking
- Catastrophic failure

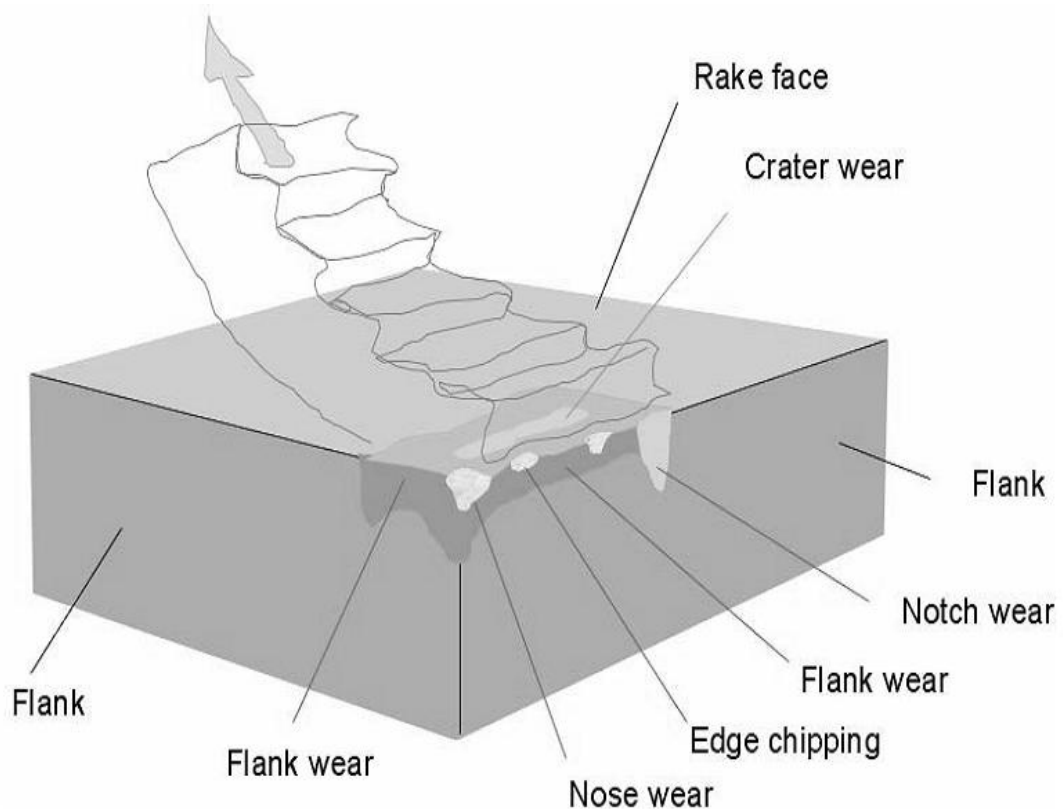


Fig. 1.6: Different Modes of Wear

Cutting tools are subjected to an extremely severe rubbing process. They are in metal-to-metal contact between the chip and work piece, under conditions of very high stress at high temperature. The situation is further aggravated (worsened) due to the existence of extreme stress and temperature gradients near the surface of the tool. During machining, cutting tools remove material from the component to achieve the required shape, dimension and surface roughness (finish). However, wear occurs during the cutting action, and it will ultimately result in the failure of the cutting tool. When the tool wear reaches a certain extent, the tool or active edge has to be replaced to guarantee the desired cutting action.

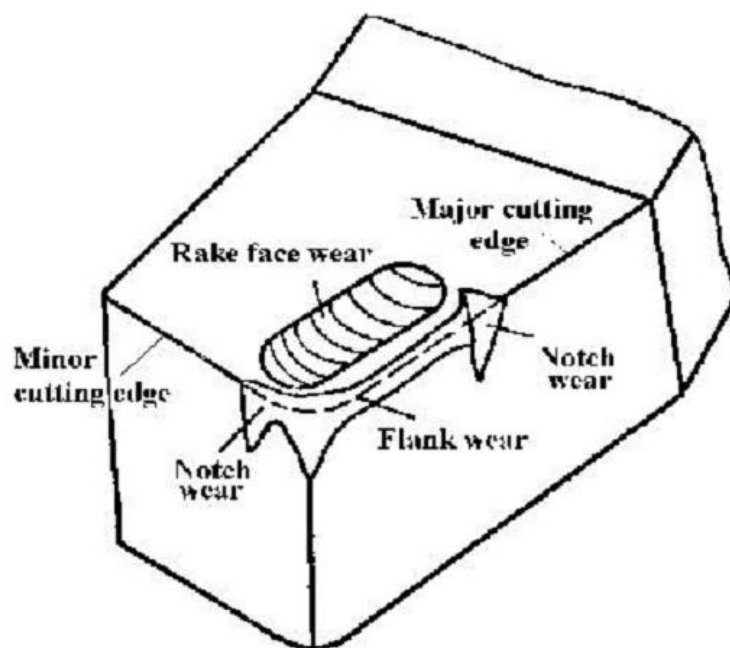


Fig 1.7: Tool wear phenomenon

1.2.1: TYPES OF TOOL WEAR

CRATER WEARS:

The chip flows across the rake face, resulting in severe friction between the chip and rake face, and leaves a scar on the rake face which usually parallels to the major cutting edge. The crater wear can increase the working rake angle and reduce the cutting force, but it will also weaken the strength of the cutting edge. The

parameters used to measure the crater wear can be seen in the diagram. The crater depth KT is the most commonly used parameter in evaluating the rake face wear.

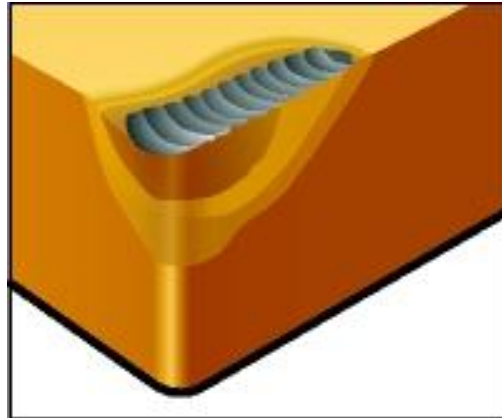


Fig 1.8: Crater Wear

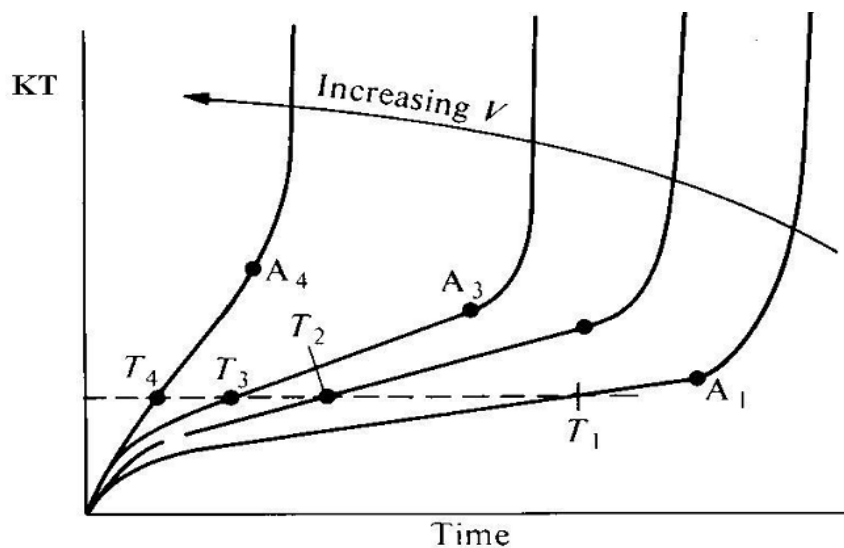


Fig. 1.9: Effects of cutting speed V and cutting time T on crater wear depth KT

FLANK WEAR (Clearance Surface):

Wear on the flank (relief) face is called Flank wear and results in the formation of a wear land. Wear land formation is not always uniform along the major and minor cutting edges of the tool. Flank wear most commonly results from abrasive wear of the cutting edge against the machined surface. Flank wear can be monitored in production by examining the tool or by tracking the change in size of the tool or machined part. Flank wear can be measured by using the average and maximum wear land size V_B and $V_{B \max}$.

Due to micro-cracking, surface oxidation and carbon loss layer, as well as micro-roughness at the cutting tool tip in tool grinding (manufacturing). For the new cutting edge, the small contact area and high contact pressure will result in high wear rate. The initial wear size is $VB=0.05-0.1\text{mm}$ normally. After the initial (or preliminary) wear (cutting edge rounding), the micro-roughness is improved, in this region the wear size is proportional to the cutting time. The wear rate is relatively constant.

When the wear size increases to a critical value, the surface roughness of the machined surface decreases, cutting force and temperature increase rapidly, and the wear rate increases. Then the tool loses its cutting ability. In practice, this region of wear should be avoided. Flank wear and chipping will increase the friction, so that the total cutting force will increase. The component surface roughness will be increased, especially when chipping occurs. Flank wear will also affect the component dimensional accuracy. When form tools are used, flank wear will also change the shape of the component produced.

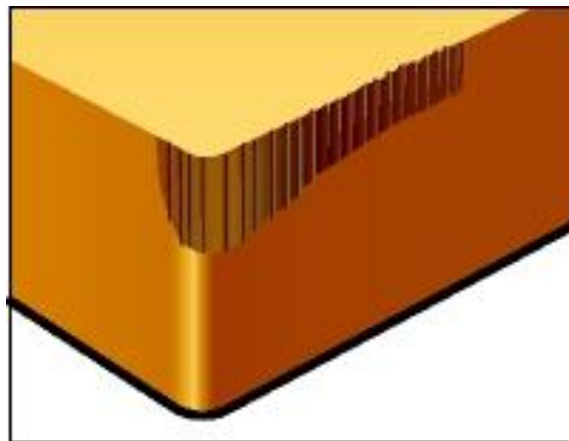


Fig. 1.10 : Flank Wear

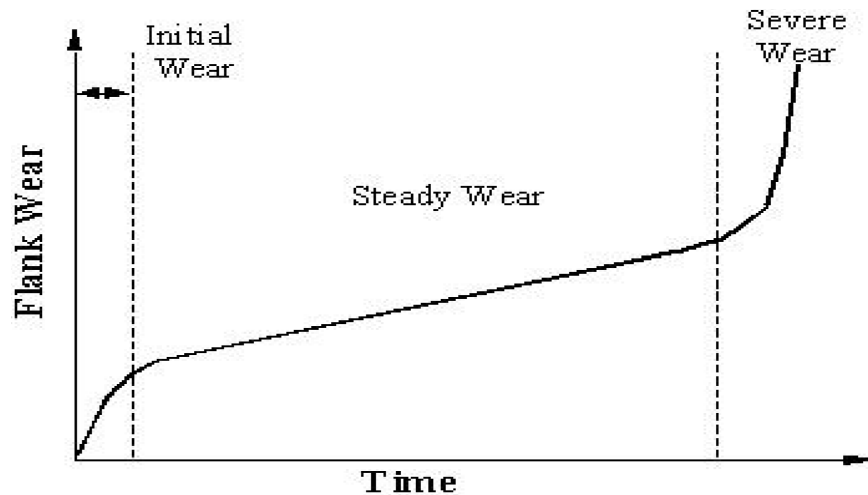


Fig. 1.11: Different regions of wear

NOTCH WEAR:

Wear on the flank (relief) face is called Flank wear and results in the formation of a wear land. Wear land formation is not always uniform along the major and minor. This is a special type of combined flank and rake face wear which occurs adjacent to the point where the major cutting edge intersects the work surface. The gashing (or grooving, gouging) at the outer edge of the wear land is an indication of a hard or abrasive skin on the work material. Such a skin may develop during the first machine pass over a forging, casting or hot-rolled work piece. It is also common in machining of materials with high work-hardening characteristics, including many stainless steels and heat-resistant nickel or chromium alloys. In this case, the previous machining operation leaves a thin work-hardened skin.

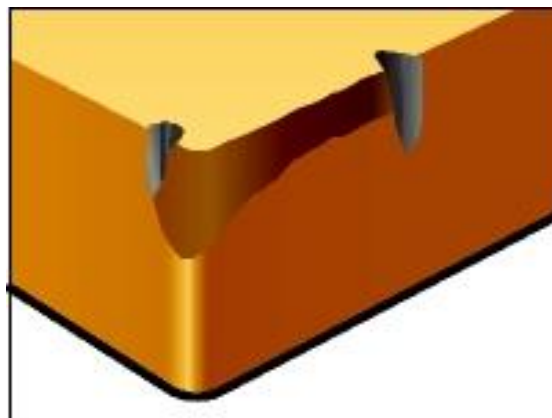


Fig. 1.12 : Notch Wear

CHIPPING:

Chipping of the tool, as the name implies, involves removal of relatively large discrete particles of tool material. Tools subjected to discontinuous cutting conditions are particularly prone to chipping. Chipping of the cutting edge is more like micro-breakages rather than conventional wear. Built-up edge formation also has a tendency to promote tool chipping. A built-up edge is never completely stable, but it periodically breaks off. Each time some of the built-up material is removed it may take with it a lump (piece) of tool edge

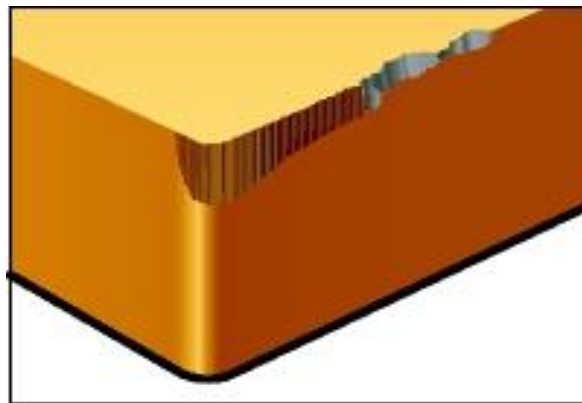


Fig. 1.13: Chipping Wear

ATTRITION WEAR:

Sometimes called Adhesion wear, this pattern is found on very slow surface feed operations. It is characterized by a very rough surface on the land and face of the tool. Usually, a built up edge (BUE) is observed. Chips will be thick and not curl. Severe streaking of the finished part will be apparent.

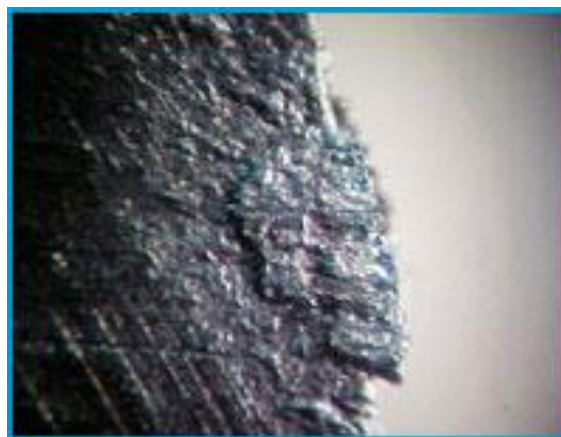


Fig. 1.14: Attrition Wear

ABRASIVE WEAR:

Deep, multiple scratches or scores are observed on the land (flank) of the tool. The scoring may appear predominantly on front rows of cutting teeth or it may appear randomly anywhere on the broach tool. The scoring will not appear uniform in length and will be at different positions across the land of the tool.

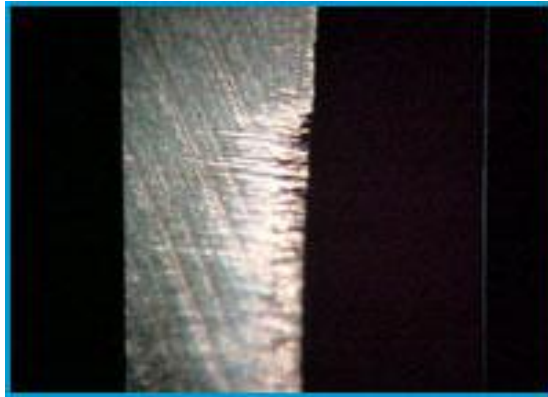


Fig. 1.15: Abrasive Wear

FRACTURE:

Often the evidence is lost when the insert is shattered. It may be the result of over use or severe overload. If it occurs very late in the life of the tool, other wear patterns probably existed such as Chipping, Crater, Deformation or Flaking and the tool was overrun.

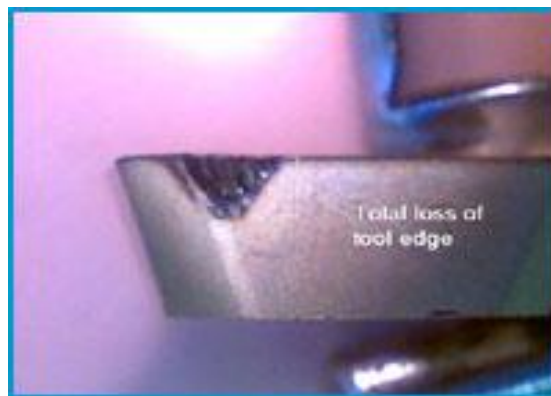


Fig. 1.16: Fracture

SPALLING:

This wear pattern is difficult to observe as it occurs relatively early in the life of the tool. If left in place, the tool will eventually demonstrate failure modes such as Crater, Flaking, Flank or Fracture wear. If Spalling and Thermal Cracking are both observed, condition should be treated as thermal shock first. Since spalling occurs early, other wear patterns develop that mask and may mislead the observer.

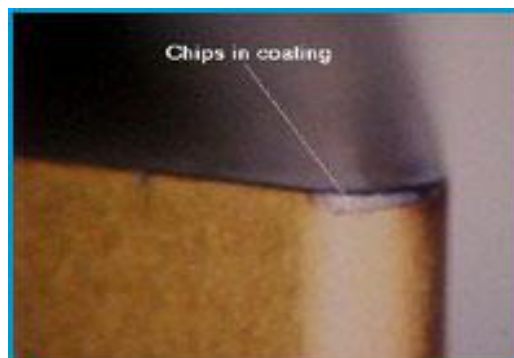


Fig. 1.17: Spalling

BUILT UP EDGE:

This common problem is identified by work piece material sticking to the face of the tool. The BUE often leads to chipping of the tool cutting edges. Often it will be an irregular wear pattern and will generate poor surface micro-finish on the part. Remnants of a built up edge may show on the finished part as a streak left behind when the tool is extracted from the work piece.

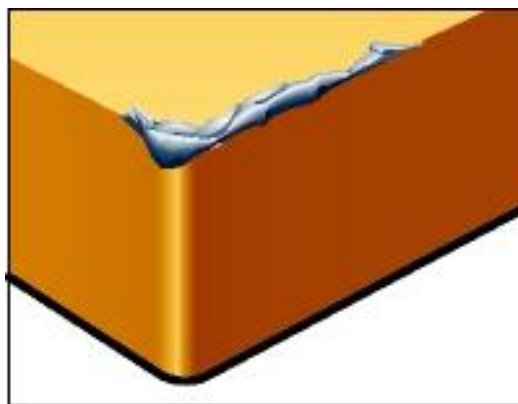


Fig. 1.18: Built up edge

THERMAL CRACKING:

This wear pattern is unique as shows up as hairline cracks that are perpendicular to the cutting edge. Many times the parallel cracks are uniformly distributed long the cutting edge. These edge chips will appear to be very uniform in depth and are in line with the direction of tool travel.

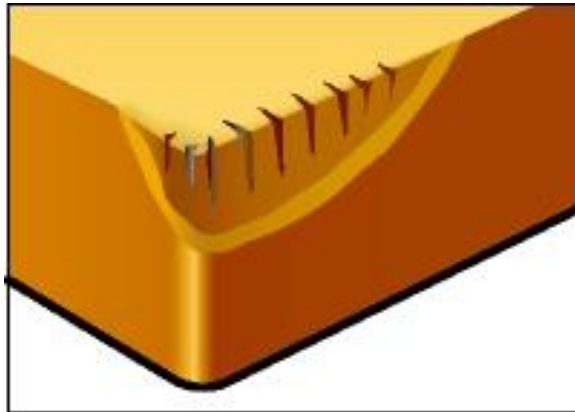


Fig. 1.19: Thermal Cracking

PLASTIC DEFORMATION:

This is caused by the plastic deformation of edge, depression or flank impression, leading to poor chip control, poor surface finish and insert breakage. Another factor contributing on plastic deformation is the cutting temperature and high pressure. It can be avoided by selecting a more wear resistant or harder grade of tool, reducing cutting speed or reducing the feed.

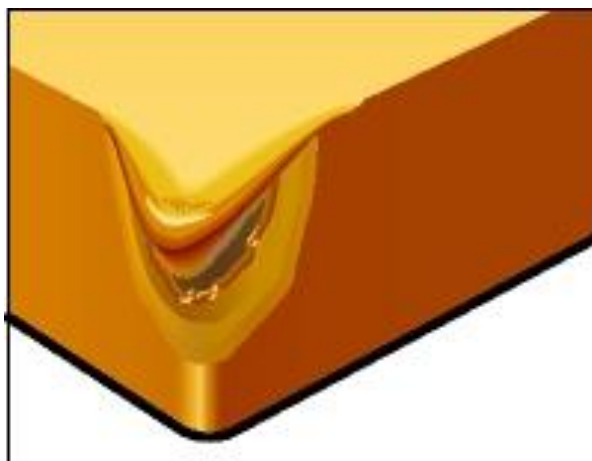


Fig. 1.20: Plastic Deformation

ULTIMATE FAILURE:

The final result of tool wear is the complete removal of the cutting point - ultimate failure of the tool. This may come about by temperature rise, which virtually causes the tool tip to soften until it flows plastically at very low shear stress. This melting process seems to start right at the cutting edge and because material flow blunts the edge, the melting process continues back into the tool; within a few seconds a piece of tool almost as large as the engaged depth of cut is removed. An alternative mechanism of ultimate failure is the mechanical failure (usually a brittle fracture) of a relatively large portion of the cutting tip. This often results from a weakening of the tool by crater formation. Ultimate failure by melting and plastic flow is most common in carbon and high-speed-steel tools, while fracture failures are most common in sintered carbide or ceramic tools.

1.2.2 : TOOL WEAR EVOLUTION

Tool wear curves illustrate the relationship between the amount of flank (rake) wear and the cutting time, τ_m , or the overall length of the cutting path, L . Figure 1.21(a) shows the evolution of flank wear $V_{B \max}$, as measured after a certain length of cutting path. Normally, there are three distinctive regions that can be observed in such curves. The first region (region I in Figure 1.21(a)) is the region of primary or initial wear. The relatively high wear rate (an increase of tool wear per unit time or length of the cutting path) in this region is explained by accelerated wear of the tool layers damaged during manufacturing or re-sharpening. The second region (region II in Figure 1.21(a)) is the region of steady-state wear. This is the normal operating region for the cutting tool. The third region (region III in Figure 1.21(a)) is known as the tertiary or accelerated wear region. Accelerated tool wear in this region is usually accompanied by high cutting forces, temperatures and severe tool vibrations. Normally, the tool should not be used in this region. In practice, the cutting speed is of prime concern in the consideration of tool wear. As such, tool wear curves are constructed for different cutting speeds keeping other machining parameters constant. In Figure 1.21(b), three characteristic tool wear curves (mean values) are shown for three different cutting speeds, v_1 , v_2 , and v_3 . Because v_3 is greater than the other

two, it corresponds to the fastest wear rate. When the amount of wear reaches the permissible tool wear VB_{Bc} , the tool is said to be worn out.

Typically VB_{Bc} is selected from the range 0.15–1.00 mm depending upon the type of machining operation, the condition of the machine tool and the quality requirements of the operation. It is often selected on the grounds of process efficiency and often called the criterion of tool life. In Figure 1.21(b), T_1 is the tool life when the cutting speed v_1 is used, T_2 – when v_2 , and T_3 – when v_3 is the case. When the integrity of the machined surface permits, the curve of maximum wear instead of the line of equal wear should be used (Figure 1.21(b)). As such, the spread in tool life between lower and higher cutting speeds becomes less significant. As a result, a higher productivity rate can be achieved, which is particularly important when high-speed CNC machines are used.

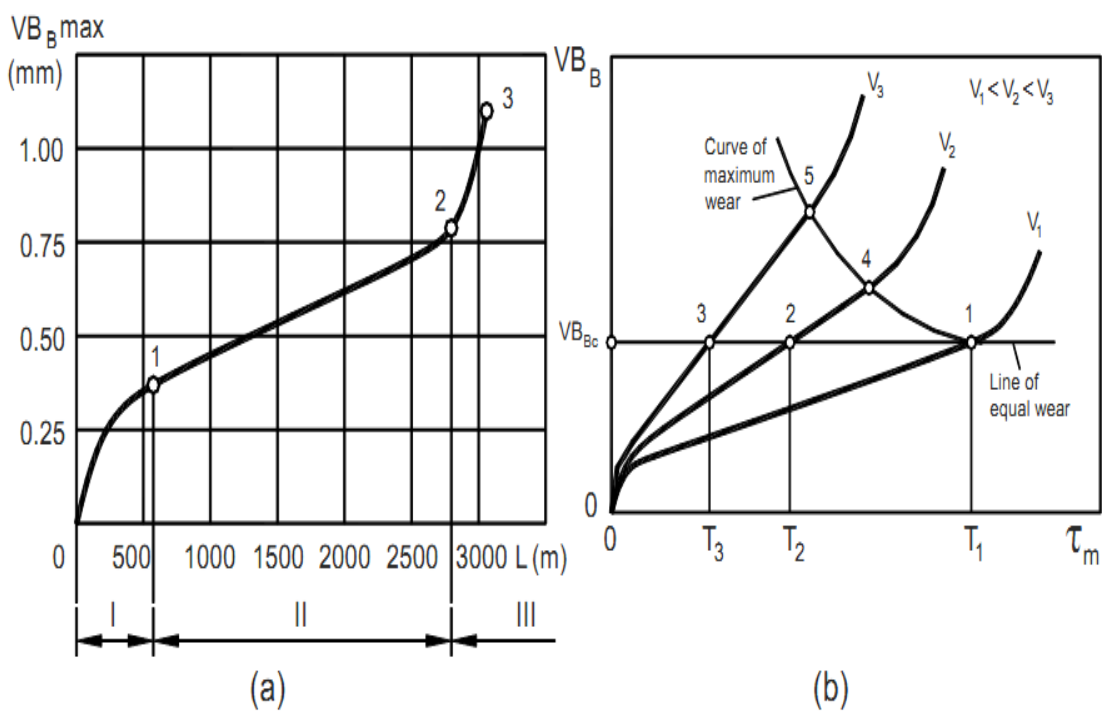


Fig. 1.21 : Wear curves: (a) normal wear curve, (b) evolution of flank wear land

VB_B as a function of cutting time for different cutting speeds

MECHANISM OF TOOL WEAR:

The general mechanisms that cause tool wear, summarized in Figure 1.22, are

- (i) Abrasion

- (ii) Diffusion
- (iii) Oxidation
- (iv) Fatigue and
- (v) Adhesion

The fundamentals of these tool wear mechanisms are explained for several authors, for example, Shaw [1] and Trent and Wright [2]. Most of these mechanisms are accelerated at higher cutting speeds and consequently cutting temperatures.

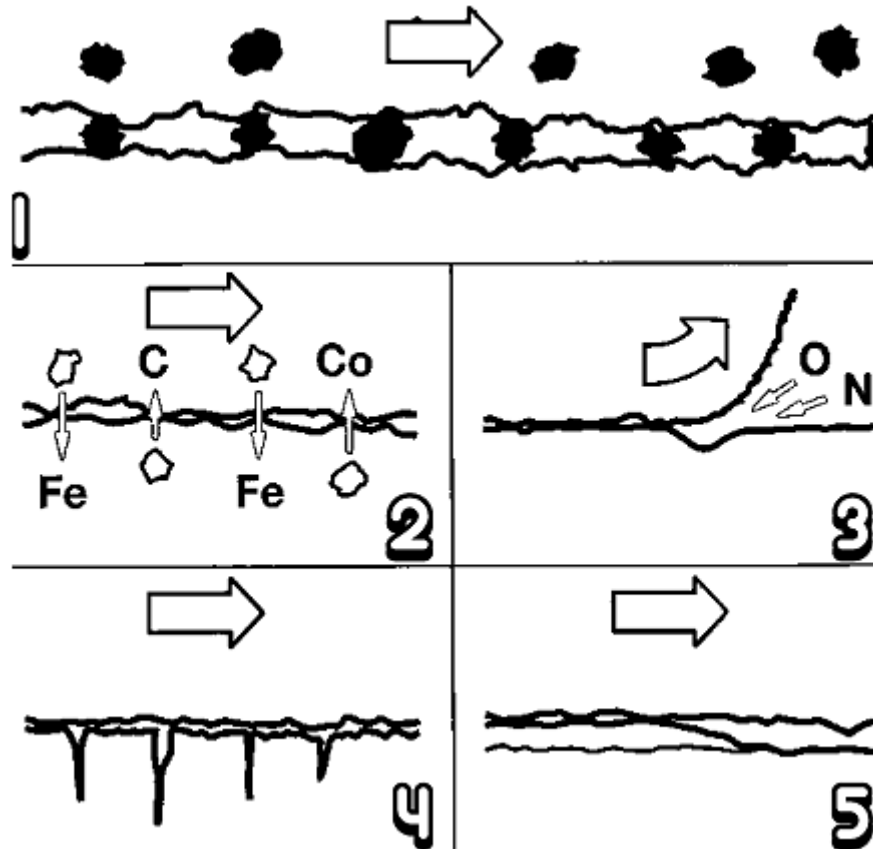


Fig. 1.22: Evolution of the flank wear land V_B as a function of cutting time for different cutting speeds [3]

1.2.3 : EFFECT OF TOOL WEAR ON PERFORMANCE MEASURES

Consequences of Tool Wear:

- (i) Increase the cutting force
- (ii) Increase the surface roughness
- (iii) Decrease the dimensional accuracy

- (iv) Increase the temperature
- (v) Vibration
- (vi) Lower the production efficiency, component quality
- (vii) Increase the cost

Influence on cutting forces:

Crater wear, flank wear (or wear-land formation) and chipping of the cutting edge affect the performance of the cutting tool in various ways. The cutting forces are normally increased by wear of the tool. Crater wear may, however, under certain circumstances, reduce forces by effectively increasing the rake angle of the tool. Clearance-face (flank or wear-land) wear and chipping almost invariably increase the cutting forces due to increased rubbing forces.

Surface finish (roughness):

The surface finish produced in a machining operation usually deteriorates as the tool wears. This is particularly true for a tool worn by chipping and generally the case for a tool with flank-land wear; although there are circumstances in which a wear land may burnish (polish) the work piece and produces a good finish.

Dimensional accuracy:

Flank wear influences the plan geometry of a tool; this may affect the dimensions of the component produced in a machine with set cutting tool position or it may influence the shape of the components produced in an operation utilizing a form tool. (If tool wear is rapid, cylindrical turning could result in a tapered work piece)

Vibration or chatter:

Vibration or chatter is another aspect of the cutting process which may be influenced by tool wear. A wear land increases the tendency of a tool to dynamic instability. A cutting operation which is quite free of vibration when the tool is sharp may be subjected to an unacceptable chatter mode when the tool wears.

1.2.4 : TOOL LIFE

There is no single universally accepted definition of tool life. The life needs to be specified with regard to the process aims. A common way of quantifying the end of a tool life is to put a limit on the maximum acceptable flank wear, V_B or $V_{B \max}$. Typical figures are given in table 1.1. Tool wear is almost always used as a lifetime criterion because it is easy to determine quantitatively. The flank wear land V_B is often used as the criterion because of its influence on work piece surface roughness and accuracy. Figure 1.23 shows the wear curves (V_B versus cutting time) for several cutting velocities (1, 2 and 3) and the construction of the life curve (cutting velocity vs. tool life). Taylor [4] presented the following equation:

$$V_c T^n = C \quad (1.4)$$

where V_c is the cutting speed (m/min), T is the tool life (min) taken to develop a certain flank wear (V_B), n is an exponent that depends on the cutting parameters and C is a constant. C is equal to the cutting speed at $T = 1$ min. Therefore, each combination of tool material and work piece and each cutting parameter has its own n and C values, to be determined experimentally.

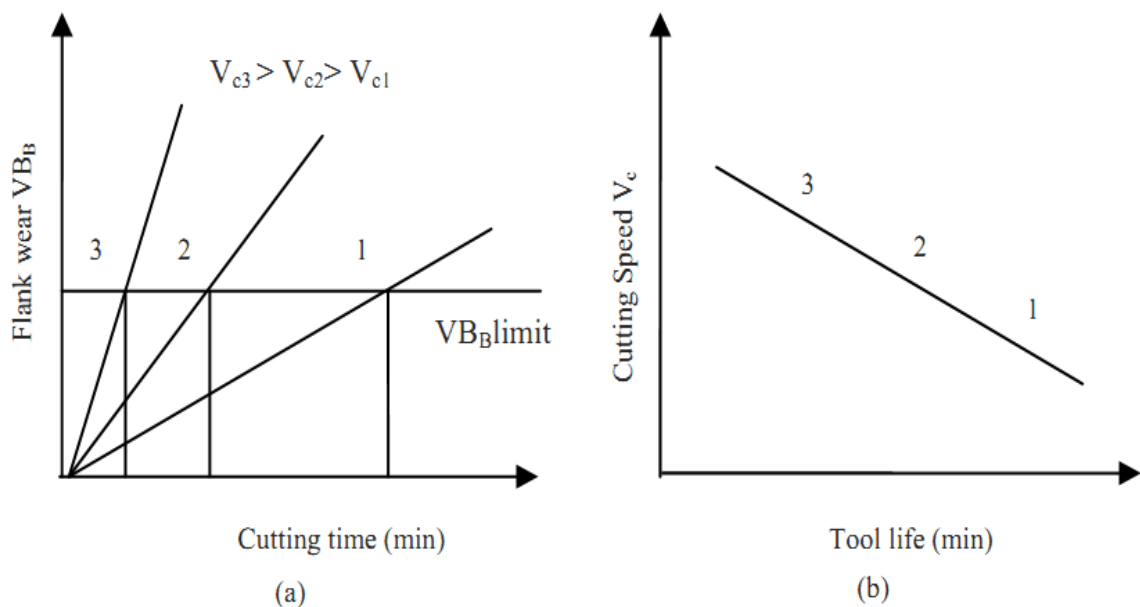


Fig. 1.23: (a) Wear curves for several cutting speeds (1, 2 & 3) and (b) tool life curve

Table 1

HSS tools, roughing	1.50 mm
HSS tools, finishing	0.75 mm
Carbide tools	0.70 mm
Ceramic tools	0.60 mm

1.2.5 EXPANDED TAYLOR'S TOOL LIFE FORMULA:

According to the original Taylor tool life formula, the cutting speed is the only parameter that affects tool life. This is because this formula was obtained using high-carbon and high-speed steels as tool materials. With the further development of carbides and other tool materials, it was found that the cutting feed and the depth of cut are also significant. As a result, the Taylor's tool life formula was modified to accommodate these changes as:

$$V_c T^n f^a d^b = C \quad (1.5)$$

Where d is the depth of cut (mm) and f is the feed (mm/rev). The exponents a and b are to be determined experimentally for each combination of the cutting conditions. In practice, typical values for HSS tools are $n = 0.17$, $a = 0.77$ and $b = 0.37$ [4]. According to this information, the order of importance of the parameters is: cutting speed, then feed, then depth of cut. Using these parameters, Equation (1.5) for the expanded Taylor's tool life formula model can be rewritten as:

$$T = C^{\frac{1}{n}} V_c^{-\frac{1}{n}} f^{\frac{-a}{n}} d^{\frac{-b}{n}} \quad \text{or} \quad T = C^{5.88} V_c^{-5.88} f^{-4.53} d^{-2.18} \quad (1.6)$$

Although cutting speed is the most important cutting parameter in the tool life equation, the cutting feed and the depth of cut can also be the significant factors. Finally, the tool life depends on the tool (material and geometry); the cutting parameters (cutting speed, feed, depth of cut); the brand and conditions of the cutting fluid used; the work material (chemical composition, hardness, strength, toughness, homogeneity and inclusions); the machining operation (turning, drilling, milling), the

machine tool (for example, stiffness, run out and maintenance) and other machining parameters. As a result, it is nearly impossible to develop a universal tool life criterion.

1.2.6 RECENT TRENDS IN TOOL LIFE EVALUATION:

Although Taylor's tool life formula is still in wide use today and lies at the very core of many studies on metal cutting, including at the level of national and inter-national standards, one should remember that it was introduced in 1907 as a generalization of many years of experimental studies conducted in the 19th century using work and tool materials and experimental technique available at that time. Since then, each of these three components has undergone dramatic changes. Tool life is not an absolute concept but depends on what is selected as the tool life criteria. In finishing operations, surface integrity and dimensional accuracy are of primary concern, while in roughing operations the excessive cutting force and chatter are limiting factors. In both applications, material removal rate and chip breaking could be critical factors. These criteria, while important from the operational point of view, have little to do with the physical conditions of the cutting tool. To analyze the performance of cutting tools on CNC machines, production cells and manufacturing lines, the dimension tool life is understood to be the time period within which the cutting tool assures the required dimensional accuracy and required surface integrity of the machined parts. Although there are a number of representations of the dimension tool life, three of them are the most adequate [5].

- The dimension wear rate is the rate of shortening of the cutting tip in the direction perpendicular to the machined surface taken within the normal wear period (region II in Figure 1.21(a)), i.e.,

$$v_h = \frac{dv_r}{dT} = \frac{h_r - h_{r-i}}{T - T_i} = \frac{vh_{l-r}}{1000} = \frac{vfh_s}{100} \quad (\mu m/min) \quad (1.6)$$

Where h_{r-i} and l_i are the initial radial wear and initial length of the tool path, respectively, and l is the total length of the tool path. It follows from Equation

(1.6) that the surface wear rate is reverse proportional to the overall machined area and, in contrast, does not depend on the selected wear criterion.

- The specific dimension tool life is the area of the work piece machined by the tool per micron of radial wear

$$T_{UD} = \frac{dS}{dh_r} = \frac{1}{h_s} = \frac{(l-l_i)f}{(h_r-h_{r-i})100} \quad (10^3 \text{ cm}^2 / \mu\text{m}) \quad (1.6)$$

- The surface wear rate and the specific dimension tool life are versatile tool wear characteristics because they allow the comparison of different tool materials for different combinations of the cutting speeds and feeds using different criteria selected for the assessment of tool life.

1.3: SURFACE ROUGHNESS

1.3.1 SURFACE STRUCTURE OF METALS

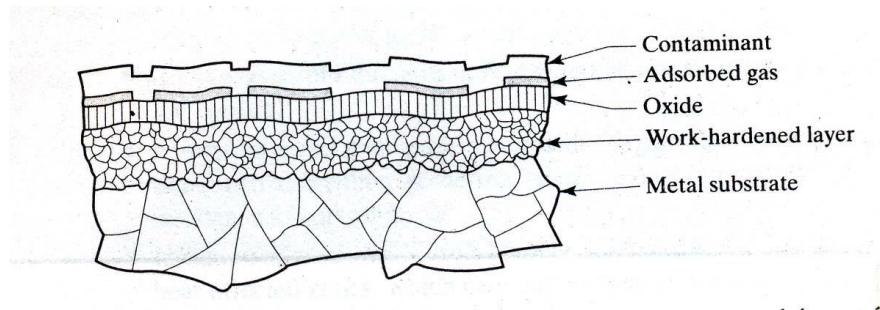


Fig. 1.24: Cross section of surface structure of metals

The characteristics of different layers of the surface of a metal are discussed below:

- The bulk metal, also known as the metal substrate, has a structure that depends on the composition and processing history of the metal.
- Above “metal substrate”, the layer is known as “work-hardened layer”. The depth and properties of the work-hardened layer depend on such factors as the processing method used and how much frictional sliding the surface undergoes. The use of sharp tools and the selection of appropriate processing parameters result in surfaces with little or no disturbance.

Unless the metal is processed and kept in an inert (oxygen-free) environment, or is a noble metal such as gold or platinum, an oxide layer forms over the work hardened layer. Iron has an oxide structure with FeO adjacent to the bulk metal, followed by a layer of Fe₃O₄ and then a layer of Fe₂O₃, which is exposed to the environment. Aluminum has a dense, amorphous (without crystalline structure) layer of Al₂O₃, with a thick, porous hydrated aluminum-oxide layer over it.

- Under normal environmental conditions, surface oxide layers are generally covered with absorbed layers of gas and moisture. Finally, the outermost surface of the metal may be covered with contaminants such as dirt, dust, grease, lubricant residues, cleaning-compound residues, and pollutants from the environment.

1.3.2: FACTORS AFFECTING THE SURFACE ROUGHNESS

Whenever two machined surfaces come in contact with one another the quality of the mating parts plays an important role in the performance and wear of the mating parts. The height, shape, arrangement and direction of these surface irregularities on the work piece depend upon a number of factors such as:

A) The machining variables which include

- a) Cutting speed
- b) Feed, and
- c) Depth of cut.

B) The tool geometry

Some geometric factors which affect achieved surface finish include:

- a) Nose radius
- b) Rake angle
- c) Side cutting edge angle, and
- d) Cutting edge.

C) Work piece and tool material combination and their mechanical properties

D) Quality and type of the machine tool used,

E) Auxiliary tooling, and lubricant used, and

F) Vibrations between the work piece, machine tool and cutting tool.

1.4 : MAGNETIC FIELD

1.4.1: CALCULATION OF MAGNETIC FIELD

The relationship between the fundamental electromagnetic quantities can be expressed by Maxwell's equations, written in the differential or integral form. The general Maxwell's differential equations can be written as:

$$\nabla \times \mathbf{H} = \mathbf{J} + \frac{\partial \mathbf{D}}{\partial t} \quad (1.8)$$

$$\nabla \times \mathbf{E} = -\frac{\partial \mathbf{B}}{\partial t} \quad (1.9)$$

$$\nabla \cdot \mathbf{D} = \rho \quad (1.10)$$

$$\nabla \cdot \mathbf{B} = 0 \quad (1.11)$$

Where \mathbf{H} is magnetic field, \mathbf{J} is current density, \mathbf{D} is electric displacement field, \mathbf{E} is electric field, \mathbf{B} is magnetic flux density and ρ is electric charge density.

Another fundamental equation is the equation of continuity, which can be written as

$$\nabla \cdot \mathbf{J} = -\frac{\partial \rho}{\partial t} \quad (1.12)$$

Constitutive relations describing the macroscopic properties medium are included to obtain a closed system

$$\mathbf{D} = \epsilon \mathbf{E} \quad (1.13)$$

$$\mathbf{B} = \mu \mathbf{H} \quad (1.14)$$

$$\mathbf{J} = \sigma \mathbf{E} \quad (1.15)$$

Where ϵ is the permittivity of the medium, μ is the permeability of the medium and σ is the conductivity of the medium.

At interfaces between 2 media, boundary conditions can be specified to solve the Maxwell's equations as below

$$\mathbf{n}_2 \times (\mathbf{E}_1 - \mathbf{E}_2) = 0 \quad (1.16)$$

$$\mathbf{n}_2 \times (\mathbf{D}_1 - \mathbf{D}_2) = \rho_s \quad (1.17)$$

$$\mathbf{n}_2 \times (\mathbf{H}_1 - \mathbf{H}_2) = \mathbf{J}_s \quad (1.18)$$

$$\mathbf{n}_2 \times (\mathbf{B}_1 - \mathbf{B}_2) = 0 \quad (1.20)$$

Where ρ_s and \mathbf{J}_s denote surface charge density and surface current density, respectively, and \mathbf{n}_2 is the outward normal from the medium 2.

Two of these conditions are independent, one consisting of equations (1.11) and (1.14), and the other consisting of equations (1.12) and (1.13), A consequence of the above is that at the interface:

$$\mathbf{n}_2 \bullet (\mathbf{J}_1 - \mathbf{J}_2) = -\frac{\partial \rho_s}{\partial t} \quad (1.21)$$

These equations can then be used to calculate the theoretical flux densities and current densities to predict the reduction in cutting forces during the turning process.

1.4.2: EDDY CURRENT AND MAGNETIC FORCE

When using the Maxwell's equations, the variations in the currents and charges of the source are more or less synchronized with the variation in the electromagnetic field, except for a slight delay in the field as a result of the propagation speed of electromagnetic waves in the medium. To facilitate the prediction of magnetic field and Lorentz's forces, the delay effect is ignored and stationary current is assumed at every instant. The evaluation of the forces will be presented later. This quasi-static approximation is valid as long as the changes in time are small and the studied geometries are considerably smaller than the wavelength.

The quasi-static approximation implies that the equation of continuity can be rewritten as

$$\nabla \bullet \mathbf{J} = 0 \quad (1.22)$$

The time derivative of the electric displacement $\partial/\partial t$ can be disregarded in the Maxwell-Ampere's Law as well. The Lorentz's force equation, expressing the force \mathbf{F} per unit charge q , with velocity \mathbf{v} relative to the reference system is

$$\mathbf{F}/q = \mathbf{E} + \mathbf{v} \times \mathbf{B} \quad (1.23)$$

This means that to an observer in the moving frame, the force on charge q can be interpreted as caused by the electric field $\mathbf{E}' = \mathbf{E} + \mathbf{v} \times \mathbf{B}$. In a conductive medium, the current density would thus be

$$\mathbf{J} = \sigma(\mathbf{E} + \mathbf{v} \times \mathbf{B}) + \mathbf{J}^e \quad (1.24)$$

Where, \mathbf{J} is externally generated current density. This implies that the Maxwell-Ampere's law can be written as

$$\nabla \times \mathbf{H} = \mathbf{J} = \sigma(\mathbf{E} + \mathbf{v} \times \mathbf{B}) + \mathbf{J}^e \quad (1.25)$$

CHAPTER 2
LITERATURE REVIEW & PRESENT WORK

The researches on tool wear and surface roughness of the work piece and other machinability factors during the machining operation are significant in number. The quality and productivity has a lot of importance in the field of manufacturing which are listed below:

- Keeps costs down to improve profits and reduce the prices.
- Enables firms to spend more on improving customer service and supplementary services.
- Increase repeat purchases from loyal customers.
- Enables a firm to differentiate its offerings.

For years, quality and productivity have been viewed as two important indexes of company performance, especially in manufacturing industries. However, they are always emphasized separately.

To fulfill the need of a certain cutting condition, tool design focuses on the specialized insert. But by designing such specialized tool inserts an extra cost will be added up with the overall manufacturing cost. Moreover it sufficiently complex and specialized training is required to determine the specific insert under a unique cutting condition. The optimization of the cutting processes consists of establishing a simple functional dependency between input process variables such as cutting conditions, tool geometry, etc., and output parameters-amount of tool wear, tool life and thereby adjusting the cutting conditions as required. This trial and error process is usually time consuming and requires constant fine tuning. The other common process depends on the application of hard and thin wear resistant coatings to improve the tool life of inserts. Nevertheless, problems such as sudden failure of coatings and poor adhesion between thin surface coatings and insert material remains to be a challenge.

Tool wear is of many different types and also depend on the type of tool material chosen and the cutting conditions used. For this study, flank wear was measured as the maximum land wear " $V_{B \max}$ ". For continuous turning the maximum tool wear land width ($V_{B \max}$) shows a near linear increase with cutting distance after initial rapid wear. Flank wear typically results due to erosion of the flank face and excessive chipping on flank side of tool. Such flank wear compromises the stability of

the cutting edge, causing reduction dimensional tolerance and tool life, increased roughness, and tool breakage in the extreme case.

It is well accepted that, during machining of steel work materials with WC tools, several wear mechanisms such as abrasion, adhesion, oxidation, diffusion, etc. can operate simultaneously [1, 9-13]. Thus under a given set of machining condition, determination of the dominant wear mechanism is difficult. However, Hastings and Oxley [9] and Opitz and Konig [10] have pointed out that, the most likely dominant wear mechanisms and the corresponding cutting speeds/temperatures are: abrasion at low speeds/temperatures, followed by adhesion at moderate speeds/temperatures and then diffusion at high speeds/temperatures. By superposition of these wear mechanisms; they were able to explain the observed variations of tool wear over a wide range of cutting speeds [9, 10]. That is, the total wear occurring on a tool contact face (e.g. flank face) is equal to the sum of the wear occurring due to the separate effects of all the wear mechanisms. It should be noted that all the wear mechanisms will not occur simultaneously. Moreover, the dominant wear mechanism will depend on the cutting conditions and tool and work materials.

Tool wear reduction has always been always been a focus in research into machining processes. As productivity and cost are closely related to tool life, a small increase in tool life can greatly reduce the amount of machine down time for tool replacements, and also the cost of grinding and resetting the worn tool. Currently, the most common method reducing wear is to separate the surfaces by the use of fluid or solid lubricants. The second general approach is to modify materials and properties by using hard and thin wear-resistant coatings for tools to improve their lifetime. Nevertheless, there are still problems with sudden failures of the coatings and the adhesion between thin surface coatings and tool material remains a challenge[6]. Examples of this would include crating special materials and alloys for cutting tools and also hardened layers at material surfaces. In the paper by Mansori Et. Al. [7, 8], it was shown that beneficial effects on the application of magnetic field in various machining processes has been demonstrated. Many of these experiments often involve application of the magnetic field to both work piece and tool. And studies using pulse and alternating magnetic field were performed as well. However, most of the

machining processes were mostly focused on changing the material properties of the work piece and not the tool insert.

Tool wear, the gradual failure of cutting tools due to regular use, is an inevitable impediment in machining processes [14]. High speed machining uses high cutting speed and feed rate. This produces high temperature in the tool and the work piece. This high temperature not only reduces the tool life but also deteriorates the product quality, thereby affecting directly on the manufacturing cost of the product [15]. However tool life can be improved satisfactorily by using a suitable tool material and proper cutting conditions. So, there can be more number of factors like this which affect the tool wear mechanism during turning operation and this can be controlled in order to improve the tool life [16-19].

The effects of external superimposed electric current with an aim of thermo-electric compensation and consequent improvement in wear resistance of cutting tools have been studied by Bobrovskii [20], Kanji and Pal [21]. In their study an improvement in the tool life has been noticed, but they did not give any detailed reasons for this improvement. Zhou et al. [22] investigated on tool life criteria in raw turning. A new tool-life criterion depending on a pattern-recognition technique was proposed and neural network and wavelet techniques were used to realize the new criterion. The experimental results showed that this criterion was applicable to tool condition monitoring in a wide range of cutting conditions.

Braghini et al [23] studied the wear behavior of Polycrystalline Cubic Boron Nitride (PCBN) and cemented carbide tool in end milling of hardened steels. They found that the minimal wear mechanism was a combination of adhesion and abrasion. It was also stated that wear occurred predominantly on the flank face. Kumar et al [24] investigated the wear morphology of alumina based ceramic tools in the machining hardened stainless steel and found that the flank wear affects the tool wear at lower speed. Ghani et al [25] studied about the performance of TiN coated carbide inserts in semi-finish and finished end milling of hardened tool steel at high cutting speeds. Their results compared the effectiveness of TiAlN inserts under preheated room temperature condition. Once factor in the variation of performance was concluded to be tool wear.

Amin et al. [26] proposed a predictive model for the estimation of tool life under different cutting conditions in end milling of tool steel using TiAlN (Titanium Aluminium Nitride). In their investigation on tool wear, Takeyama and Murata [27] studied that the amount of tool flank wear is given by abrasive wear thermal diffusion. They considered abrasive wear to be proportional to the cutting distance and independent of tool temperature. Thermal diffusion was considered to be temperature dependent. Tool temperature and tool life results were obtained when machining steel and cast iron using P10 grade WC tools. It has been noticed that the experimental results for temperature above 800° C could be represented well by equations thus indicating that wear of tested tools was dominated by diffusion. Muju and Radhakrishna [28] proposed a generalization of the model represented by Muju and Ghosh [29-31] using a more fundamental approach by taking into account the influence of the temperature. The conclusion of the generalized model were that the application of a magnetic field to a contacting pair reduces the activation energy of wear and diffusion and is advantageous only when (H_2/H_1) is greater than or equal to 0.2, where H_1 and H_2 are the hardness's of the bodies with the lowest and highest magnetic permeability, respectively.

Muju and Ghosh [29-31] presented a physical model to explain some results obtained when conducting tool wear experiments with magnetized HSS turning tools on mild steel and brass. The wear experiments consisted of the use of mild steel tools to cut aluminium. Additional tests with the mild steel tools rubbing against brass and mild steel were also performed. The tools were magnetized using a d.c. source and an auxiliary tool was used to keep the machined surface fresh. In their observations, they found an increase in tool life by approximately 40% and a reduction of the size of wear particles, but no phase change. The authors discussed the effects of an external magnetic field from a mechanical point of view. Their analysis was performed as a phenomenological approach based on dislocation mobility during a two-body interaction in the presence of an external magnetic field. To establish a physical model, the authors assumed the uniformity of dislocation density and velocity. However, the repulsion and the temperature effect on dislocations are neglected. Predictions of the proposed model confirm that the magnetic field influences the

adhesive wear behavior in such a way as to reduce the wear rate of the body with the lowest magnetic permeability.

Oxley [32] and Arsecularatne [33-34] studied about the change in tool life in combination with the temperature. When compared with empirical methods, the theoretical method appears far more effective in predicting tool life as it allows tool geometrical parameters and cutting conditions to be combined into the single parameter of temperature. This approach was initially applied to orthogonal and oblique conditions with plane face tools investigated by Trent et al [2]. Later it was extended to tools with restricted contact and commercial chip grooves with considerable success carried out by Kitagawa et al [35]. In these investigations carried out by the authors mentioned above, diffusion was considered to be the dominant tool wear mechanism. Trent et al. [2] and Hastings et al. [9] investigated that when machining steel work materials, these mechanisms are unlikely to be dominant under the conditions normally used in practice (i.e. at relatively high cutting speeds). This is due to- the insufficient amount of abrasions present in the work piece, insufficient hardness of abrasives to abrade WC and inability to detect any significant signs of abrasive wear in extensive metallurgical studies. However, there are certain conditions under which abrasive wear of WC tools have been observed.

Kitagawa et al. [35] studied that, under practical conditions, wear of WC tools was due to adhesion, that wear rate could be represented by a relation and that wear should increase with the normal stress on the tool flank. This is one of the major drawbacks of these studies since reliable experimental results or an analytical method to determine this stress is not yet available. Another is that the predicted results indicate elastic contact at flank/work interface in spite of experimental evidence of plastic contact investigated by Trent and Wright [2]. Iwata et al. [36] showed that adhesion between WC and steel (hence adhesive wear rate) becomes a maximum at 600° C and thereafter falls off rapidly with further increase in temperature.

Choudhury and Bartarya [37] focused on design of experiments and the neural network for prediction of tool wear. The input parameters were cutting speed, feed and depth of cut; flank wear, surface finish and cutting zone temperature were selected as outputs. Empirical relation between different responses and input variables

and also through neural network (NN) program helped in predictions for all the three response variables and compared which method was best for the prediction.

Chien and Tsai [38] developed a model for the prediction of tool flank wear followed by an optimization model for the determination of optimal cutting conditions in machining 17-4PH stainless steel. The back-propagation neural network (BPN) was used to construct the predictive model. The genetic algorithm (GA) was used for model optimization.

Bagchi and Ghosh [39-40] seem to be the first investigators to have studied the effect of an EMF created by a magnetic field on the wear characteristics of cutting HSS tools while machining mild steel. Flank wear was measured and a wear gain factor (wear decrease) due to the applied magnetic field was considered. They found that within the range of speeds investigated, the gain factor was always found to be positive. This improvement depended both on magnetic field intensity and cutting speed although there were particular cutting speeds at which the extended tool life was maximum, irrespective of field intensity. To provide some reasons of why a magnetized cutting tool has greater life, Chakrabarti proposed a qualitative model in which he assumed a physical reorientation of the elements of the magnets [41]. Although the results of the modeling analysis were encouraging, the model itself was subject to question. Two years later, Pal and Gupta [42] investigated the effect of an alternating magnetic field on the wear behavior of HSS drills in drilling gray cast iron and malleable cast iron under dry cutting condition. In the case of gray iron, the alternating magnetic field was applied both on tool and work piece simultaneously using a solenoid. In drilling malleable iron, the same solenoid was used but instead of encircling the job, it was placed on top of the SG iron block so that the magnetic field was mainly applied on the tool. The authors observed that considerable increase in the tool lifetime has been achieved for both test configurations. Mansori et al. studied the magnetic field effect on the HSS tool durability during machining [43]. Cutting tests consisted of turning experiments to establish some relation between the applied magnetic field intensity and the HSS tool durability. The tool durability was defined as the necessary time for the outage (catastrophic failure criteria) of the cutting tool during machining. In their study, it has been observed that high values of tool

durability at a higher level of magneto-mechanical excitation which is characterized by higher magnetic field intensities and cutting speed.

Kumanan et al. [44] proposed the methodology for prediction of machining forces using multi-layered perceptron trained by genetic algorithm (GA). The data obtained from experimental results of a turning process were explored to train the proposed artificial neural networks (ANNs) with three inputs to get machining forces as output. The optimal ANN weights were obtained using GA search. This function-replacing hybrid made of GA and ANN was found computationally efficient as well as accurate to predict the machining forces for the input machining conditions.

Mahmoud and Abdelkarim [45] studied on turning operation using High-Speed Steel (HSS) cutting tool with 45° approach angle. This tool showed that it could perform cutting operation at higher speed and longer tool life than traditional tool with 90° approach angle. The study finally determined optimal cutting speed for high production rate and minimum cost, tool life, production time and operation costs.

Natarajan et al. [46] presented the on-line tool wear monitoring technique in turning operation. Spindle speed, feed, depth of cut, cutting force, spindle-motor power and temperature were selected as the input parameters for the monitoring technique. For finding out the extent of tool wear; two methods of Hidden Markov Model (HMM) such as the Bar-graph Method and the Multiple Modeling Methods were used. A decision fusion centre algorithm (DFCA) was used for increasing the reliability of this output which combined the outputs of the individual methods to make a global decision about the wear status of the tool. Finally, all the proposed methods were combined in a DFCA to determine the wear status of the tool during the turning operations.

Srikanth and Kamala [47] evaluated optimal values of cutting parameters by using a Real Coded Genetic Algorithm (RCGA) and explained various issues of RCGA and its advantages over the existing approach of Binary Coded Genetic Algorithm (BCGA). They concluded that RCGA was reliable and accurate for solving the cutting parameter optimization and construct optimization problem with multiple

decision variables. These decision variables were cutting speed, feed, depth of cut and nose radius. The authors highlighted that the faster solution can be obtained with RCGA with relatively high rate of success, with selected machining conditions thereby providing overall improvement of the product quality by reduction in production cost, reduction in production time, flexibility in machining parameter selection.

The productivity of a machining operation is not only determined by the use of low cost-high performance but also by the capability to transform specific steel alloys to the required surface finish and geometry by machining at sufficiently high speed. Surface roughness is the dimensional accuracy of the finished product and is one of the most important quality requirements of the finished product. Therefore in most machining situations, minimization of surface roughness is a prime issue which is carried out by optimizing the machining process parameters in order to attain minimal surface roughness.

Lin et al. [48] adopted an additive network to construct a prediction model for surface roughness and cutting force. Once the process parameters: cutting speed, feed rate and depth of cut were given; the surface roughness and cutting force could be predicted by this network. Regression analysis was also adopted as second prediction model for surface roughness and cutting force. Comparison was made on the results of both models indicating that additive network was found more accurate than that by regression analysis. Investigation was also carried out for the prediction of surface roughness in finish turning operation by developing an empirical model through considering working parameters: work piece hardness (material), feed, cutting tool point angle, depth of cut, spindle speed, and cutting time. Data mining techniques, nonlinear regression analysis with logarithmic data transformation were employed for developing the empirical model to predict the surface roughness.

Lee and Chen [49] highlighted on artificial neural networks using a sensing technique to monitor the effect of vibration produced by the motions of the cutting tool and work piece during the cutting process developed an on-line surface recognition system. The authors employed tri-axial accelerometer for determining the direction of vibration that significantly affected surface roughness.

Kirby et al. [50] developed the prediction model for surface roughness in turning operation. The regression model was developed by a single cutting parameter and vibrations along three axes were chosen for in-process surface roughness prediction system. By using multiple regression and Analysis of Variance a strong linear relationship among the parameters (feed rate and vibration measured in three axes) and the response (surface roughness) was found. The authors demonstrated that spindle speed and depth of cut might not necessarily have to be fixed for an effective surface roughness prediction model.

Özel and Karpaz [51] studied for prediction of surface roughness and tool flank wear by utilizing the neural network model in comparison with regression model. The data set from measured surface roughness and tool flank wear were employed to train the neural network models. Predictive neural network models were found to be capable of better predictions for surface roughness and tool flank wear within the range in between they were trained. They also carried out theoretical and experimental studies to investigate the intrinsic relationship between tool flank wear and operational conditions in metal cutting processes using carbide cutting inserts. The authors developed the model to predict tool flank wear land width which combined cutting mechanics simulation and an empirical model. The study revealed that cutting speed had more dramatic effect on tool life than feed rate.

Sing and Kumar [52] studied on optimization of feed force through setting of optimal value of process parameters namely speed, feed and depth of cut in turning of EN24 steel with TiC coated tungsten carbide inserts. The authors used Taguchi's parameter design approach and concluded that the effect of depth of cut and feed in variation of feed force were affected more as compare to speed.

Ahmed [53] developed the methodology required for obtaining optimal process parameters for prediction of surface roughness in Aluminium turning. For development of empirical model nonlinear regression analysis with logarithmic data transformation was applied. The developed model showed small errors and satisfactory results. The study concluded that low feed rate was good to produce reduced surface roughness and also the high speed could produce high surface quality within the experimental domain.

Abburi and Dixit [54] developed a knowledge-based system for the prediction of surface roughness in turning process. Fuzzy set theory and neural networks were utilized for this purpose. The authors developed rule for predicting the surface roughness for given process variables as well as for the prediction of process variables for a given surface roughness.

Zhong et al. [55] predicted the surface roughness of turned surfaces using networks with seven inputs namely tool insert grade, work piece material, tool nose radius, rake angle, depth of cut, spindle rate, and feed rate.

Doniavi et al. [56] used response surface methodology (RSM) in order to develop empirical model for the prediction of surface roughness by deciding the optimum cutting condition in turning. The authors showed that the feed rate influenced surface roughness remarkably. With increase in feed rate surface roughness was found to be increased. With increase in cutting speed the surface roughness decreased. The analysis of variance was applied which showed that the influence of feed and speed were more in surface roughness than depth of cut.

Kassab and Khoshnaw [57] examined the correlation between surface roughness and cutting tool vibration for turning operation. The process parameters were cutting speed, depth of cut, feed rate and tool overhanging. The experiments were carried out on lathe using dry turning (no cutting fluid) operation of medium carbon steel with different level of aforesaid process parameters. Dry turning was helpful for good correlation between surface roughness and cutting tool vibration because of clean environment. The authors developed good correlation between the cutting tool vibration and surface roughness for controlling the surface finish of the work pieces during mass production. The study concluded that the surface roughness of work piece was observed to be affected more by cutting tool acceleration; acceleration increased with overhang of cutting tool. Surface roughness was found to be increased with increase in feed rate.

Al-Ahmari [58] developed empirical models for tool life, surface roughness and cutting force for turning operation. The process parameters used in the study were

speed, feed, depth of cut and nose radius to develop the machinability model. The methods used for developing aforesaid models were Response Surface Methodology (RSM) and neural networks (NN).

Sahoo et al. [59] studied for optimization of machining parameters combinations emphasizing on fractal characteristics of surface profile generated in CNC turning operation. It was concluded that feed rate was more significant influencing surface finish in all three materials. It was observed that in case of mild steel and aluminium feed showed some influences while in case of brass depth of cut was noticed to impose some influences on surface finish. The factorial interaction was responsible for controlling the fractal dimensions of surface profile produced in CNC turning.

Wang and Lan [60] used Orthogonal Array of Taguchi method coupled with grey relational analysis considering four parameters viz. speed, cutting depth, feed rate, tool nose run off etc. for optimizing three responses: surface roughness, tool wear and material removal rate in precision turning on an ECOCA-3807 CNC Lathe. The MINITAB software was explored to analyze the mean effect of Signal-to-Noise (S/N) ratio to achieve the multi-objective features. This study not only proposed an optimization approaches using Orthogonal Array and grey relational analysis but also contributed a satisfactory technique for improving the multiple machining performances in precision CNC turning with profound insight.

Biswas et al. [61] studied that on-line flank wear directly influenced the power consumption, quality of the surface finish, tool life, productivity etc. The authors developed a model for prediction of the tool wear. From the orthogonal machining of aluminium with high-speed steel tool for various rake angles, feed and velocity the experimental data were obtained and input along with other machining parameters ratio between cutting force and tangential forces was collected. These were used to predict the tool wear. The final parameters of the model were obtained by tuning the crude values obtained from mountain clustering method by using back-propagation learning algorithm and finally predicted the flank wear with reasonable accuracy and proved it to be a potent tool in estimating flank wears on-line.

In his study, Kang T. Y. [62] has shown the improvement of tool life with the application of external electromagnetic force. His study extended to the measurement of the cutting force at the cutting contact point during the machining operation when electromagnetic force is applied. The study emphasizes on the increase in tool life with higher intensity in the magnetic field. The author has also investigated the effect of changing the pole orientation of the magnetic field.

Patwari et al [63] investigated the effect of the magnetic field created by a permanent magnet on the machinability factors such as tool wear, surface roughness and chip morphology. This study shows a significant improvement in the above mentioned machinability factors.

SCOPE OF THE PRESENT WORK:

This literature review gives the idea of the vast amount of works that have been done in the field of manufacturing in order to achieve the improvement in the machinability factors. All of the researches carried out on the field of magnetic cutting have shown a significant improvement of tool life, surface roughness and other machinability factors during turning operation. However an elaborate study combining the optimization and the orientation of the magnetic field lines have not yet been studied. The use of magnetic treatment to improve the tool life of inserts has much economic importance. The treatment usually involves low intensity, easy to produce and control magnetic field that are applied at room temperature. The use of magnetic field during machining operation is still not widely appreciated and is underexploited in today's industry. Hence the main objective of this study is to find an optimum orientation of magnetic field that will result in an improvement in tool life, surface roughness and other machinability factors and thereby reducing the total manufacturing cost.

CHAPTER 3

DETAILS OF EXPERIMENTATION

3.1 : INTRODUCTION

Primarily the experiment is carried out to study the effect of electromagnetic field on turning operation. Suitable result obtained in the machinability compared to normal cutting condition which suggested us to further experimentation on various design. During experimentation the effect of three different designs of electromagnets i.e changing the orientation of electromagnetic field lines for different machinability parameter such as tool wear, surface roughness, temperature profile, cutting force etc has observed.

3.2 : EXPERIMENTAL SET UP

3.2.1 : DESIGN 1 ELECTROMAGNET

This design magnetizes the tool holder, so the chips get attached to the holder and damages the surface. Chips around the insert also obstacle smooth cutting. However at high rpm when it is difficult for the chips to get attached, we got better result in tool life with this design.

In the following figure the set up is shown.

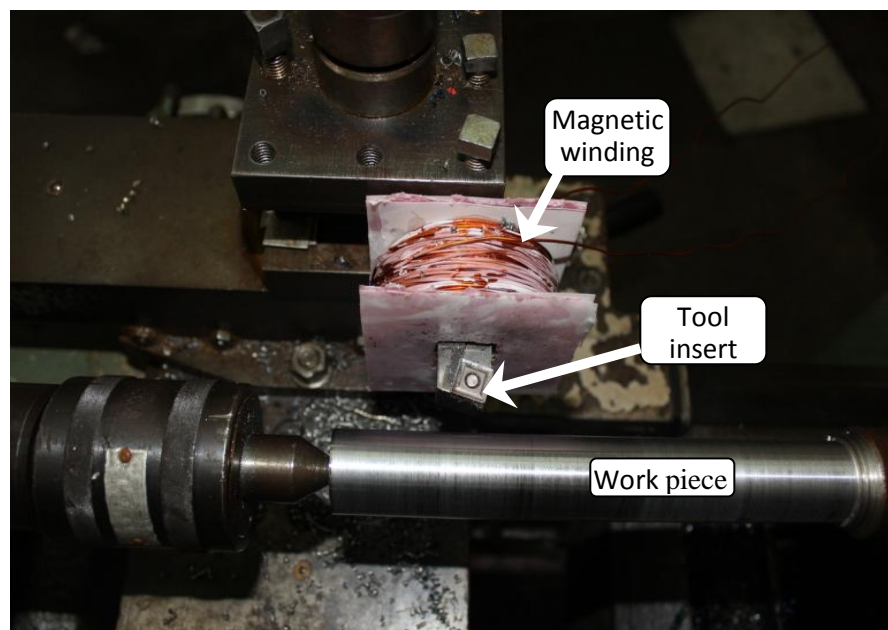


Fig. 3.1 : Experimental set up with the first design of electromagnet

Here the tool is magnetized. Controlled supply of electricity from an external source ensures constant magnetism during the cutting process.

3.2.2 : DESIGN 2 ELECTROMAGNET

This Design has a very strong magnetic field. Here also the chips create problem. The magnets on the tool holder are not in a stable position due to huge amount of chips attached to it which might result in difficulties in getting a smooth trend.

In this design two magnets is placed in the two opposite side of the tool holder. Here current entrance is maintained i.e. pole directions is given priority. During each cutting the pole direction was maintained same.

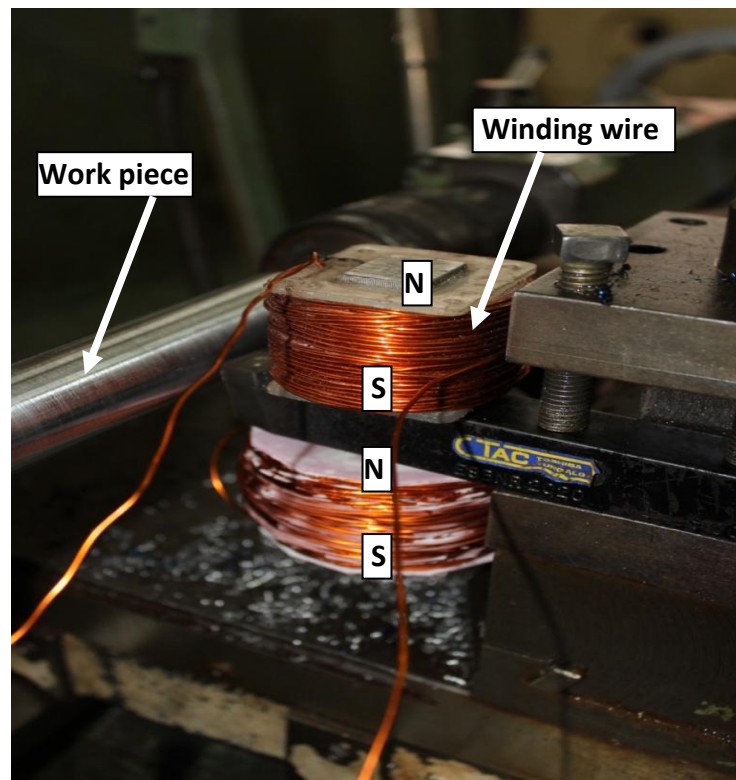


Fig. 3.2: Experimental setup of the second design of electromagnet

3.2.3 : DESIGN 3 ELECTROMAGNET

This electromagnet has been designed mainly to concentrate all the magnetic flux lines over the tool holder. The transformer core consisting of laminated iron plates minimizes the loss of magnetism in the core due to eddy current. Beside this the escape of the field lines in the surrounding air is greatly reduced. It does not move from its position even if there are huge amount of chips attached to it. Chips get attached to the side, not around the tool holder.

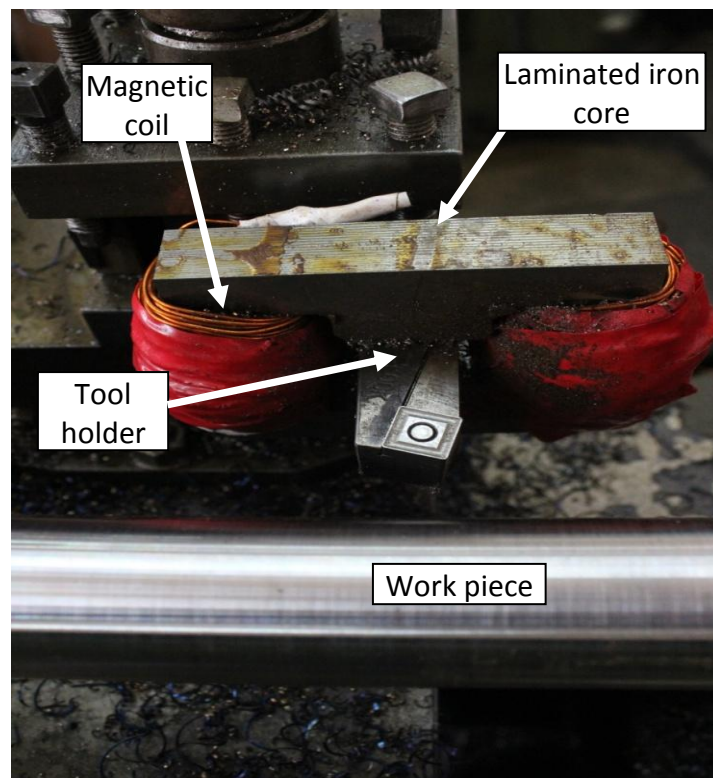


Fig. 3.3 : Experimental setup of the third design of electromagnet

The core shown in the figure consists of 37 plates having 300 copper wire turns in each side. Controlled current is supplied from an external source to maintain constant magnetism.

The specification of copper wire used to make all three designs of electromagnets is SWG 19 having a diameter of 1.02 mm.

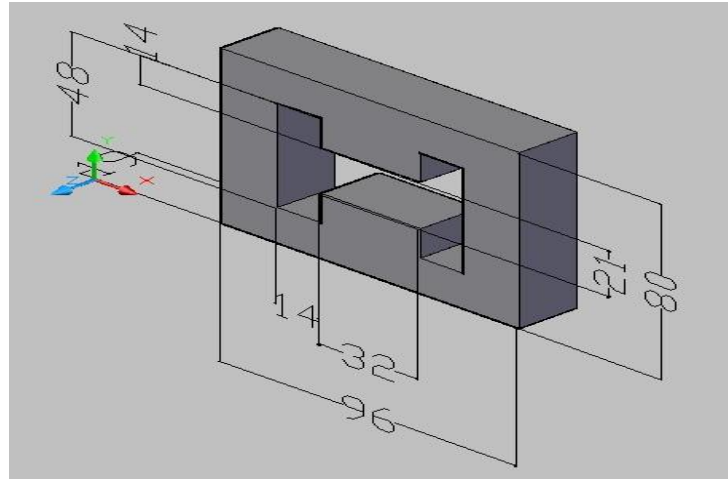


Figure: 3.4 CAD Model of the core of electromagnet

3.3 : MACHINING PARAMETERS

In any basic turning operation speed, feed and depth of cut are the three primary factors. Though there are some other parameters that influence the cutting condition such as kind of material, tool material, coolant used but these three are the ones which can be changed by adjusting the controls in the machine.

Feed has been kept constant throughout the experiment. The changing cutting parameters used in this experiment are the cutting speed and the depth of cut.

The kind of speed in turning operation is rotational and it is expressed in revolution per minute (rpm). The important feature for a particular turning operation is the surface speed or the speed at which the work piece material is moving past the cutting tool. It is simply the product of the rotating speed times the circumference of the work piece before the cut is started.

Though rpm can be fixed by the desire of operator but there are some limitations of using it. The lathe used for the experiment allows 9 different rpm to be used during turning operation.

Feed always refers to the cutting tool, and it is the rate at which the tool advances along its cutting path. On most power-fed lathes, the feed rate is directly related to the spindle speed and is expressed in mm (of tool advance) per revolution (of the spindle), or mm/rev. Lathe machine allows feed to be fixed by operator and different charts having variable value of feed is written in the body of the machine.

Depth of cut refers to the amount of material that is to be removed in each cutting (in a single pass of the cutting tool). It is the thickness of the layer being removed from the work piece or the distance from the uncut surface of the work to the cut surface. It is expressed in mm.

Operator fixes the depth of cut by rotating the circular scale attached in the carriage of the lathe machine. Once it is fixed, the tool is allowed to move axially past the job piece and it removes the given distance around the job piece as long as it is in action.

3.4 : EXPERIMENTAL DETAILS

The scope and objectives of the present work have already been mentioned in the previous chapter. Accordingly the present study has been done through the following plan of experiment.

- One particular lathe is selected for carry out whole operation.
- Checking and preparing the centre lathe before starting operation.
- Cutting MS bars of desired length by power saw and to fix it in the three jaw chuck.
- Performing facing and centre drilling of job piece for fixing it in between chuck and tail stock.
- Performing straight turning operation on specimens in various cutting environments involving various combinations of process control parameters like: spindle speed, feed, depth of cut and magnetic field.
- Measuring tool flank wear using microscope and image processing.
- Determining surface roughness using image processing algorithms in MATLAB or using scopetech software.
- Collecting chip in each condition and calculating chip serration frequency.
- Analysis and comparison of collected data.

The whole process of the experimentation can be shown as the flowchart given below:

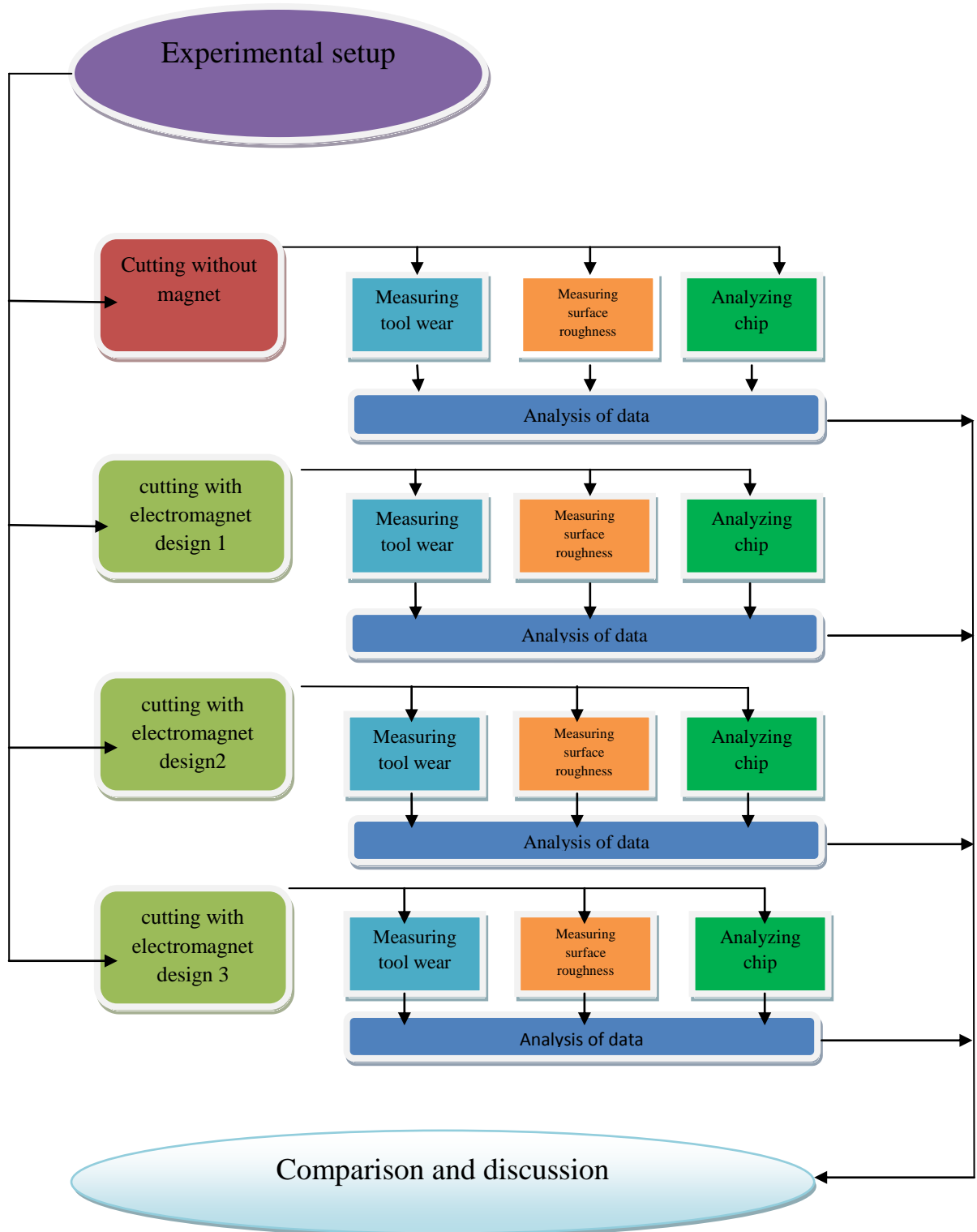


Fig 3.5: Flow sequence of the experimentation

3.5 : PROCESS VARIABLES AND THEIR VALUES

In the present experimental study, spindle speed, feed rate and depth of cut have been considered as process variables. The process variables with their units (and notations) are listed in Table 3.2

Process Variables		
Spindle Speed (N) (RPM)	Feed (f) (mm/sec)	Depth of cut (D) (mm)
530	1.0	0.5, 0.75, 1.0
860	1.0	0.5, 0.75, 1.0
1400	1.0	0.5, 0.75, 1.0

Table: 3.1 Process variables and their values

3.6 : EQUIPMENT USED

3.6.1 : CENTER LATHE

The turning machines are, of course, every kind of lathes. Lathes used in manufacturing can be classified as engine, turret, automatics, and numerical control etc. They are heavy duty machine tools and have power drive for all tool movements. They commonly range in size from 12 to 24 inches swing and from 24 to 48 inches center distance, but swings up to 50 inches and center distances up to 12 feet are not uncommon. Many lathes are equipped with chip pans and built-in coolant circulating system. The lathe used in this study is

Manufactured by: GATE INC. (United Kingdom)

Model: L-1/180

3.6.2 : OPTICAL MICROSCOPE

The model of the microscope used for the DIP technique is Metallurgical Microscope MMB2300. Figure 3.3 and table 3.3 give more details of the microscope.

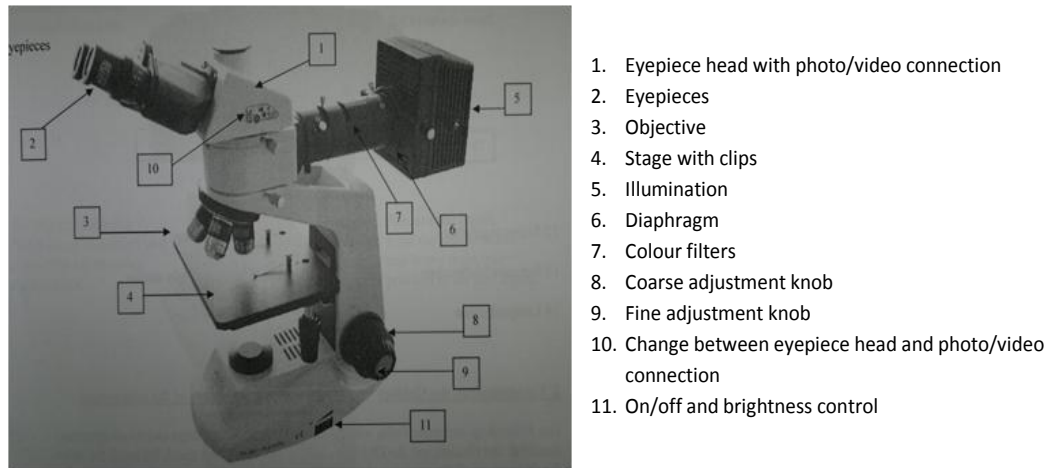


Figure: 3.6 Photograph and details of the optical microscope

Plano eyepieces	10X
Lenses	Plan achromatic 4X,10X,40X
Magnification	40 to 400
Filter	Blue
Power supply	90 to 240 VAC
Fuse	3.15 A
Illumination	Built in lamp 6V 30W, bright-field condenser
Stage moving range	132 x 140 mm
Photo-/video-mounting	Photo-adapter with eyepiece Video-adapter with eyepiece
Weight	10kg net, 15kg cross

Table: 3.3 Detail specification of the microscope

Optical microscope is used to take the image of wear of the tool insert, surface roughness and chip structure. Image processing software is used to capture the microscopic view and the image taken and saved in the laptop for further analysis. The microscope along with the laptop used during the experiment is shown below

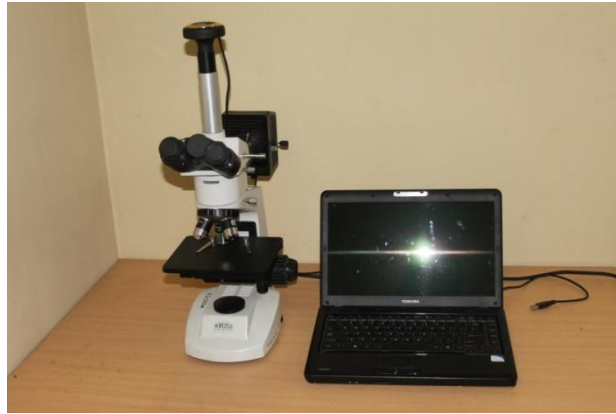


Fig 3.7: Optical microscope connected with laptop for taking image.

3.7.3 : WORK PIECE USED

Mild steel shafts (Diameter 40mm and length 250mm) were used as the work piece material of the experiments. The steel contains 0.25% Carbon and little impurities.

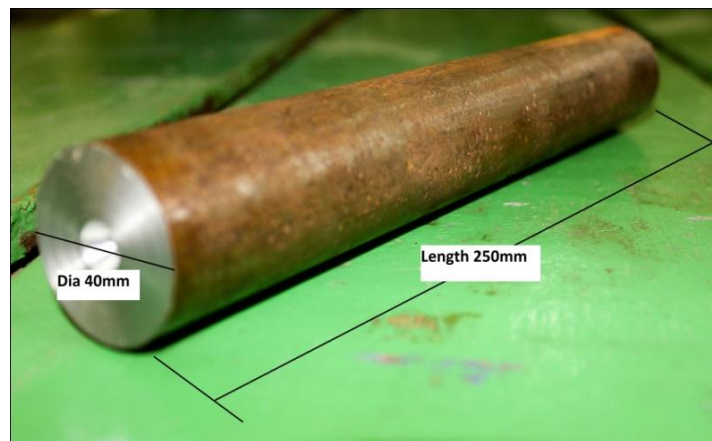


Figure: 3.8 Work piece

Shaft length: 250 mm

Cutting length: 200 mm each time (total 5 times i.e. 1000mm for one side of insert)

Shaft diameter: 40 mm

Shaft material: mild steel

3.6.4 : CUTTING TOOL USED:

Tool: Tungsten carbide coated insert

Model: TX 20

Dimension: 10mm ×10mm ×5mm

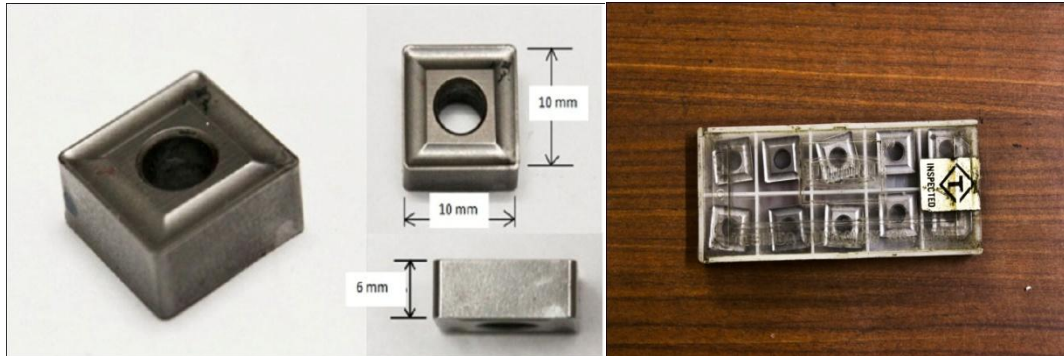


Figure: 3.9 Insert with dimension

3.6.5 : MECHANISMS USED FOR ELECTROMAGNET

An electromagnet is a type of magnet in which the magnetic field is produced by the flow of electric current. An electric current flowing in a wire creates a magnetic field around the wire. To concentrate the magnetic field, in an electromagnet the wire is wound into a coil with many turns of wire lying side by side. The magnetic field of all the turns of wire passes through the centre of the coil, creating a strong magnetic field there. A coil forming the shape of a straight tube is called a solenoid. Much stronger magnetic fields can be produced if a "core" of ferromagnetic material, such as soft iron, is placed inside the coil. The ferromagnetic core increases the magnetic field to thousands of times the strength of the field of the coil alone, due to the high magnetic permeability (μ) of the ferromagnetic material. This is called a ferromagnetic-core or iron-core electromagnet.

The material of the core of the magnet (usually iron) is composed of small regions called magnetic domains that act like tiny magnets. Before the current in the electromagnet is turned on, the domains in the iron core point in random directions, so their tiny magnetic fields cancel each other out, and the iron has no large scale magnetic field. When a current is passed through the wire wrapped around the iron, its magnetic field penetrates the iron, and causes the domains to turn, aligning parallel to

the magnetic field, so their tiny magnetic fields add to the wire's field, creating a large magnetic field that extends into the space around the magnet. The larger the current passed through the wire coil, the more the domains align, and the stronger the magnetic field is. Finally all the domains are lined up, and further increases in current only causes slight increases in the magnetic field; this phenomenon is called saturation.

In this study three different design of electromagnet is constructed which are shown earlier on experimental setup. For each magnet same source of electricity is used. An electrical circuit has to be made in order to convert 220 volt ac voltage to 12 volt dc voltage. The circuit constructed is shown below.

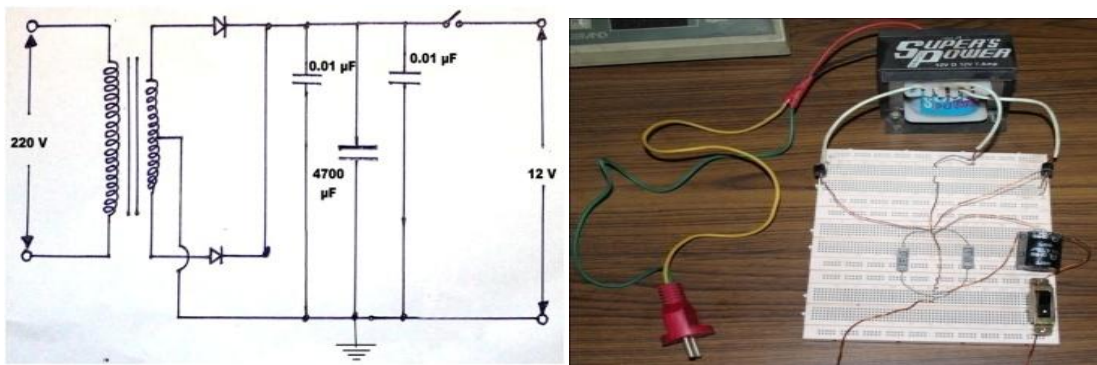


Figure: 3.10 Electrical Circuit to produce electromagnetic field

3.7 : MEASUREMENT TECHNIQUE USED IN THIS STUDY

3.7.1 : MEASUREMENT OF TOOL WEAR

The sequence used in the analysis is illustrated by figure 3.10 below. The flank wear observed were always hemispherical in shape and thus, utilization of image processing for wear analysis was possible.

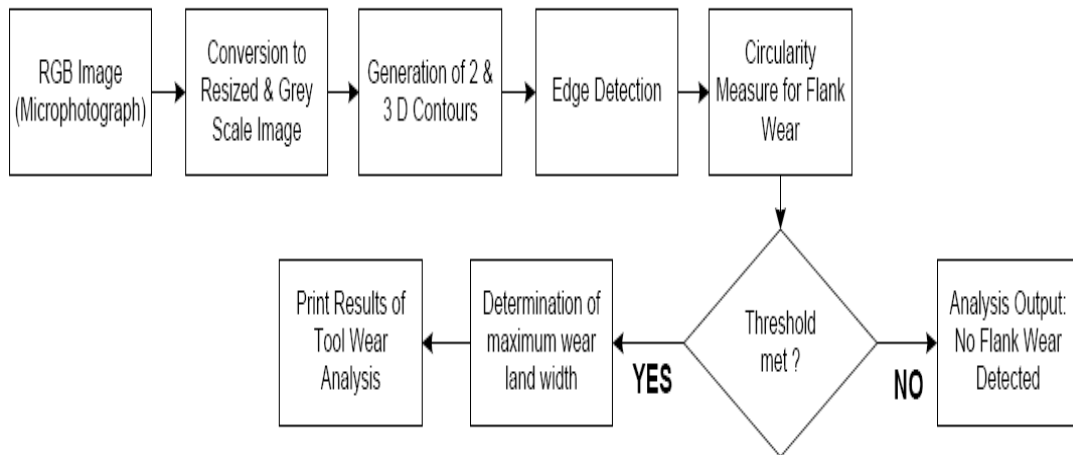


Figure: 3.11 Process logic sequence flowchart for measuring tool wear

Digital image processing comprises the application of computer algorithm and logic to process and analyze digitized images. It is a subcategory of digital signal processing and has many advantages over analog image processing, such as: application of a wider range of algorithms to the input data and avoidance of signal distortion build-ups. An additional advantage is that images are defined over two or more dimensions, in digital image processing, and thus, can be easily modeled in the form of multidimensional systems in software dealing with Matrices, like MATLAB. For their analysis, the authors used MATLAB 2008a image processing toolbox, which can efficiently process the samples' images, in n by m 2-D matrices form.

The microphotograph of interest, obtained at 10x zoom, was obtained and saved as an RGB digital image. The image is subsequently resized and converted to grayscale for standardization in comparison and reducing the calculation load by a third, respectively. The surface topography and contour, in 2 and 3-D respectively, were then generated using the algorithm developed by Patwari et al. [64].

The resized grayscale image was then analyzed for edge detection. The sharp edge of the tool, defined by the principal and auxiliary flank surfaces, was clearly identified by the algorithm along with the measure of its uniform straightness. The algorithm then was then used to detect and evaluate the circularity of the flank wear, which manifests as small craters. The principal axis of the crater was then determined in number of pixels. This pixel information along with the edge detection and original

tool dimensions were then used to calculate the maximum flank wear land width, „ V_{Bmax} ,“ in millimeters.

The results of the wear analysis are then compared by the software against a ‘threshold’ land wear value, obtained from Patwari et al. [64] work, to determine whether the wear is a flank wear. This is achieved by a decision subroutine in the software. The utility of this screening process for flank wear is that most tools display other types of wear such as: built-up edge, rake wear, and edge wear etc. which are not very significant to cutting edge stability. Depending upon the evaluation of the decision subroutine, the software outputs either that ‘no flank wear is detected’ or that ‘flank wear detected’ along with the calculated value of land wear V_{Bmax} . The same analysis was conducted for eight different lengths of cut and compared with the results obtained by Patwari et al. [64].

A new measure, called the circularity metric ‘ CM ’, was developed to detect and analyze flank tool wear land width V_B . The metric evaluates the extent to which feature in the tool’s image is circular and decides that it is a flank wear if the metric threshold of 0.80 was reached. Once the wear is detected the algorithm then determines the length of the wears principal axis in pixels; which is subsequently converted to millimeters by the process already mentioned above. Equation (1), below, is the mathematical definition of the circularity metric used.

$$CM = \frac{4\pi(area)}{(Perimeter)^2} \quad (3.1)$$

Figure 3.13, below, shows the sample results of image processing for tool (with flank wear) used for turning with length of cut 800 mm.

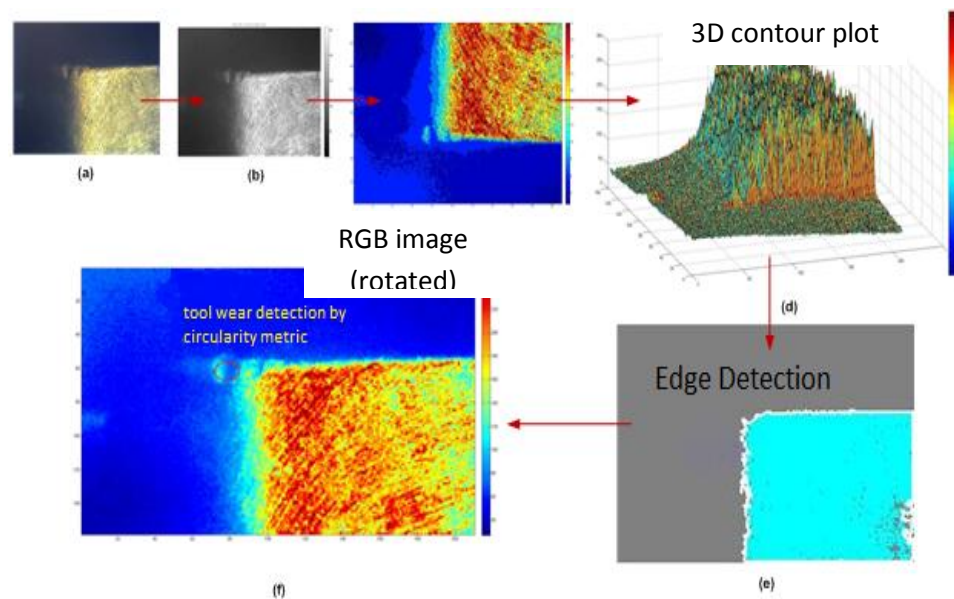


Figure: 3.12 Image processing result sample for measuring tool wear [64]

Another method used in case of measuring some image of tool wear was the software named scopetek. The measurement of tool wear using this software is described below.

1. The image of the tool wear that is to be measured is opened in the window.
2. From the layout bar new layer is selected.
3. Then from the bar we have to go in draw option. Here we have to select vertical line.
4. Now putting the cursor on the image will allow drawing vertical line. The vertical line drawn upon the wear will give the measurement of the tool wear in pixel.
5. This value is then converted to mm using a standard converter.

3.7.2 : MEASUREMENT OF SURFACE ROUGHNESS

The image processing technique for determining surface roughness is described below:

1. Optical microscope was used to take the image of surface roughness after cutting 1000 mm length of work piece.
2. The work piece was cut by power saw to make it small so that it can be placed under the eyepiece of the microscope and can be focused.

3. Same magnification and illuminating conditions were used for maintaining same quality and environment in all photographs
4. The photographs are converted to grey scale and then to binary images in order to speed up the calculation process. As the process is dependent on the intensity of the reflected light from the surface to the microscope it is convenient to convert the image to grayscale image in order to compare the intensity of each point with others. The binary image stores the values of each point as binary values. This way it is easier to analyze the image later.
5. The binary images are then analyzed using a digital image processing algorithm to generate profile plot and colored contour plot.
6. First the program adds up all the values of each point over the whole region and then finds out the average value. This average value is the average surface roughness of the work piece.
7. Then a profile plot is generated by plotting the average value of light intensity on each plane against distance. This helps to understand the waviness of the surface in two dimensional views.
8. Next a colored contour plot of the whole region is generated to observe the location of peak points and bottom points. The contour color map thus gives an overall idea of the surface quality.
9. Finally a 3D contour plot of the surface is generated for the whole region to reconstruct the real surface in the software. This 3D contour plot represents as the 3D model of the actual surface that has been taken in the study.

The whole sequence is illustrated by the following flowchart (figure 3.14) and by figure 3.15.

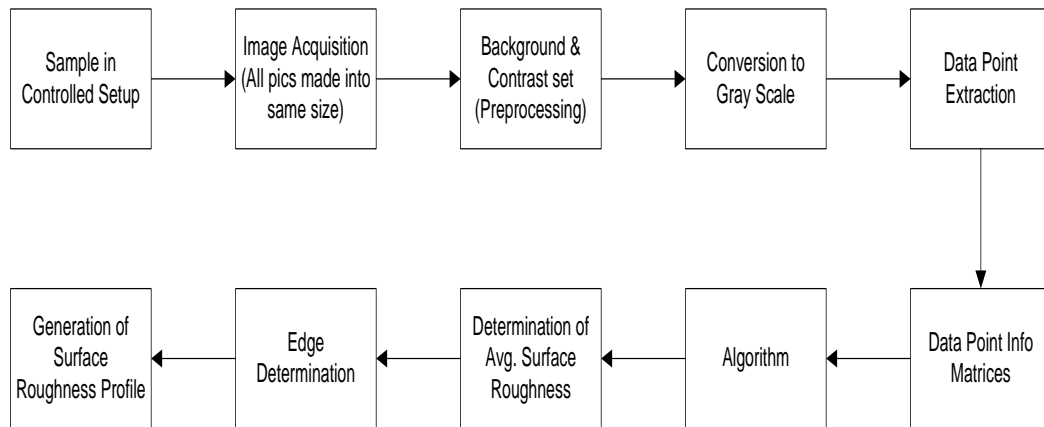


Figure: 3.13 Flow diagram of image processing for surface roughness

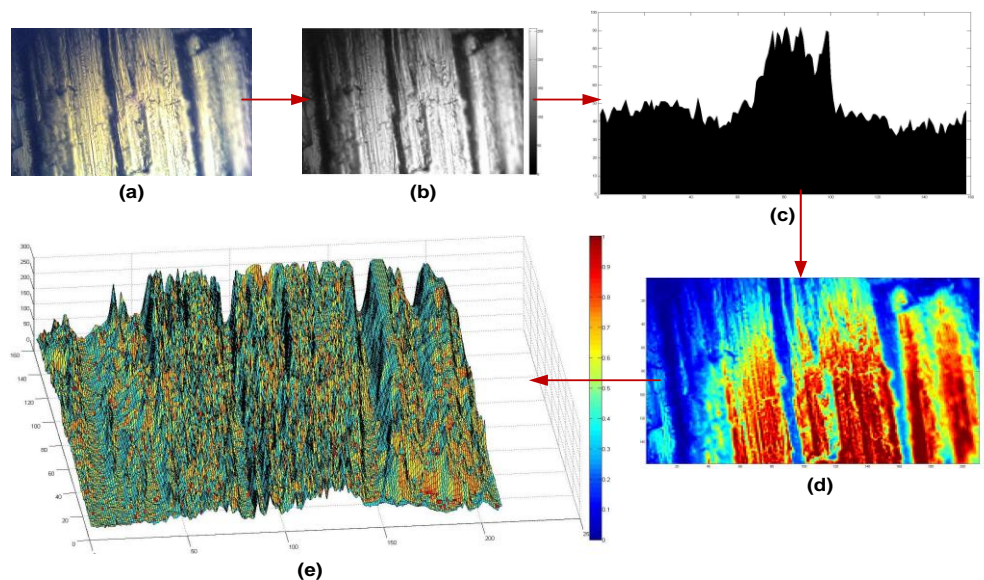


Figure: 3.14 DIP results (work-piece surface roughness, without magnet) (a) 10x zoom RGB microphotograph, (b) grayscale, (c) profile plot, (d) 2-D colored contour plot, (e) 3-D colored contour plot [65-66]

3.7.3 : OBSERVATION OF CHIP BEHAVIOR

The chips formed during turning were mainly investigated and it has been found that at some specific cutting conditions chip formation presents extreme cases of secondary and primary chip serration. Firstly, the chip at different cutting conditions were collected, labeled and kept accordingly. Then each chip was mounted using a mixture of resin and hardener. The mixture was stirred for about one minute and left to solidify. The solidified mixture is called mounting. The next step is to

grind the mounting surface in order to reveal the chip to the surface. Various grade of abrasive paper are used starting with grade 240 followed by 400, 800 and 1200. In order to remove the scratches on the surfaces, the mounting is then polished using alumina solution starting from grain size $6.0\ \mu$, followed by $1.0\ \mu$, $0.3\ \mu$ and $0.01\ \mu$. As a safety precaution, before polishing; the mounting is viewed under the microscope to ensure that the chip is visible on the surface. Finally, nitol is applied to the surface to reveal the grain boundaries of the ferrite and pearlite. Then the mounting is ready to be viewed under the microscope to capture the structure of the chip.



Figure: 3.15 Samples of mounted chip



Figure: 3.16 Instruments used for chip analysis. a) Polishing wheel, b) optical microscope

3.7.4 : MEASUREMENT OF TEMPERATURE

Digital thermocouple was used to measure the temperature of the tip of the insert. The hot end of the thermocouple was welded to the tip of the insert. Readings were continuously displayed on the screen of the thermocouple as the turning process is carried on. Final Reading is taken from the display of the thermocouple after cutting 200mm at different cutting speed and depth of cut.

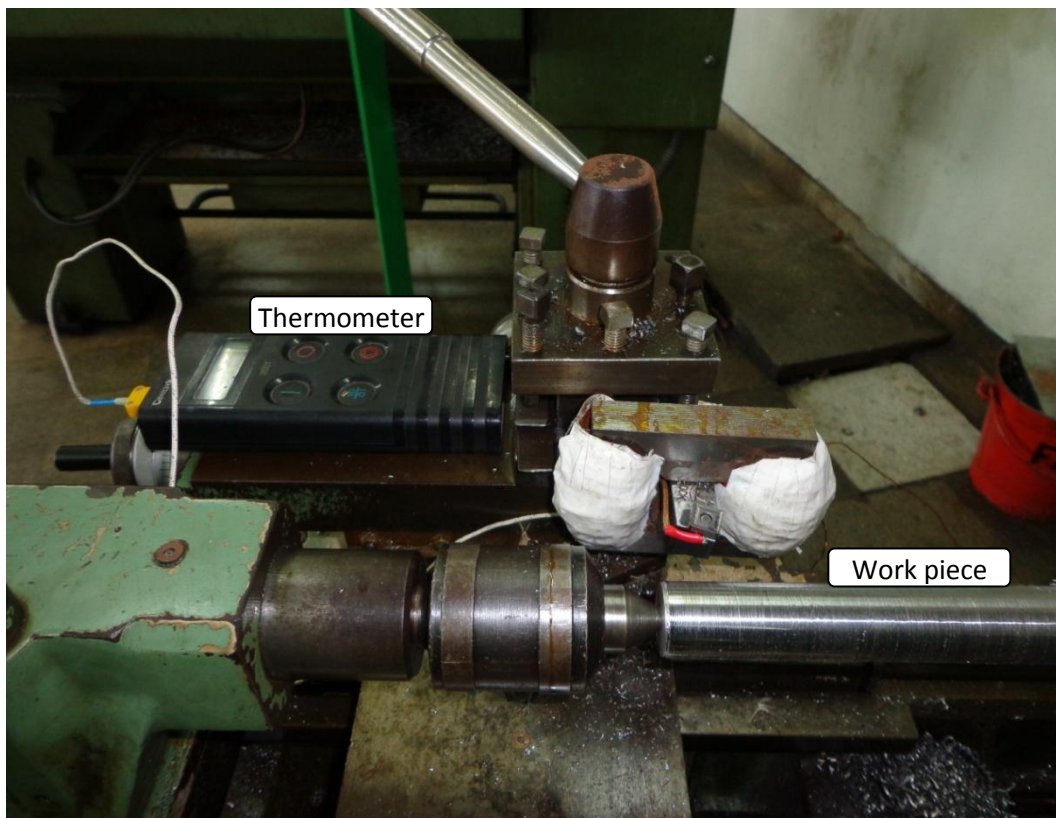


Fig. 3.17: Set up for temperature measurement

3.7.5 : MEASUREMENT OF CUTTING FORCE

To measure the cutting force a digital strain meter was used. Two strain gauges (Mfg- JP Tech, model- PA13-062AB-120 EN, gauge factor- 2.07) were attached to the tool holder. A half Wheatstone bridge circuit was used to connect the strain gauges to the digital strain meter. One strain measure was attached on top portion of the tool holder to measure the tension and one was attached on the bottom

side to measure the compression. These two strain meters acted as two active arms of the bridge. The other two resistors of the bridge circuit were activated internally in the strain meter. The connection and the circuit diagram are shown in the following section.

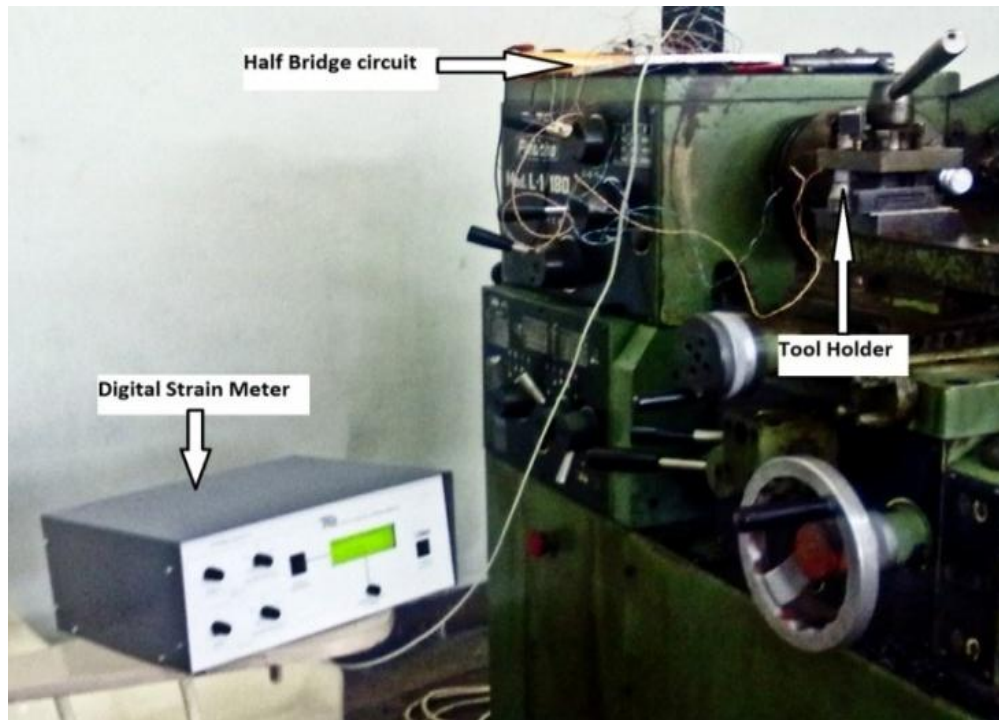


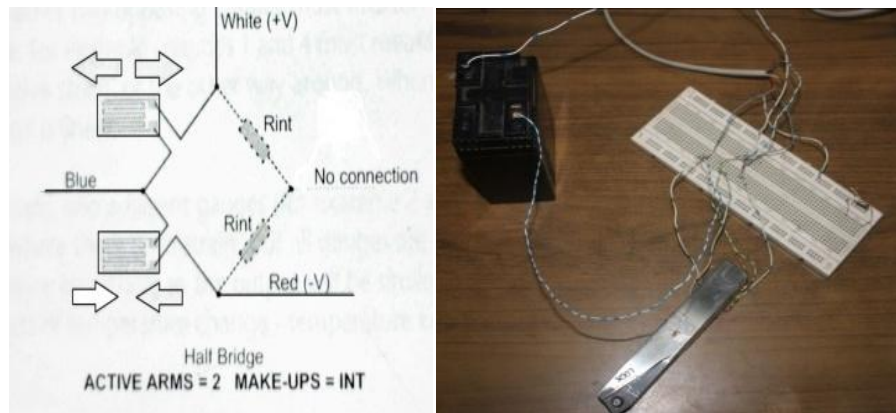
Figure: 3.18 Arrangement for measuring cutting force with half bridge circuit and strain meter

The strain meter measured the strain on the tool holder because of tangential cutting force in micro strain. Later this strain was related to force using Young's formula. The empirical equation shows a proportional relationship in between strain and force. Later these data were plotted.



Figure: 3.19 SM 1010 Digital Strain Display

The circuit diagram of the half bridge circuit with the connection terminal to strain meter is shown below:



Rint- 'make up' resistors inside (built into) the digital strain display
Figure: 3.20 Circuit used to connect strain gauges to the strain meter [67]

There were four wires in the input cable of the strain display. They had four different colors. The white wire was attached to the power line and the red wire was connected to the ground. The blue wire was connected in between the strain gauges. As the dummy or make up resistors were built into the strain gauge so no connection was required to the green wire. The specifications of the strain display are given in the table below:

Item	Details
Standard strain display range	+/- 10000 $\mu\epsilon$
Dynamic strain range	+/- 2000 $\mu\epsilon$
Gauge factor range	1.9 to 2.3
Nominal warm up time	10 minutes
Connections	Quarter, half & full bridge
Channels	16 (14 standard & 2 extra dynamic outputs)

Table: 3.21 Technical details of SM1010 digital strain display [67]

CHAPTER 4
RESULT AND DISCUSSIONS

4.1 : TOOL WEAR:

The image processing tool for determining flank wear developed by Patwari et al. [64] has been verified. The results of the analysis were compared with those previously determined by Patwari et al. [64], who used Kruss metallurgical microscope's analysis software to determine V_{Bmax} . Table 4.1 lists the average accuracy and repeatability of the analysis technique. From the table, it was observed that, the accuracy was higher for greater wear or larger wear land V_{Bmax} .





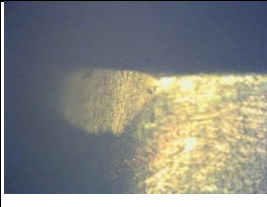



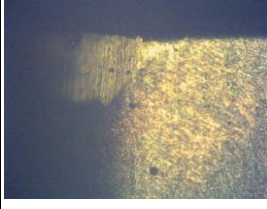











No.	Cut Length (mm)	Actual Wear (mm)	Calc. Wear (mm)	Error %	Repeatability %
1	0	0	0	0	100
2	200	0	0	0	100
3	400	0.0057	0.0063	10.52631579	100
4	500	0.0281	0.0298	6.049822064	100
5	600	0.0323	0.031	-4.024767802	100
6	700	0.0374	0.036	-3.743315508	100
7	800	0.0393	0.039	-0.763358779	100
8	1000	0.0412	0.04105	-0.36407767	100
Avg. Error % =				3.183957201	

Table: 4.1 Accuracy and repeatability of the automated tool wear analysis technique

The image processing technique for tool wear measurement showed good accuracy and consistency. It was observed that the technique was simple, fast, and economical. The only major investment is the requirement for an optical microscope and laptop, hardware that is readily available in most modern industries or research institutes. The shortcoming observed was that the software was less precise in evaluating tool wear when the flank land wear was very small ($V_{Bmax} < 0.3$ mm approx.). For detection of larger tool flank wear the accuracy of the system was markedly improved. Also, the algorithm displayed a tendency to overestimate small tool wear and underestimate larger tool wear. The consistency to detect tool wear, however, was always 100%, as shown by the first two data points. The explanation for this behavior is that the software relies on contrast difference or grey level intensity variation to detect and evaluate tool wear. Hence, when small amount of wear is concerned, the contrast is less, which leads to increased chances of error.

The following table shows the sample picture of the flank wear of the tool insert for different length cut at a cutting condition of 860 rpm and 0.75 mm depth of cut. The pictures are shown for non magnetic cutting and cutting with all three designs of electromagnets.

Table 2 : 860 rpm, depth of cut: 0.5 mm

Length of cut (mm)	Non magnet	Electromagnet (design 1)	Electromagnet (design 2)	Electromagnet (design 3)
200				
400				
600				
800				
1000				

The table 2 shows that there is always significant reduction in the tool wear when external magnetic field is used during the machining operation. Built up edge is seen during magnetic cutting. Only in case of the cutting with electromagnet of design

3, built up edge formed is lower in amount. It is seen only in the second picture, i.e. cutting after 400 mm of the work piece. This finer fragmented chips which, adhering to the tool insert, form the built up edge. It is in loose contact and may act as a lubricant, thereby improving tool life [8]. Thus it is obvious that the magnetic field promotes the formation of a controlled third body film which prevents direct contact between the contacting pair, i.e. the tool insert and the work piece.

The built up edge formed in case of first two designs refers to the spreading up of the magnetic field lines around the tool holder and mainly at the tip of the insert. During cutting with these two electromagnets it has been observed that chips are getting attached to the front portion of the tool which was almost absent for the third design of the electromagnet. This enables some fragment of the chips to adhere to the cutting edge of the insert, thereby forming this built up edge.

The values of the tool wear measured are plotted in graph to show the comparison between the tool wear found for different cutting condition using all three designs of electromagnet. Some sample graphs are shown below.

From the graphs showing the tool wear with the change in the length of cut of the work piece at different cutting condition during non magnetic cutting and cutting with all three designs of electromagnet, it has been observed that the tool wear increases with the increase in the cutting speed. The tool wear is always reduced when external electromagnetic field is applied during machining operation. For example in case of the cutting condition of 530 rpm and 0.5 mm depth of cut, the maximum tool wear, $V_{B \max}$ has been reached after cutting about 600 mm of the work piece for non magnetic cutting and beyond 1000 mm for all three designs of electromagnets. In this graph it is shown that initially, after cutting 200 mm of the work piece, the tool wear is more for design 2 than that of non magnetic cutting. However beyond this cutting length, the tool wear has decreased significantly for magnetic cutting condition.

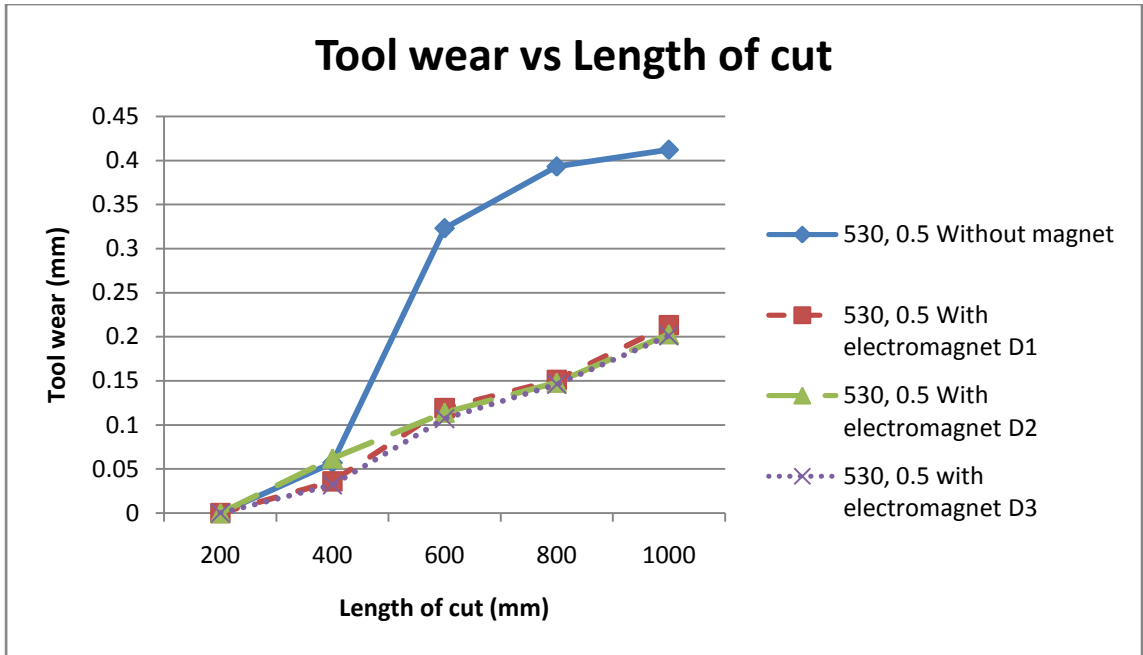


Fig. 4.1: Comparison of tool wear at 530 rpm and 0.5 mm depth of cut

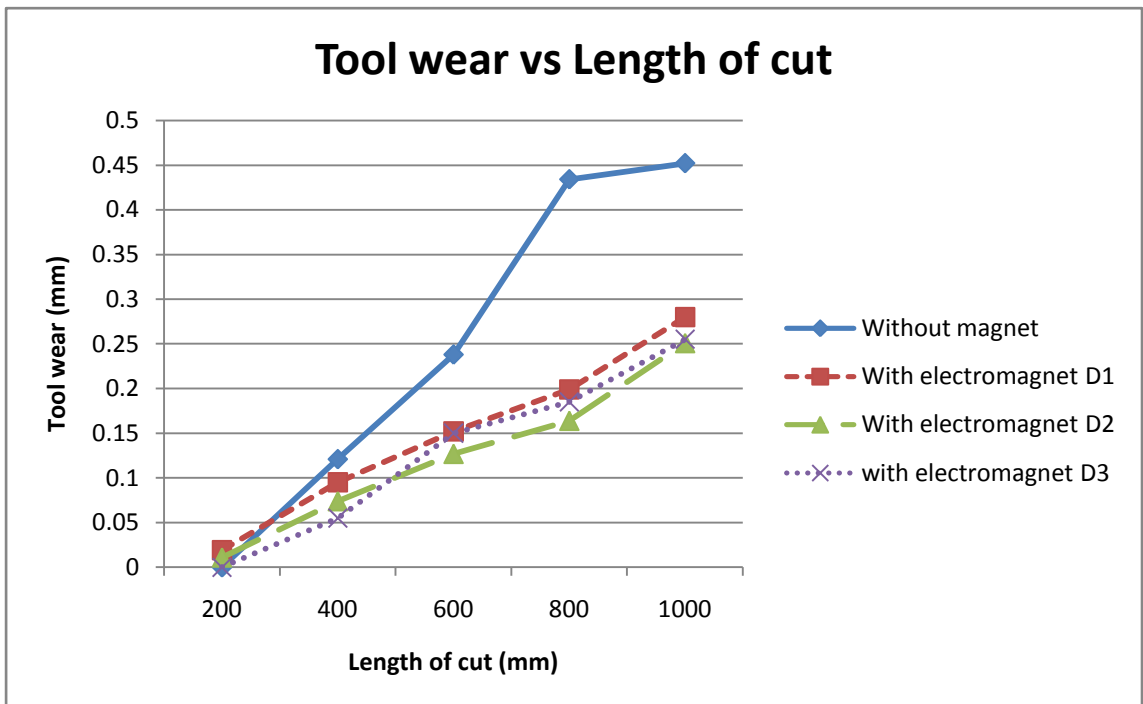


Fig. 4.2 : Comparison of tool wear at 530 rpm and 0.75 mm depth of cut

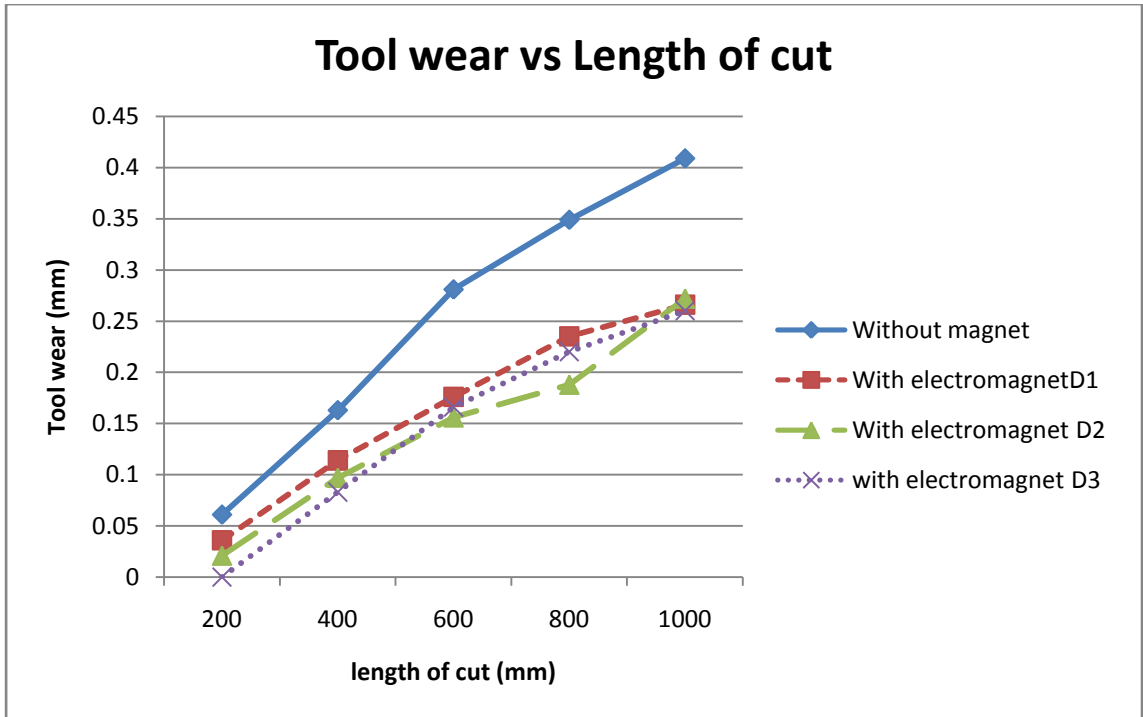


Fig. 4.3: Comparison of tool wear at 530 rpm and 1.0 mm depth of cut

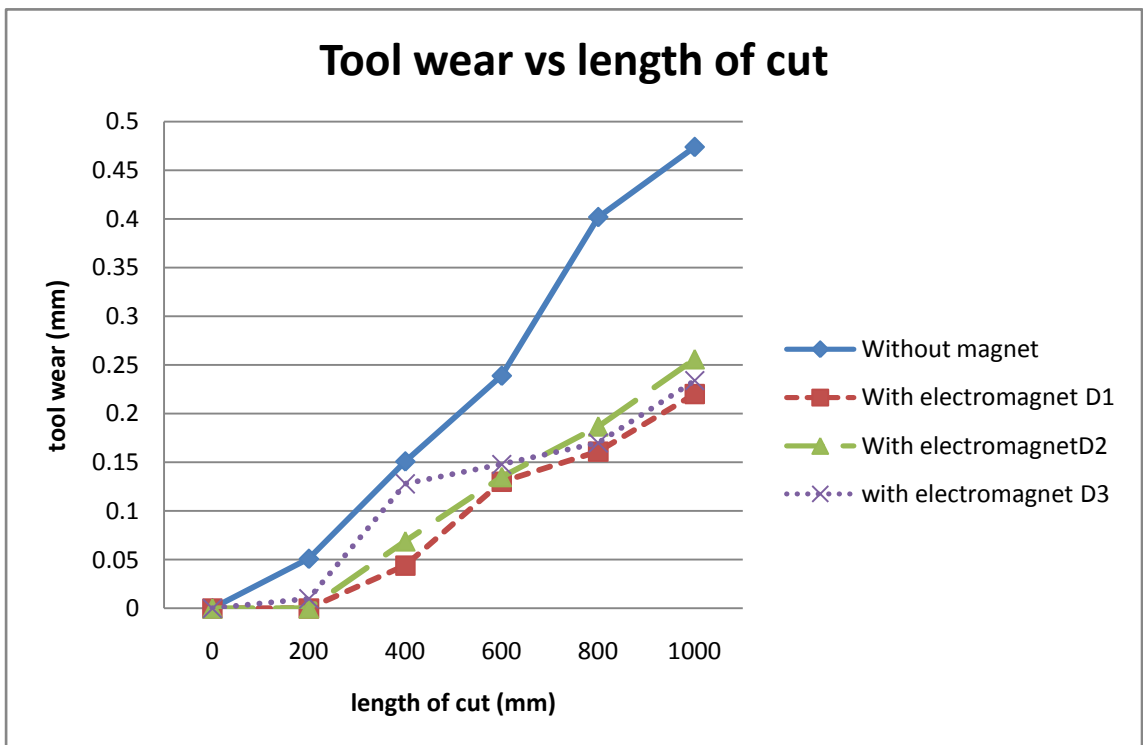


Fig. 4.4 : Comparison of tool wear at 860 rpm and 0.5 mm depth of cut

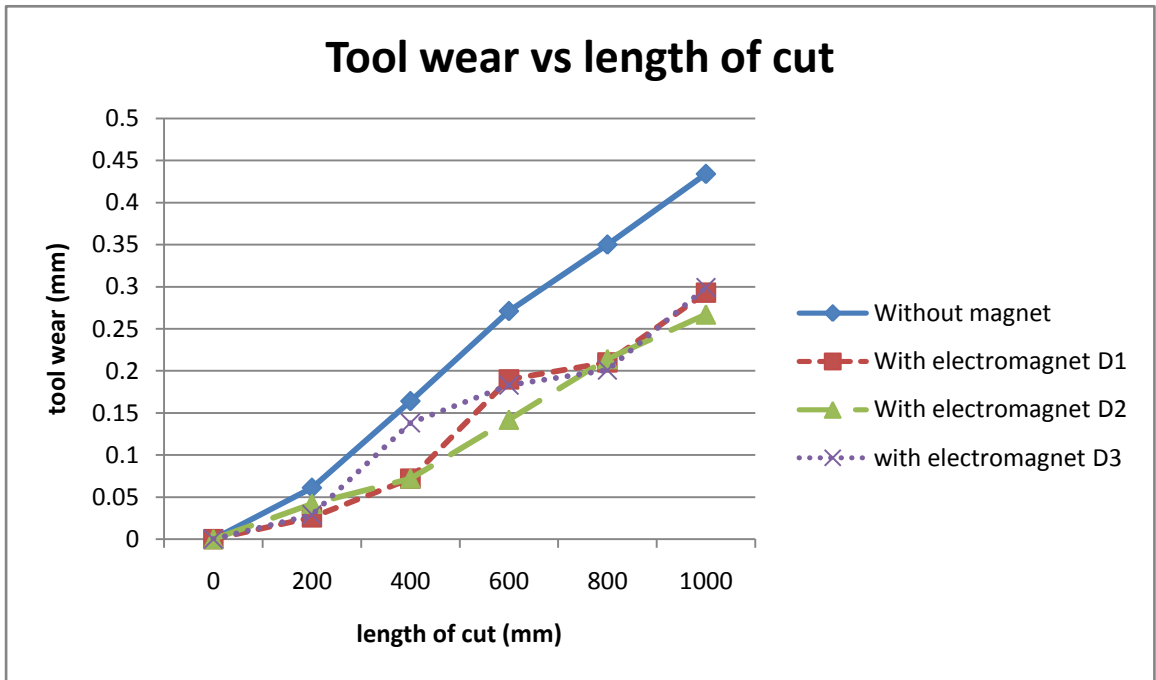


Fig. 4.5 : Comparison of tool wear at 860 rpm and 0.75 mm depth of cut

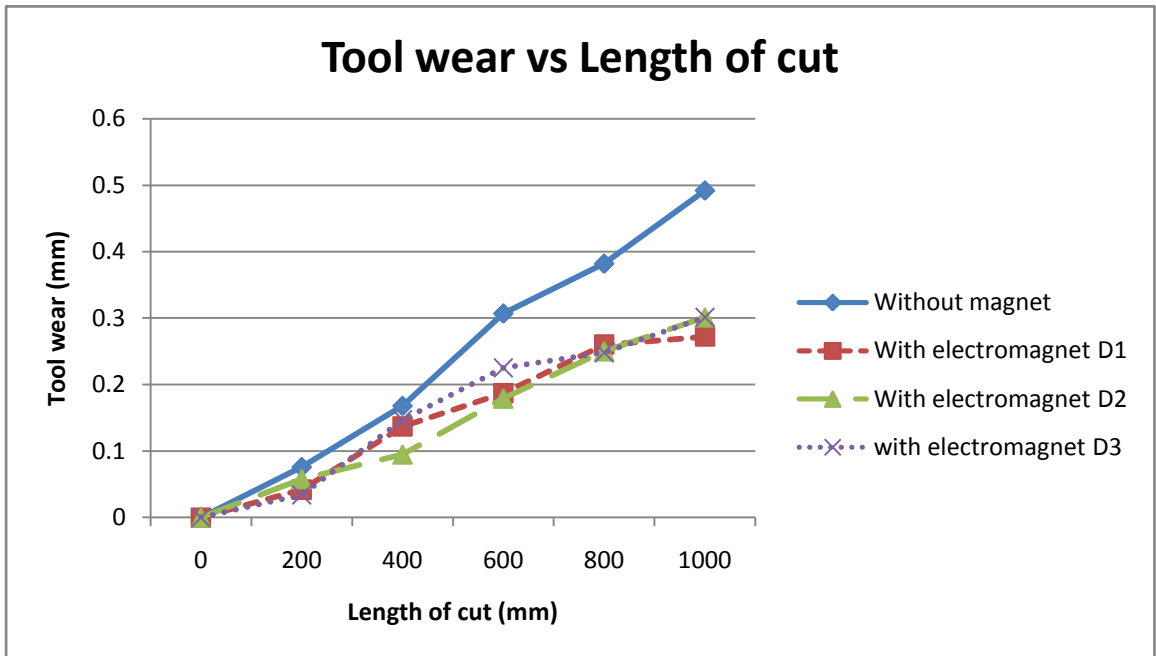


Fig. 4.6 : Comparison of tool wear at 860 rpm 1.0 mm depth of cut

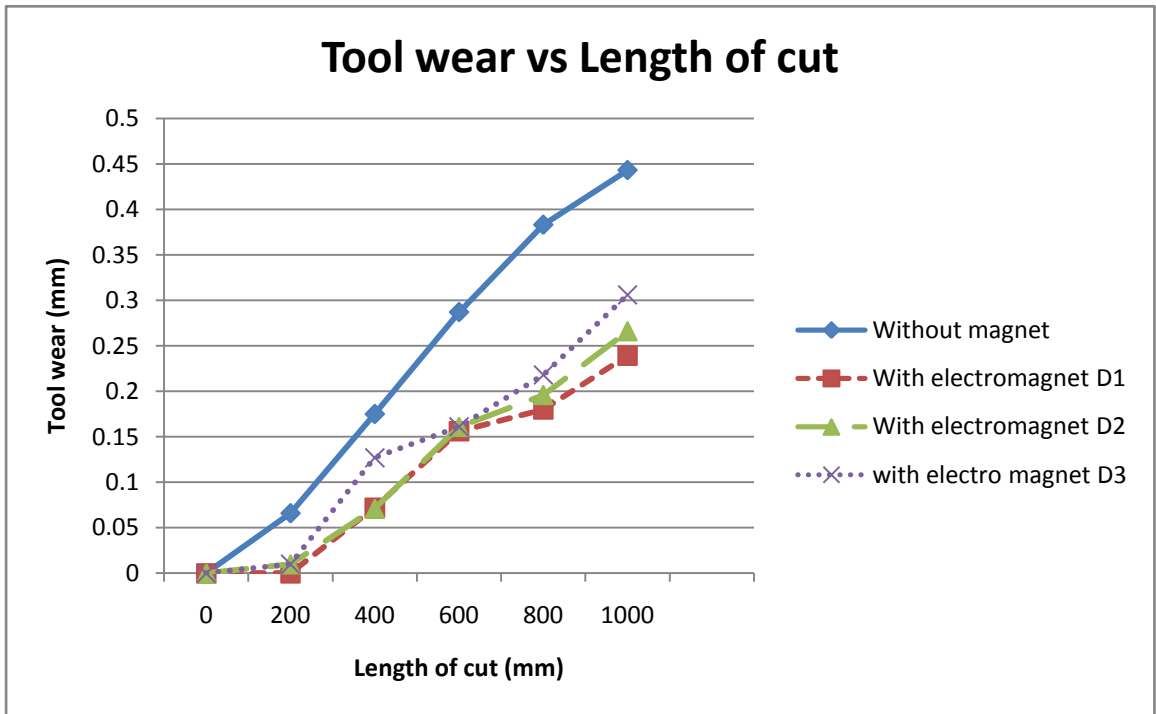


Fig. 4.7: Comparison of tool wear at 1400 rpm and 0.5 mm depth of cut

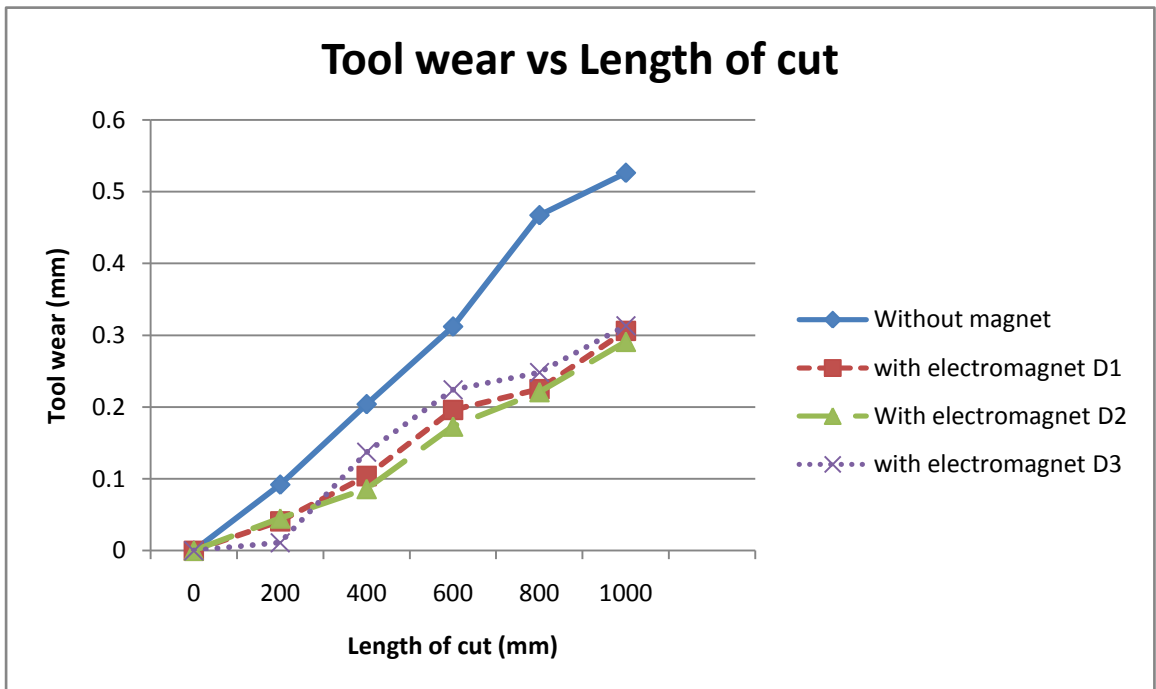


Fig. 4.8: Comparison of tool wear at 1400 rpm and 0.75 mm depth of cut

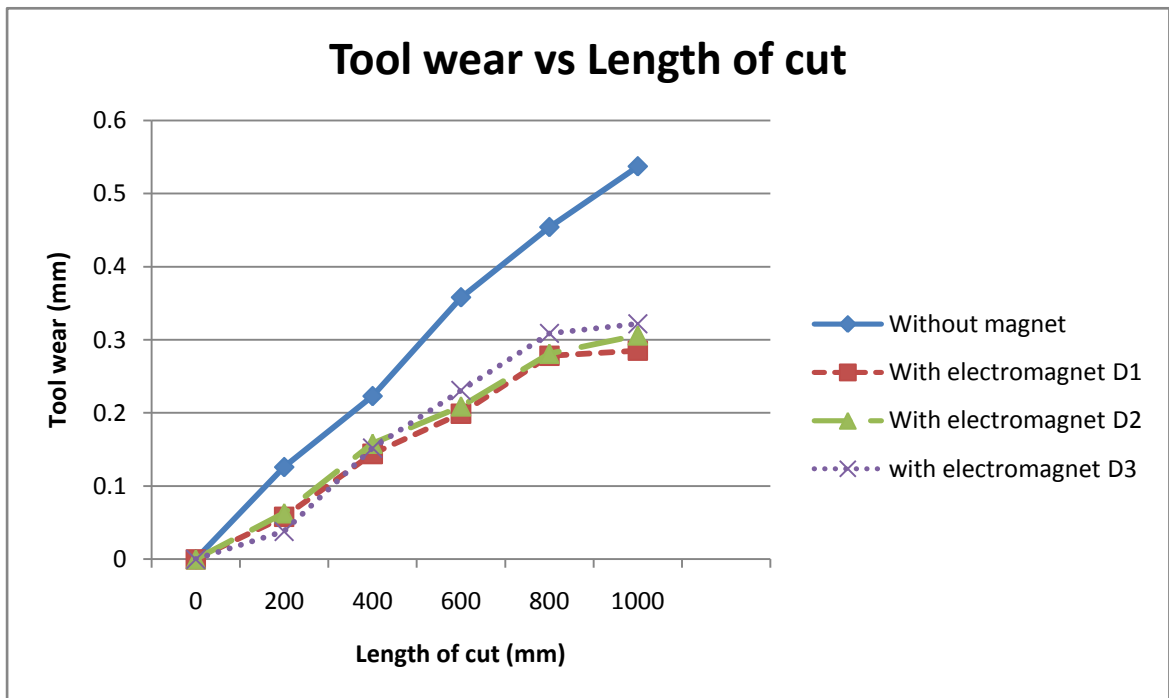


Fig. 4.9: Comparison of tool wear at 1400 rpm and 1.0 mm depth of cut

There is always improvement in the tool life when external electromagnetic field is applied during machining operation. However the graphs show some trend for the different designs of electromagnets at different cutting condition.

For lower cutting speed and lower depth of cut, the results obtained from design 1 electromagnet shows more tool wear than those obtained from cutting with electromagnet 2 and electromagnet 3. This is because of magnetizing the tool holder itself. During cutting the chips produced get attached to the tool holder and damages the preceding surface. Therefore during the next cutting operation, the tool needs to cut a comparatively rough surface. This increases the tool wear. However at higher cutting speed and higher depth of cut the chips produced are thick and cannot get attached to the tool. Therefore the preceding surface remains fresh and the next cut by the same tool will not be affected by the surface. This can be seen by looking at the graph of 530 rpm 1400 rpm. Another trend can be seen by changing the depth of cut. When the depth of cut is more design 1 and design 2 shows more sensitivity than design 3. At lower rpm and lower depth of cut the third design improves the tool life more than the other two designs. However for all cutting condition design 3 shows almost consistent results. The main purpose of using the third design of electromagnet

is to eliminate the effect produced by the chips get adhered to the tool during cutting process. And this electromagnet mainly emphasizes on the reduction of chatter phenomenon of turning operation.

To study the effect of changing the cutting speed of the turning operation, graphs of tool wear against cutting length have been plotted for different cutting speed keeping depth of cut constant. The graphs are shown for each design of electromagnets separately.

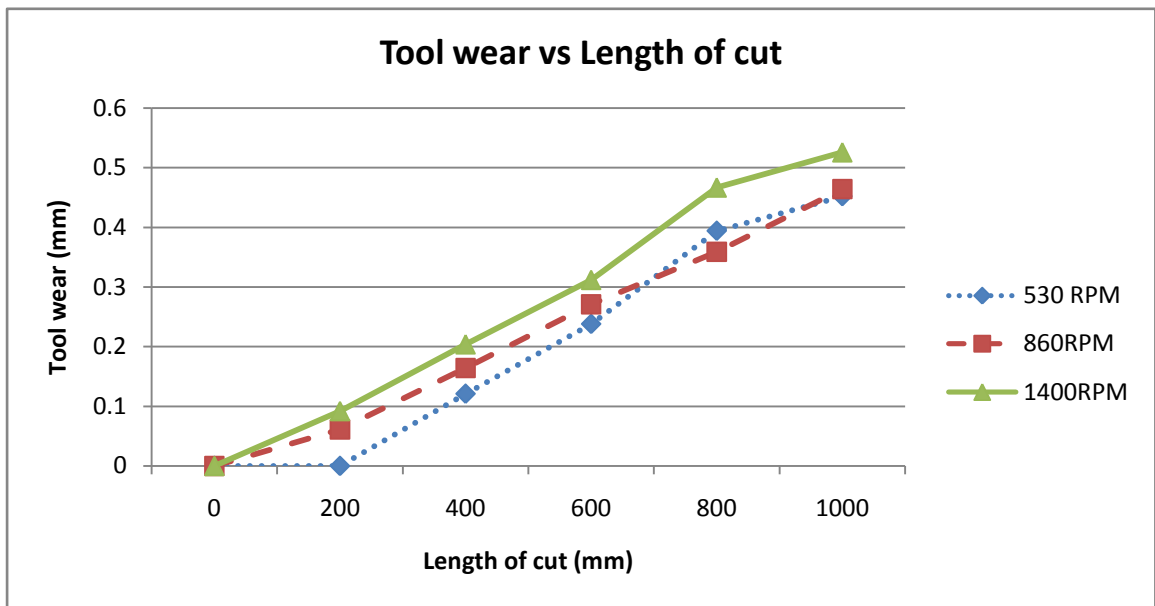


Fig. 4.10: Non magnetic cutting at 0.5 mm depth of cut

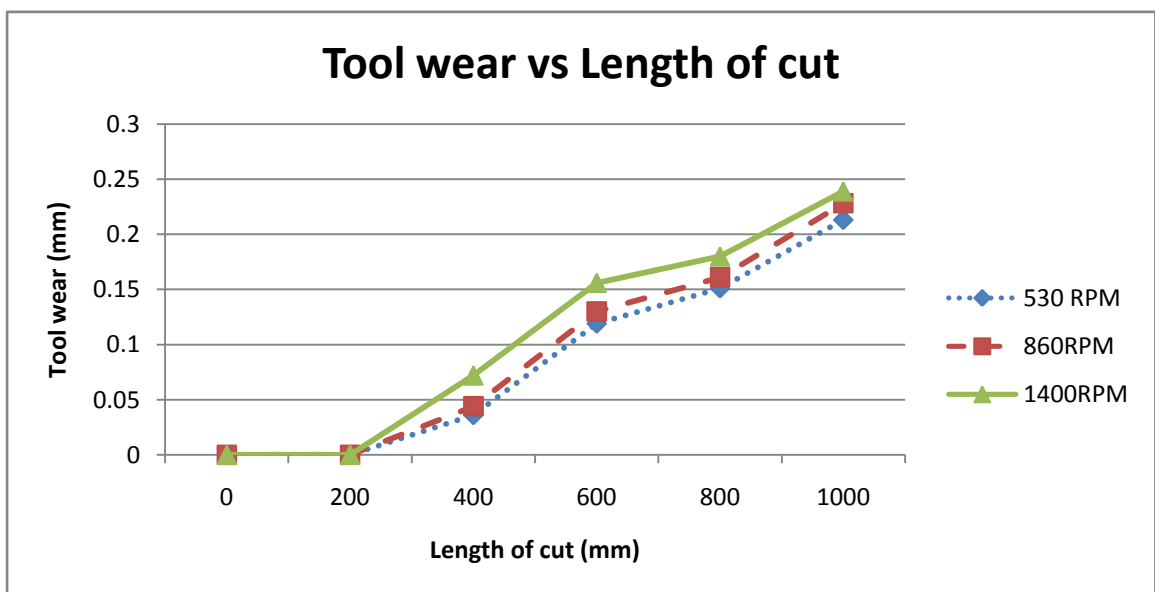


Fig. 4.11: Cutting with Design 1 electromagnet at 0.5 mm depth of cut

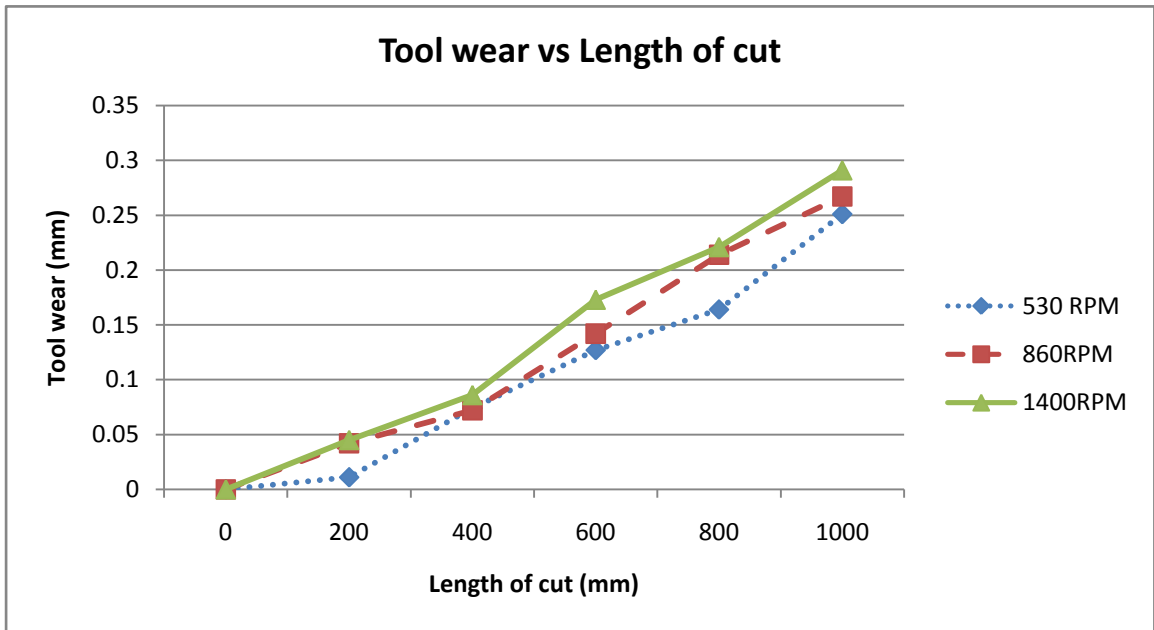


Fig. 4.12: Cutting with Design 2 Electromagnet at 0.75 mm depth of cut

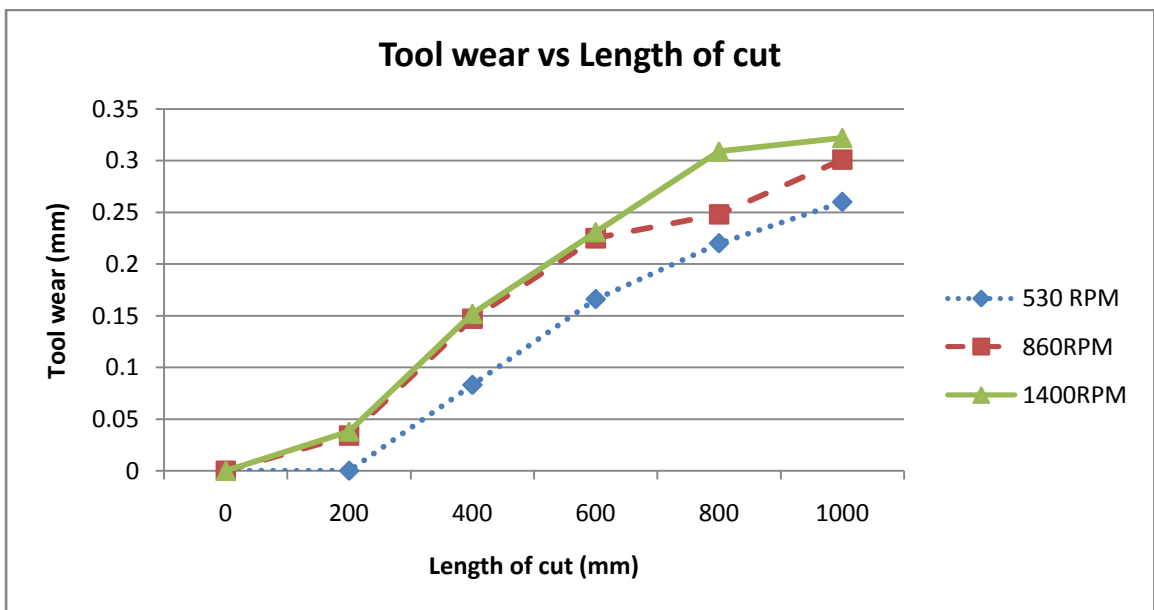


Fig. 4.13: Cutting with Design 3 Electromagnet at 1.0 mm depth of cut

From the above graphs it is obvious that with the increase in cutting speed the tool wear increases. This phenomenon is independent of external environment and other cutting parameter. For example, we have changed the depth of cut and used different designs of electromagnets to carry out the cutting operation under external electromagnetic field. However this trend of increasing tool wear at a higher cutting speed is always the same.

The effect of change in depth of cut on the tool wear has been studied by plotting the tool wear against the length of cut for different depth of cut at a constant cutting speed. This analysis was done for non magnetic cutting as well as all three designs of electromagnets. Some sample graphs are shown here and the rest of the graphs are given in Appendix 1.

From the graphs it is obvious that with the increase in depth of cut, the tool wear increases, but less significantly than the trend obtained for changing cutting speed at constant depth of cut. In this case also the effect of other cutting parameters and external environment of the cutting operation is negligible to this trend of increasing tool wear with the increase in depth of cut.

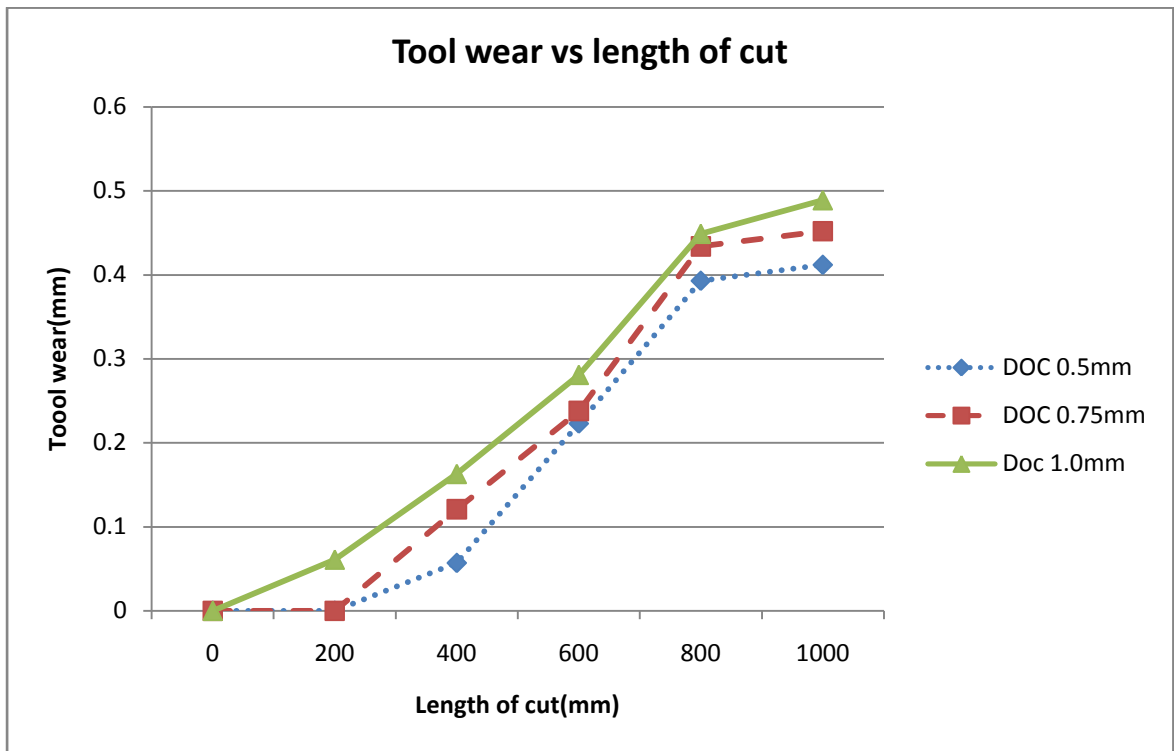


Fig. 4.14: Non magnetic cutting at a cutting speed of 530 rpm

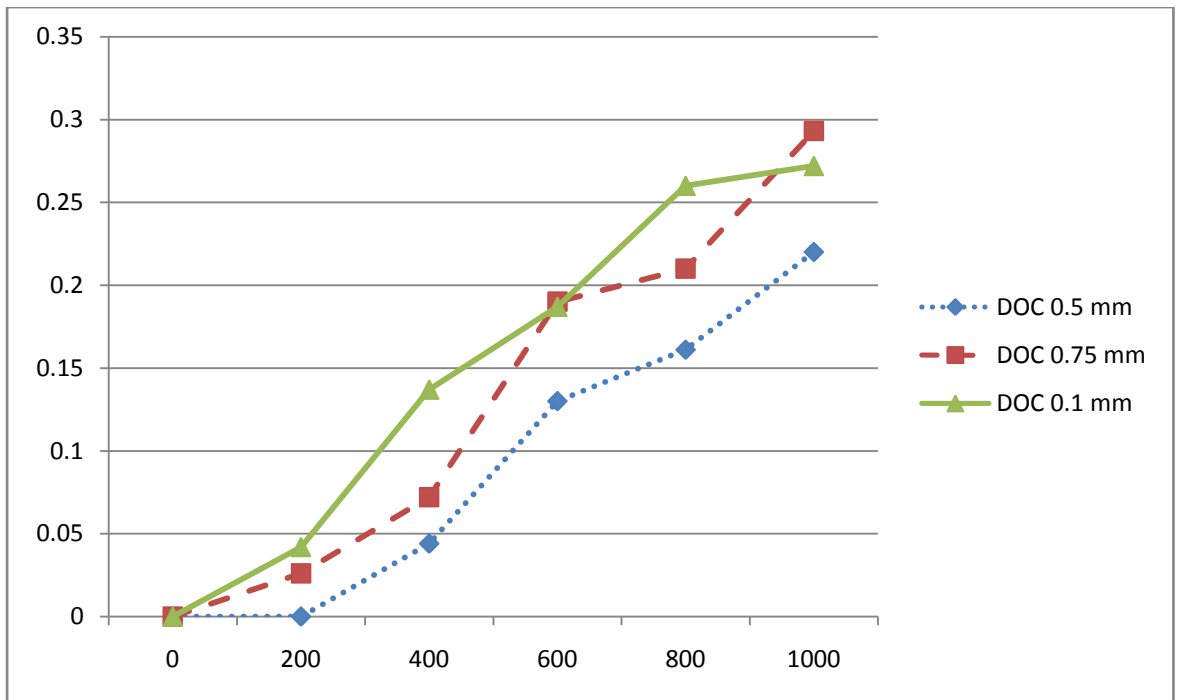


Fig. 4.15: Cutting with design 1 electromagnet at 860 rpm

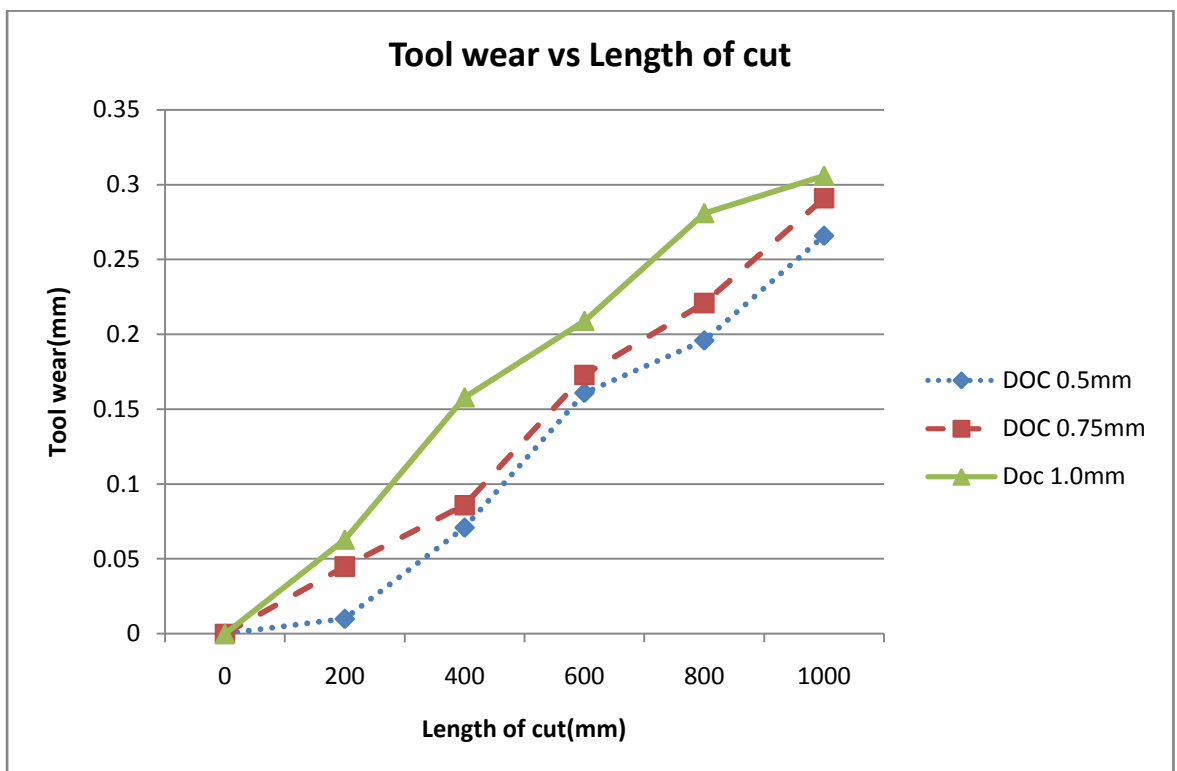


Fig. 4.16: Cutting with design 2 electromagnet at 1400 rpm

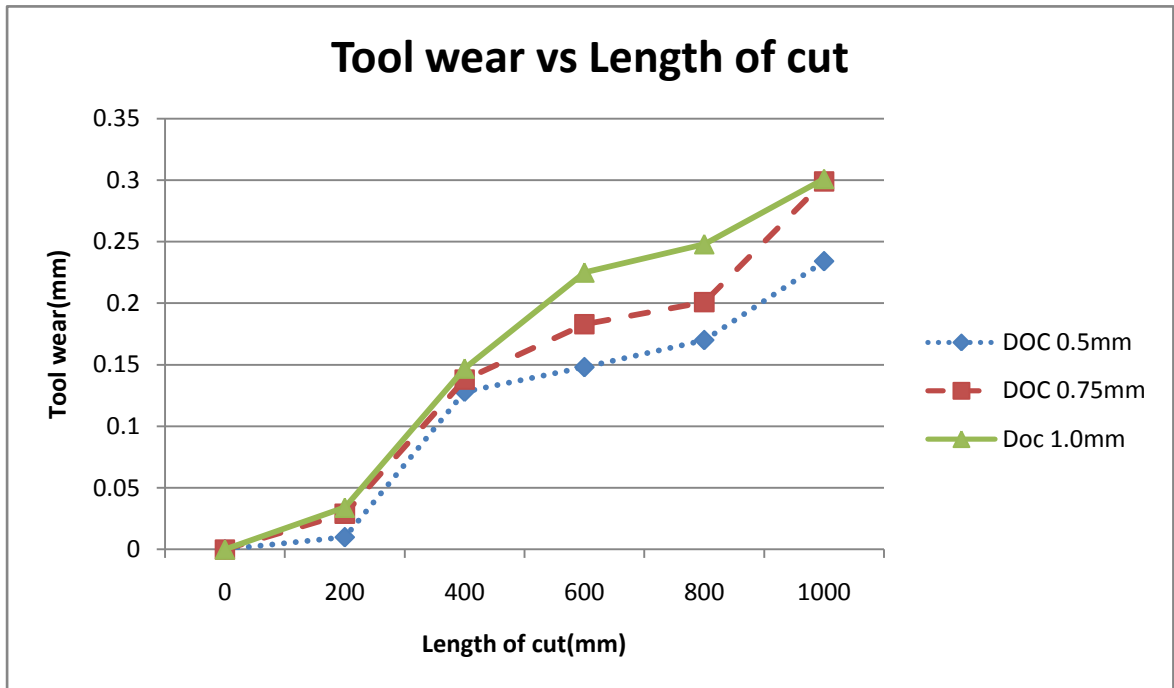


Fig. 4.17: Cutting with design 3 electromagnet at 860 rpm

Almost all the graphs show a consistent trend, however some points have deviated from its expected position. This may occur due to any error during experimentation, and beside this the experiments are huge in number for which it is very difficult to maintain constant experimental condition every time the machining operation is performed. For example the depth of cut has been given by using a rotating wheel in the carriage. This may cause some variation in the depth of cut.

The accuracy of tool wear measurement also depends on the quality of the captured image by the microscope. The built up edge also created some problem. As tool wear occurs on the edge of insert it is very difficult to focus at the exact point of the maximum flank wear. Because of these reasons some points in the graphs may have been deviated. But as each experimental condition is compared against several numbers of other experimental conditions and the characteristic of each graphs is almost similar to the ideal cases the minor dislocation of some points have little effect on the overall result. Due to the quality of the captured image of the tool flank wear, image processing technique developed by Patwari et al [64] could not be used in many of the experimental results. In this case the software “Scopetek”, which have been mentioned in the experimentation part, has been used.

In this experiment, when the tool wear showed too much deviation from the ideal position, the whole cutting was repeated by using a new corner of the tool insert. In some cases it has been done several times for the same experiment and the average has been taken.

It would give more precise results if each experiment was performed several times and the average would be taken. However, since too many cutting operation have been carried out in this experiment, it was not possible to repeat all the experiments.

4.2: SURFACE ROUGHNESS

The image of the surface was captured by the metallurgical microscope after cutting 1000 mm of the work piece. This image is then processed in MATLAB to find out the average roughness of the surface. The following figure shows the comparison among the images of the surfaces obtained for each cutting condition: non magnetic cutting and cutting with all three designs of electromagnets. The contour plots are given for the corresponding surfaces, which is obtained from the analysis using the image processing technique.





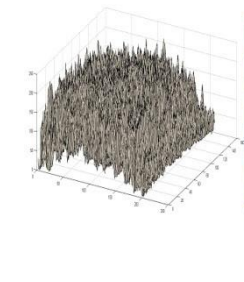
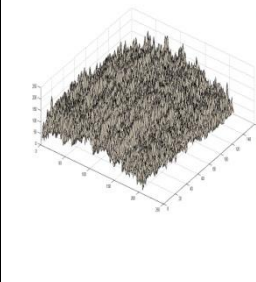
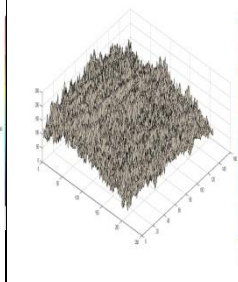
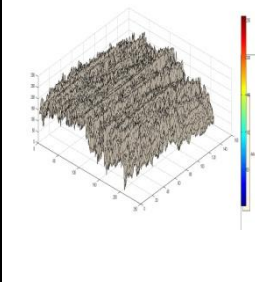
	Non Magnet	Electromagnet Design 1	Electromagnet Design 2	Electromagnet Design 3
Images of the Surface After machin - ing				
Cont- our plot				
Rough- ness (μm)	0.751	0.732	0.746	0.673

Fig. 4.18: Images of the surface of the work piece and corresponding contour plot for the cutting under different condition

The charts shown below illustrate the change in surface roughness when magnetic field is applied during cutting operation. The charts are given for each cutting condition. Sample figures are given in this text. The rest of the charts are given in the Appendix 2.

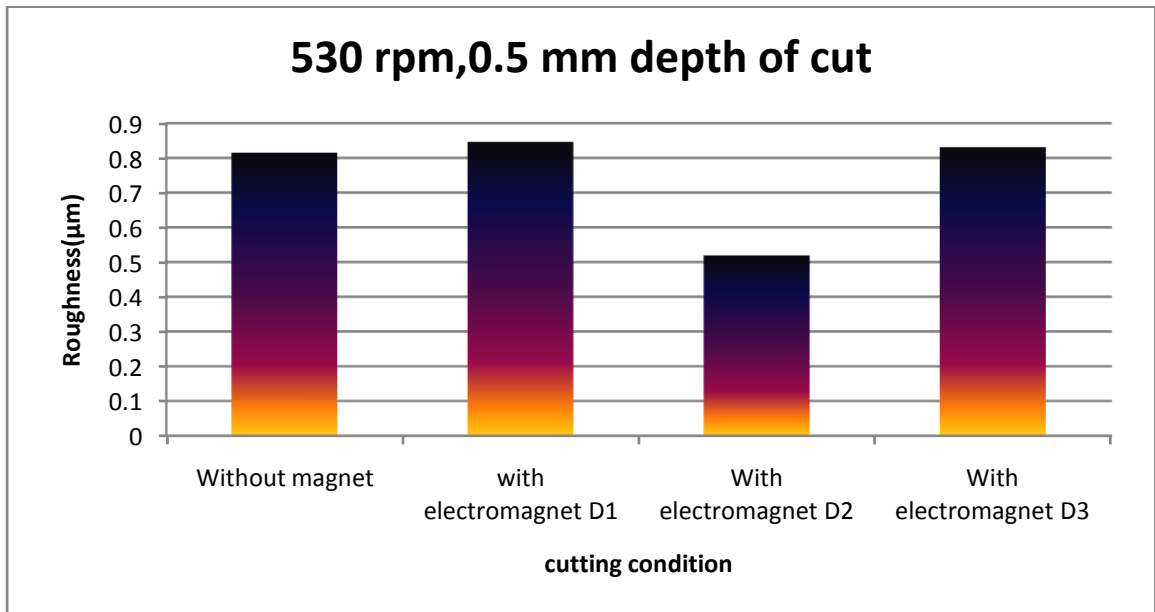


Fig. 4.19: Comparison of surface roughness at 530 rpm and 0.5 mm depth of cut

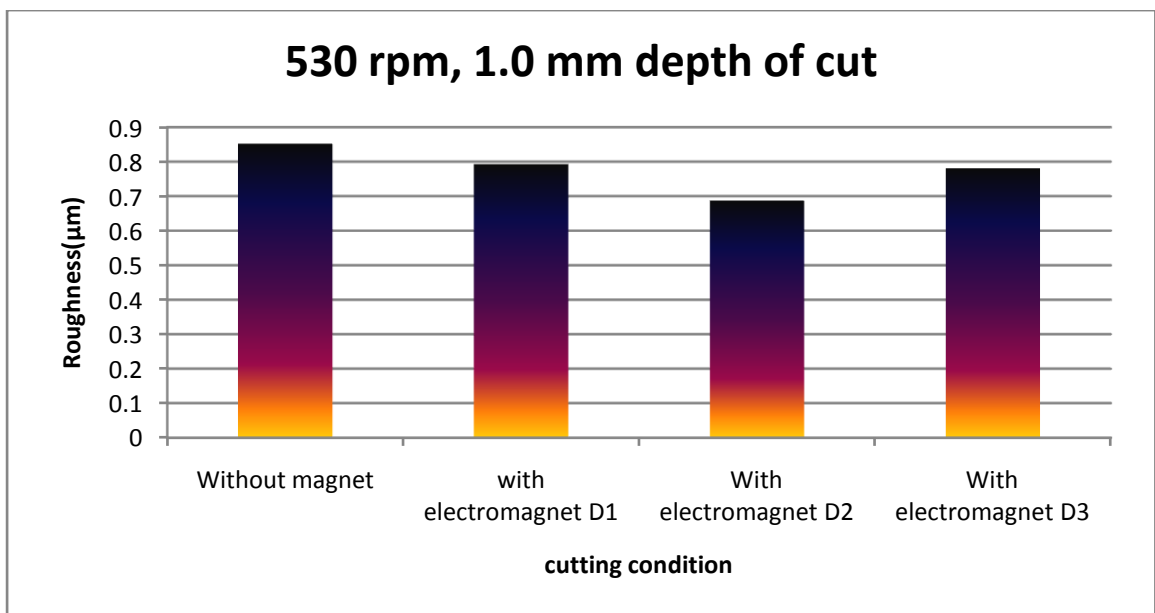


Fig. 4.20: Comparison of surface roughness at 530 rpm and 1.0 mm depth of cut

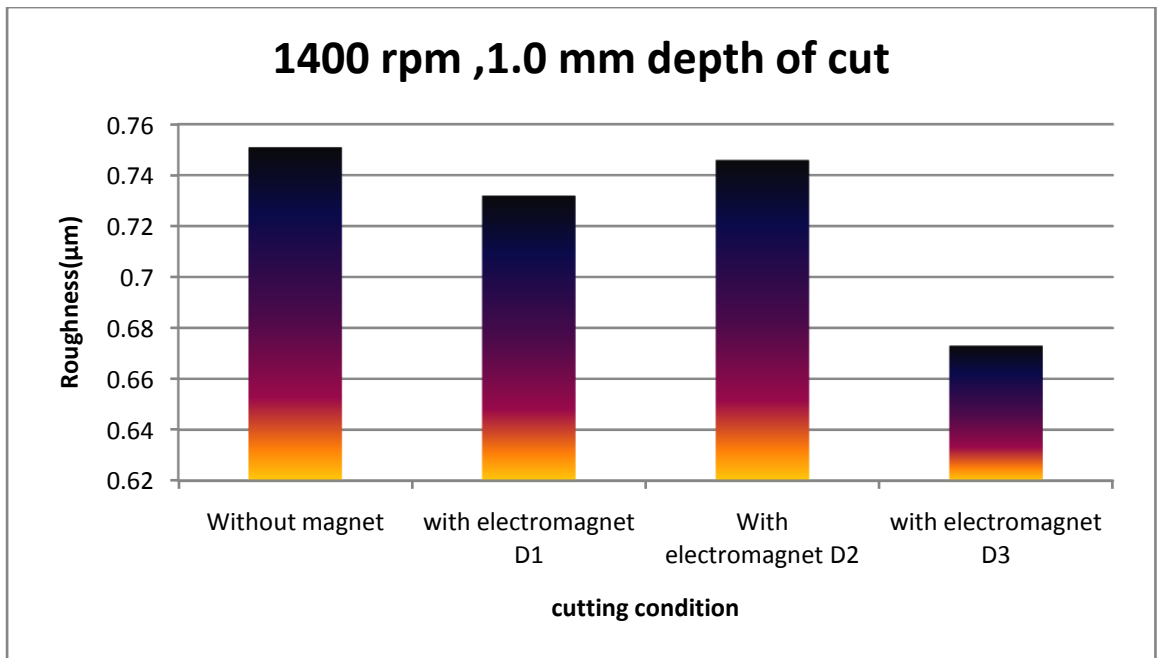


Fig. 4.21: Comparison of surface roughness at 1400 rpm and 1.0 mm depth of cut

From the above charts and the charts given in the Appendix, it is clear that the surface of the work piece improves with the application of external magnetic field. However the surface at lower rpm and lower depth of cut is sometimes worse than that of non magnetic cutting. The surface quality improves with the increase in cutting speed. Because this electromagnet magnetizes the tool holder itself and a lot of chips get attached to the tool during cutting operation. The chips adhered to the tool damages the preceding surface. Thus after cutting 1000 mm of the work piece the surface obtained in case of lower cutting speed is not better than that of non magnetic cutting. However in case of higher cutting speed the chips cannot get attached to the tool holder. For this reason at a higher speed the effect of magnetic field is more sensitive and thereby results in the reduction of surface roughness.

Another trend which is seen, especially in case of design 3 electromagnet, that the surface quality improves with the increase in the depth of cut. At lower depth of cut (0.5 mm and 0.75 mm) the surface roughness in magnetic cutting condition is higher. But in higher depth of cut (1.0 mm), the surface quality is significantly higher. This phenomenon can be explained by the formation of built up edge. In case of electromagnetic condition the higher flux density at the tip of the insert helps the accumulation of fragmented chips produced in the cutting action on the insert tip. This built up edge scratches the surface of the work piece in lower

cutting speed and depth of cut. However at a higher depth of cut, the chips produced is thicker and contain very few amount of fragmented chips or metal powder. So the built up edge formed is very thin or lighter. This easily gets removed by the cutting operation and thereby cannot scratch the work piece surface. At higher speed this removal process is more and aided by the thicker chips. This phenomenon also aids the tool wear at higher speed.

4.3 : Temperature:

Due to the application of external magnetic field during the turning operation the temperature of the system rises. This is because the work piece is constantly rotating. The magnetic field lines that cut the work piece produce an induced e.m.f. on the surface of the work piece and thus create an eddy current. Due to this eddy current the temperature which is produced at cutting junction of the tool and the work piece get assisted and becomes higher. In this experiment the temperature after cutting 200 mm length of the work piece has been measured for different cutting speed (rpm) and depth of cut (mm) in different condition, i.e. non magnetic cutting and cutting with all three designs of electromagnets.

The following figures illustrate the variation of temperature at different cutting parameters under different conditions of turning operation.

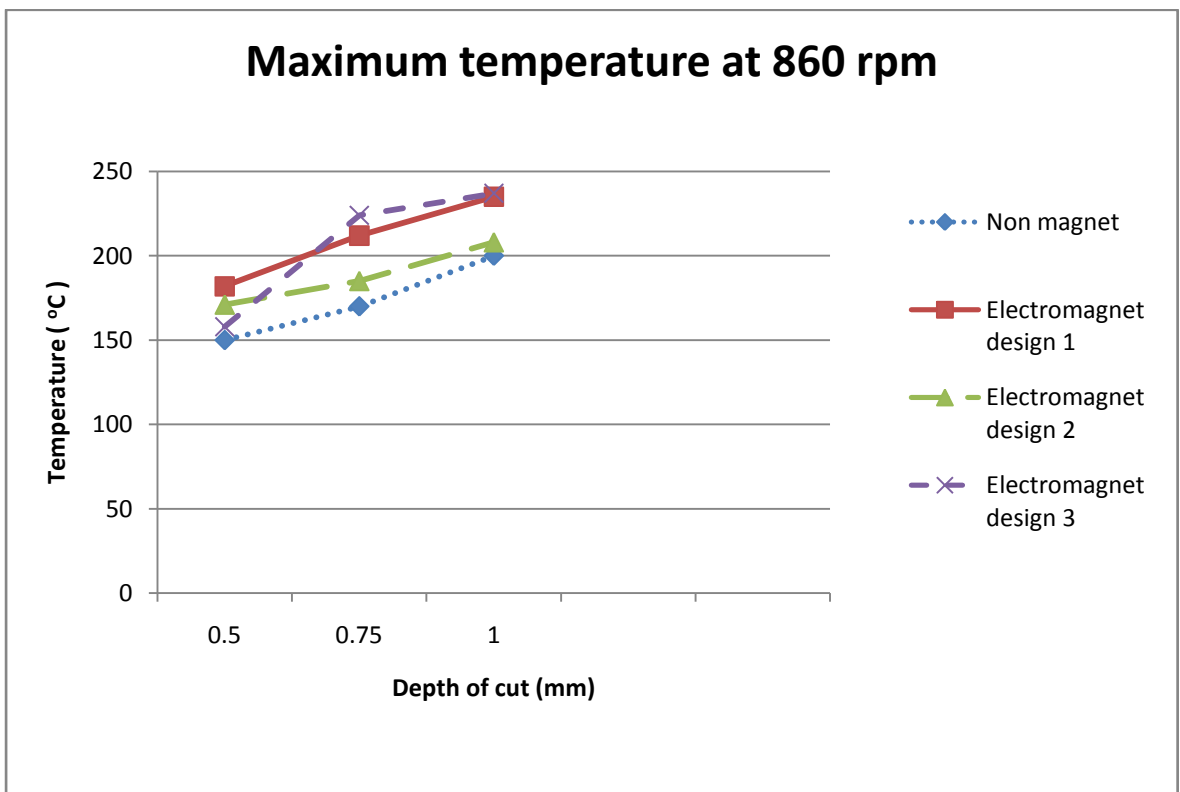
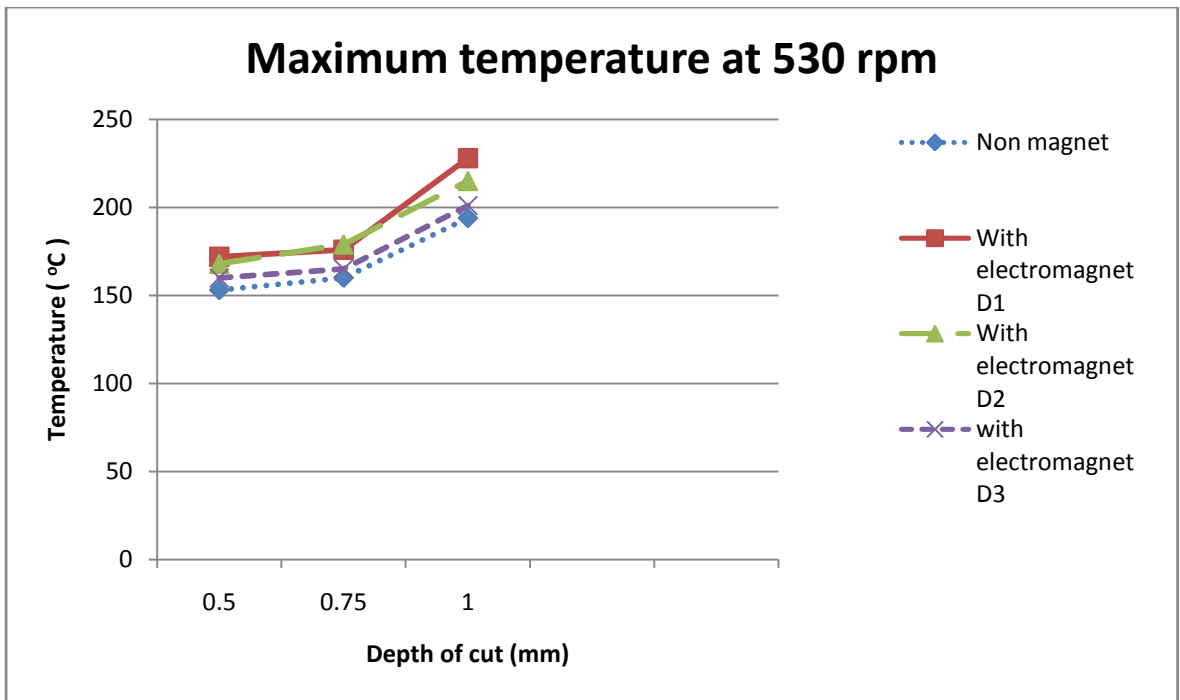


Fig. 4.22: Variation of temperature with depth of cut at 530 rpm and 860 rpm

From the above graphs of temperature it is seen that the temperature is higher for electromagnet assisted turning process. The temperature is relatively higher for the design 1 and design 2 electromagnet. This is because of the chips getting attached with the tool during turning process. These chips make more friction with the work piece and increase the temperature. But for design 3 electromagnet, there is almost no chips adhered to the tool during cutting operation for which the temperature is lower than the case of first two designs of electromagnets.

Moreover the temperature increases with the increase in depth of cut. And with higher cutting speed the temperature is higher whatever the cutting condition is, i.e. non magnetic cutting or cutting with all three designs of electromagnets.

4.4: CHIP MORPHOLOGY

The chips produced during the cutting operation after cutting 1000 mm of the work piece with a single corner of the insert for each cutting condition, are collected and then analyzed as described in the experimentation part. In each case several behavior of the chips have been studied.

4.4.1: CONTINUITY OF CHIPS

Chips collected during non magnetic condition are discontinuous and for magnetic condition it is continuous and very closely packed. The figure below illustrates this.



Fig. 4.23 (a) Discontinuous chips during non magnetic cutting

(b)continuous chips during magnetic cutting

4.4.2 : TOOTH FORMATION OF THE CHIPS

The chips produced during machining operation consist of some teeth along their side. The figure below shows the magnified view of the teeth of the chips. This illustrates the serration behavior of the chips. In our experiment we have taken the length wise view of the chips under optical microscope.

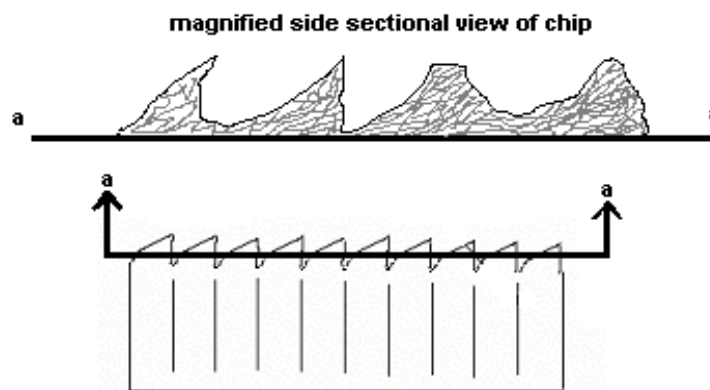


Fig. 4.24: Cross section of chips

The cross section of the chips obtained in our experiment has shown in the figure below which illustrates the behavior of chips. It is clearly visible that the tooth of serrated chips is larger in case of non magnetic cutting. The size is much smaller in case of electromagnet assisted turning process. The comparative serration nature of the chips for different designs of the electromagnet is in this figure.


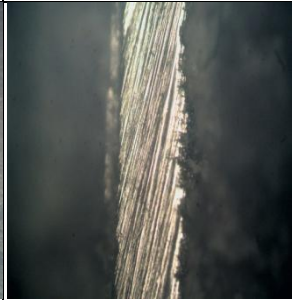

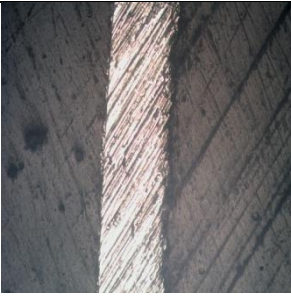
Non magnet	Electromagnet design 1	Electromagnet design 2	Electromagnet design 3
			

Fig. 4.24: Microscopic view of the chip cross section at 860 rpm and 0.75 mm depth of cut

The microscopic view of the chip cross section shows that the serration behavior of the chips decreases from non magnet condition to design 3 electromagnet condition.

4.4.3 : COLOUR OF CHIPS



Fig. 4.25: (a) chips produced during non magnetic cutting condition (b) chips produced during magnetic cutting condition

The above figure shows that burnt chips are produced during electromagnet assisted turning process. This is the consequence of the increased temperature than that of non magnetic cutting condition when electromagnets are used.

4.5: CUTTING FORCE

During any machining operation the force acting on the tool causes it to have a strain which is measured in this experiment by using digital strain meter. The value of the strain was measured in micro strain at interval of thirty seconds. Five readings were taken for each of the experimental condition and from that the average strain was obtained. The depth of cut was kept constant and the RPM of the machine was changed. Later data were taken at different depth of cut while keeping the cutting speed constant. For obtaining the value of tangential cutting force from the strain of the tool holder the Young's formula for rigidity of material was used. In that formula the value of the Young's modulus was taken as 210 GPa based on the material of the

tool holder. The area was taken as the cross section of the tool holder (2cm X 2cm). So a relationship between the force and the strain was found. This relationship shows proportionality between the tangential cutting force and the strain of the tool holder. Finally after obtaining the values of the force graphs were plotted to compare the result at different experimental conditions.

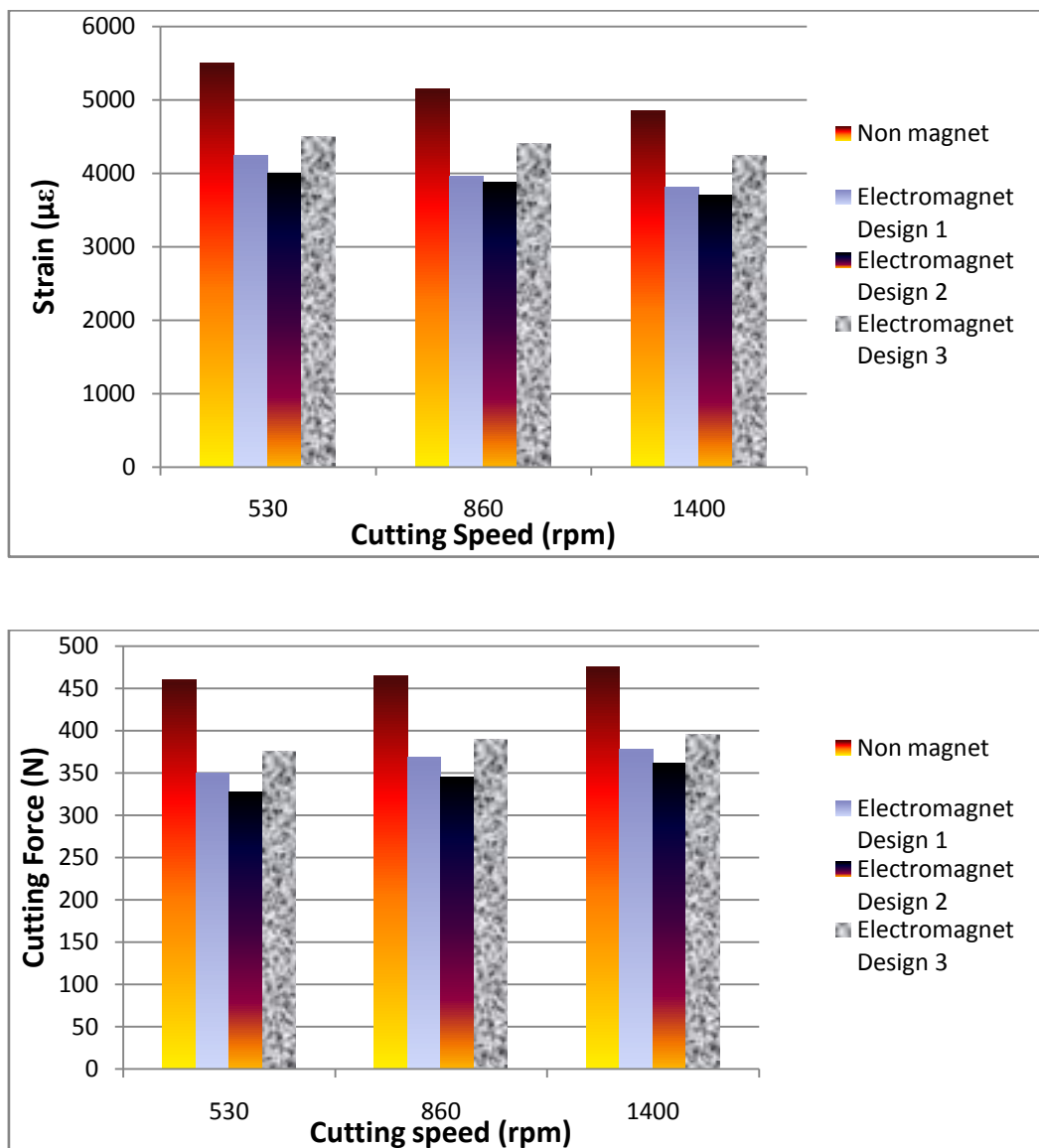
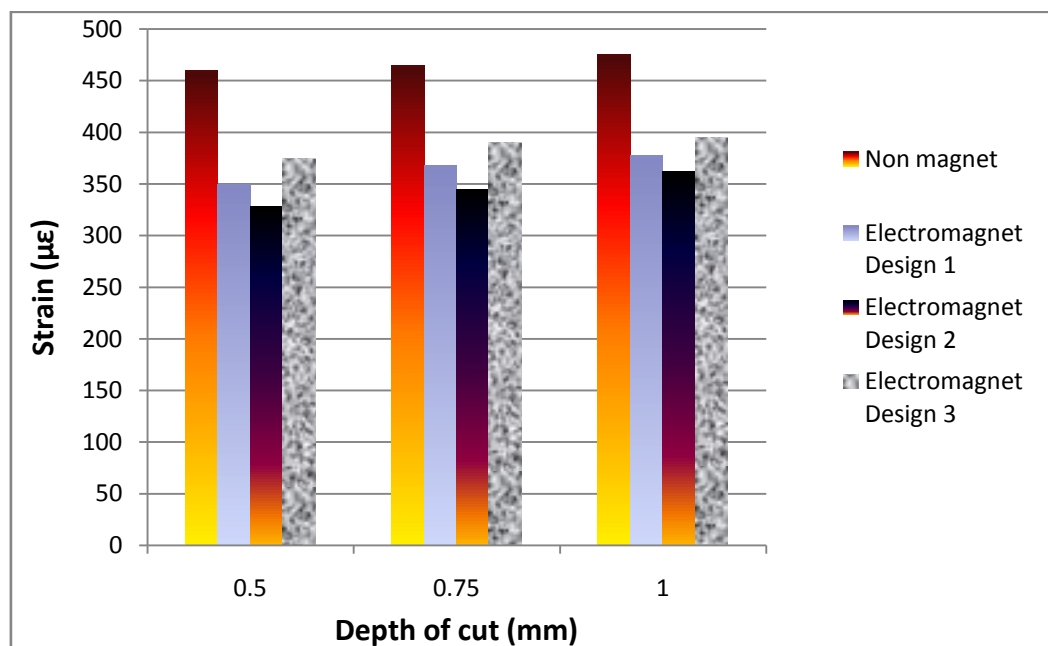


Fig. 4.26: Strain and Cutting force with respect to cutting speed

From the above figures it is obvious that the tangential cutting force always decreases with the application of external magnetic field whatever the cutting parameter is for cutting under all the conditions, i.e. non magnetic cutting, cutting with all three designs of electromagnets. Design 1 and 2 shows more reduction in the

cutting force than that for design 3. This can be explained by the reason why this cutting force is decreasing. As the work piece is turning, it cuts the magnetic field. Eddy currents are generated on the surface of the work piece and according to Lenz's law, the induced currents generates a magnetic field that opposes the change in the flux that produces it. This has the result of inducing a force on the work piece that has a damping effect, as can be seen from the reduction forces. Now, for design 1 and 2, the field lines of the electromagnets spread up much more than that of electromagnet of design 3. So there is more rate of change magnetic flux linkage with the work piece in case of first two designs of electromagnets. This is why the tangential cutting force for the first two electromagnets decreases more than the third design of electromagnet. In design 3 electromagnet, the magnetic field lines are mainly concentrated on the tool holder. Due to shape of the transformer core, the field lines cannot escape in the air, and therefore there is lower rate of flux linkage with work piece.



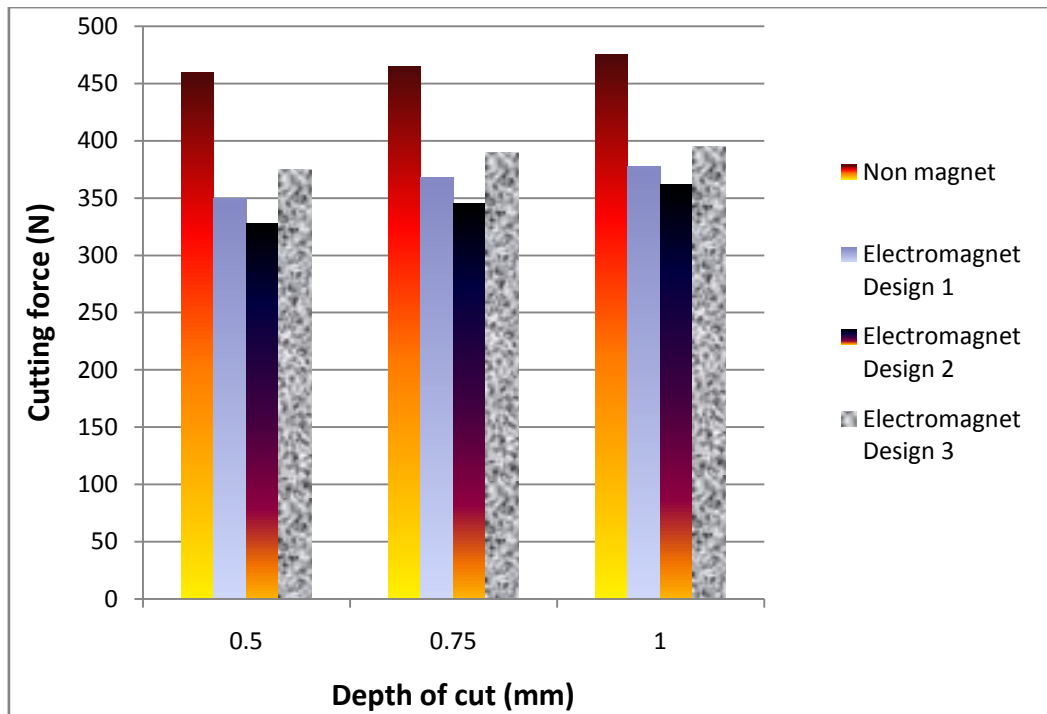


Fig. 4.27 : Strain and Cutting speed with respect to depth of cut (mm)

From the above graph, it is observed that the tangential cutting force decreases with the application of magnetic field. However, the tangential cutting force increases with the increase in the cutting speed. In this case also the reduction in cutting force is more for the case of the first two designs of electromagnets, the reason of which has been already explained in the previous section.

CHAPTER 5

**CONCLUSIONS AND RECOMMENDATIONS FOR
FURTHER STUDY**

5.1 : CONCLUSIONS

- Tool wear decreases with the application of external electromagnetic field. The improvement of tool life is independent of the position of the application of the magnetic field. It depends on both the orientation of the magnetic field as well as the cutting parameters.
- The electromagnet of design 3 shows consistent result compared to other two designs of electromagnets. Not only the lubrication effect of the built up edge is responsible for the improvement of tool life but also other factors like the reduction in chatter is one of the main reasons for this reduction of tool wear. The electromagnet of design 3, where the most of the magnetic fluxes are applied on the tool holder, ensures this phenomenon.
- The tool wear increases with the increase in cutting speed and the depth of cut and this is independent of the cutting parameters and external environment for cutting operation e.g. non magnetic cutting and cutting with the application of the three designs of electromagnets
- The surface quality improves with the application of external magnetic field. This can be explained by the reduction of the vibration of tool and work piece system in case of magnetic cutting. The improvement of tool life is another factor for this improvement. However the improvement of surface quality is not always achieved. Built up edge formation during magnetic cutting is a problem for the surface finish since it scratches the work piece surface. At higher depth of cut during machining the surface quality is better for all three designs of electromagnets. Therefore to obtain a better surface finish the magnetic environment, i.e. the particular design of electromagnet is selected depending on the cutting parameter. For example the surface finish is considerably better at higher cutting speed in case of the electromagnet of design 1.
- The increase in temperature and reduction of tangential cutting force are the other effects of magnetic cutting operation. This phenomenon support the reduction of tool wear. Since the cutting force is reduced, the contact junction of the tool and work piece becomes less severe and thereby the tool can remove the material with facing less force. As a result the tool wear increases.

- The effect of application of external magnetic field is not only confined to the improvement of tool life and improving the surface quality, it also affects the chip behavior during the turning operation. The chips produced are less serrated in nature when magnetic field is applied.

5.2 : RECOMMENDATIONS FOR FURTHER STUDY

- The experiment carried out in this study uses only mild steel as the work piece. Experiments with other materials as the work piece like conducting material, non ferrous, or non conducting and ferrous, can be done.
- Here in this study we have used only carbide tools. Other tool materials can be used for further study.
- Only three kinds of electromagnets are used with d.c. source of current which creates a constant magnetic field. An alternating source of current can be used to obtain a further understanding of the mechanism behind the reduction of tool wear by the application of application of magnetic field. Since cutting force is reduced due to linkage of the magnetic flux with the rotating work piece which, therefore, improves the tool life, with alternating magnetic field this result should be better under the same condition.

Today the manufacturing industries are investing huge amount of money only to optimize the processes involved. This is because a little bit of savings in the tool insert of machining process can greatly influence the overall production cost. Since magnetic field can improve the tool life, there is a great potential to use it in industries, although still now no industry uses magnetic field to improve the machinability factor. On the other hand, if this phenomenon is developed further, the machine tools can be designed having integrated magnetic field in them. Therefore to apply this technique in the machining process of various types of manufacturing industries, further study should be carried out to find out the feasibility in terms cost of production.

REFERENCE

1. Shaw MC (1984) Metal cutting principles. Oxford Science, Oxford, UK
2. Trent EM, Wright PK (2000) Metal cutting. Butterworth–Heinemann, Boston, MA
3. Modern Metal Cutting, A practical Handbook, Sandvik Coromant
4. Taylor, F.W., “On the art of metal cutting”, *Trans. ASME*, Vol. 28, pp. 31-350(1907).
5. Astakhov VP (2006) Tribology of Metal Cutting. Elsevier: London
6. K. Holmberg, A. Matthews, Coatings tribology: properties, techniques and applications in surface engineering, in: D. Dowson (Ed.), Tribology Series 28, Elsevier Science, Amsterdam, 1994, p. 351.
7. Mansori, M. El. and Klamecki, B.E., “Magnetic Field Effects in Machining Processes and on Manufactured Part Mechanical Characteristic”, *Journal of Manufacturing Science and Engineering*, Vol. 128, pp. 137 – 145 (2006).
8. Mansori, M.El., Pierron, F. and Paulmier, D., “Reduction of tool wear in metal cutting using external electromotive sources”, *Surface and Coatings Technology*, Vol. 163 - 164, pp. 472-477(2003).
9. Hastings, W.F., and Oxley, P.L.B, “Predicting tool life from fundamental work material properties and cutting conditions”, *Annals of the CIRP*, pp. 33–38(1976).
10. Opitz, H. and Konig, W., “On the wear of cuttingtools”, *proceedings of the 8th International MTDR Conference*, pp. 173-190(1967).
11. Wright, P.K, “Correlation of tool wear mechanisms with slip line fields for cutting in: K. Ludema (Ed.)”, *Wear of Materials, ASME*, pp. 482–488(1981).
12. Kurimoto, T. and Barrow, G., “The influence of aqueous fluids on the wear characteristics and life of carbide cutting tool”, *Annals of the CIRP*, pp. 19-25 (1982).
13. Usui, E., “Progress of predictive theories in metal cutting”, *International Journal of Japan Society of Mechanical Engineers*, Vol. 31 (2), pp. 363–369 (1998).
14. Kalpakjian, S. and Schmid, S.R., “*Manufacturing Processes for Engineering Materials*”, 5th Edition, Pearson Education Inc., pp. 440-447(2009).
15. Ginta, T.L, Amin, A.K.M.N. and Patwari, A.U., “Tool Wear Morphology And Chip Segmentation In End Milling Titanium Alloy Ti-6AL-4V”, *Proceedings of CUTSE Int. Conference*, (2008).

16. Matsumoto, Y., Hashimoto, F. and Lahoti, G., "Surface Integrity Generated By Precision Hard Turning", *Annals of the CIRP*, Vol. 48(1), pp. 59-62 (1999).
17. Thiele, J. D., and Melkote, S. N., "Effect Of Cutting Edge Geometry And Work piece Hardness On Surface Generation In The Finish Hard Turning Of AISI 52100 Steel," *Journal of Materials Processing Technology*, Vol. 94, pp. 216-226 (1999).
18. Dawson, T. G. and Kurfess, T. R., "Machining Hardened Steel With Ceramic-Coated And Uncoated CBN Cutting Tools", Technical Paper -Society of Manufacturing Engineers, MR 02-156, pp. 1-7 (2002).
19. Özel, T., Hsu, T. K. and Zeren, E., "Effects Of Cutting Edge Geometry, Workpiece Hardness, Feed Rate And Cutting Speed On Surface Roughness And Forces In Finish Turning Of Hardened AISI H13 Steel," *International Journal of Advanced Manufacturing Technology*, (2004).
20. V.A. Bobrovskii, *Russ. Eng. J.* 18 (1966) 70.
21. M. Kanji; D.K. Pal, Proceedings of the Third AIMTDR Conference, Bombay, 1969.
22. Zhou Q., Hong G. S. and Rahman M., (1995), "A New Tool Life Criterion For Tool Condition Monitoring Using a Neural Network", *Engineering Application Artificial Intelligence*, Volume 8, Number 5, pp. 579-588.
23. Braghini, A. Jr., and Coelho, R.T, "An Investigation Of The Wear Mechanisms Of Polycrystalline Cubic Boron Nitride (PCBN) Tools When End Milling Hardened Steels At Low/Medium Cutting Speeds," *International Journal on Advanced Manufacturing Technology*, Vol. 17, pp. 244-257 (2001).
24. Kumar, S., Durai, A.R. and Sornakumar, A. "The Effect Of Tool Wear On Tool Life Of Alumina-Based Ceramic Cutting Tools While Machining Hardened Martensitic Stainless Steel," *Journal of Materials Processing Technology*, Vol. 173, pp. 151-156 (2006).
25. Ghani, J.A., Choudhury, I.A. and Hassan, H.H., "Application of taguchi method in the optimization of end milling parameters," *Journal of Materials Processing Technology*, Vol. 145, pp. 84-92 (2004).
26. Amin, A. K. M. N., Hafiz, A. M. K., Lajis, M. A. and Patwari, A. U., "Prediction of tool life and experimental investigation during hot milling of AISI H13 tool steel," *Advanced Materials Research*, Vol. 83-86, pp. 190-197 (2010).
27. Takeyama, H. And Murata, R., "Basic Investigation of Tool Wear", *Trans.ASME, J. Eng. Ind.* Vol. 85, pp. 33-38 (1963).
28. M.K. Muju, A. Radhakrishna, *Wear* 58 (1980) 49

29. M.K. Muju; A. Ghosh, ASME Paper 75-PT-5, 1975.
30. M.K. Muju, A. Ghosh, *Wear* 41 (1977) 103.
31. M.K. Muju, A. Ghosh, *Wear* 58 (1980) 137.
32. Oxley, P.L.B., “*The Mechanics of Machining: An Analytical Approach to Assessing Machinability*”, Ellis Horwood, Chichester, (1989).
33. Arsecularatne, J.A., “On prediction of tool life and tool deformation conditions in machining with restricted contact tools”, *International Journal of Machine Tools and Manufacture*, Vol. 43, pp. 657–669 (2003).
34. Arsecularatne, J.A., “Prediction of tool life for restricted contact and grooved tools based on equivalent feed”, *International Journal of Machine Tools and Manufacture*, Vol. 44, pp. 1271–1282 (2004).
35. Kitagawa, T., Maekawa, K., Shirakashi, T. and Usui, E., “Analytical prediction of flank wear of carbide tools in turning plain carbon steels (part 1)”, *Japanese Society of Precision Engineering*, Vol. 22 (4), pp. 263–269 (1988).
36. Iwata, K., Ashara, J. and Okushima, K., “On the mechanism of built-up edge formation in cutting”, *Annals of the CIRP*, Vol.19 (2), pp. 323–330 (1971).
37. Choudhury S. K. and Bartarya G., (2003), “Role of temperature and surface finish in predicting tool wear using neural network and design of experiments”, *International Journal of Machine Tools and Manufacture*, Volume 43, pp. 747–753.
38. Chien W.-T. and Tsai C.-S., (2003), “The investigation on the prediction of tool wear and the determination of optimum cutting conditions in machining 17-4PH stainless steel”, *Journal of Materials Processing Technology*, Volume 140, pp. 340–345.
39. Bagchi, P.K., Ghosh, A., “Effect of magnetization on wear characteristics of cutting tools”, *Institution of Engineers (India) Journal (PR)*, Vol. 50, pp. 264-269 (1970).
40. Bagchi, P.K., Ghosh, A., “Mechanism of a cutting tool in presence of a magnetic field”, *Indian Journal of Technology*, Vol. 9, pp. 165-168 (1971).
41. Chakrabarti, S., “Why Magnetic Cutting Tool Has Greater Life- Probable Cause”, ”, *Institution of Engineers (India) Journal (PR)*, Vol. 52, pp. 118-123 (1971).
42. Pal, D.K. and Gupta, N.C, “some experimental studies on drill wear in the presence of alternating magnetic field”, *Institution of Engineers (India) Journal (PR)*, Vol.53, pp. 195-200 (1973).
43. M.E.L. Mansori, K. Lafdi, D. Paulmier, “*Metal Cutting and High Speed Machining*”, Kluwer Academic Plenum Publishers, New York, 2002, p. 301.

44. Kumanan S., Saheb S. K. N. and Jesuthanam C. P., (2006), "Prediction of Machining Forces using Neural Networks Trained by a Genetic Algorithm", *Institution of Engineers (India) Journal*, Volume 87, pp. 11-15.
45. Mahmoud, E. A. E. and Abdelkarim, H. A., "Optimum Cutting Parameters in Turning Operations using HSS Cutting Tool with 45° Approach Angle", *Sudan Engineering Society Journal*, Vol. 53 (48), pp. 25-30 (2006).
46. Natarajan, U., Arun, P. and Periasamy, V. M., "On-line Tool Wear Monitoring in Turning by Hidden Markov Model (HMM)", *Institution of Engineers (India) Journal (PR)*, Vol. 87, pp. 31-35 (2007).
47. Srikanth T. and Kamala V., (2008), "A Real Coded Genetic Algorithm for Optimization of Cutting Parameters in Turning IJCSNS", *International Journal of Computer Science and Network Security*, Volume 8 Number 6, pp. 189-193.
48. Lin, W. S., Lee B. Y., Wu C. L., "Modeling the surface roughness and cutting force for turning", *Journal of Materials Processing Technology*, Vol. 108, pp. 286-293(2001).
49. Lee, S. S. and Chen, J. C., "Online surface roughness recognition system using artificial neural networks system in turning operations", *International Journal of Advanced Manufacturing Technology*, Vol. 22, pp. 498–509 (2003).
50. Kirby, E. D., Zhang, Z. and Chen, J. C., "Development of An Accelerometer based surface roughness Prediction System in Turning Operation Using Multiple Regression Techniques", *Journal of Industrial Technology*, Vol. 20 (4), pp. 1-8 (2004).
51. Özel, T. and Karpaz, Y., "Predictive modeling of surface roughness and tool wear in hard turning using regression and neural networks", *International Journal of Machine Tools and Manufacture*, Vol.45, pp. 467–479 (2005).
52. Singh, H. and Kumar, P., "Optimizing Feed Force for Turned Parts through the Taguchi Technique", *Sadhana*, Vol. 31(6), pp. 671–681(2006).
53. Ahmed, S. G., "Development of a Prediction Model for Surface Roughness in Finish Turning of Aluminium", *Sudan Engineering Society Journal*, Vol. 52 (45), pp. 1-5 (2006).
54. Abburi, N. R. and Dixit, U. S., "A knowledge-based system for the prediction of surface roughness in turning process", *Robotics and Computer-Integrated Manufacturing*, Vol. 22, pp. 363–372 (2006).

55. Zhong, Z. W., Khoo, L. P. and Han, S. T., "Prediction of surface roughness of turned surfaces using neural networks", *International Journal of Advance Manufacturing Technology*, Vol. 28, pp. 688–693(2006).
56. Doniavi, A., Eskanderzade, M. and Tahmsebian, M., "Empirical Modeling of Surface Roughness in Turning Process of 1060 steel using Factorial Design Methodology", *Journal of Applied Sciences*, Vol. 7 (17), pp. 2509-2513 (2007).
57. Kassab, S. Y. and Khoshnaw, Y. K., "The Effect of Cutting Tool Vibration on Surface Roughness of Work piece in Dry Turning Operation", *Engineering and Technology*, Vol. 25(7), pp. 879-889 (2007).
58. Al-Ahmari, A. M. A., "Predictive machinability models for a selected hard material in turning operations", *Journal of Materials Processing Technology*, Vol. 190, pp. 305–311(2007).
59. Sahoo, P., Barman, T. K. and Routara, B. C., "Taguchi based practical dimension modeling and optimization in CNC turning", *Advance in Production Engineering and Management*, Vol. 3(4), pp. 205-217 (2008).
60. Wang M. Y. and Lan T. S., (2008), "Parametric Optimization on Multi-Objective Precision Turning Using Grey Relational Analysis". *Information Technology Journal*, Volume 7, pp.1072-1076.
61. Biswas, C. K., Chawla, B. S., Das N. S., Srinivas, E. R. K. N. K., "Tool Wear Prediction using Neuro-Fuzzy System", *Institution of Engineers (India) Journal (PR)*, Vol. 89, pp. 42-46 (2008).
62. Kang, T. Y., "Effect of Magnetic Field on Tool life in Milling", Thesis- submitted to National University of Singapore (2006/2007).
63. Anayet U. Patwari, M.N. Mahmood, M.D. Arif, "Improvement of Machinability of Mild Steel during turning operation by Magnetic Cutting", *International Journal on Advanced Science Engineering Information Technology*, Vol. 2 (2012) No. 3
64. Patwari, A. U., Arif, M. D. and Mahmood, M.N., "An innovative application of Digital Image Processing to Analyze Tool wear in Turning Operation", *Submitted to INRIT 2012*, Thailand (2012).
65. Anayet U. Patwari, Arif M.D., Chowdhury N.A., and Chowdhury Md. S. I., "3-D contour generation and determination of surface roughness and determination of surface roughness of shaped and horizontally milled plates using digital image processing," *International Journal of Engineering, Annals of Faculty of Engineering*,

Hunedoara, Romania.

66. Arif M.D., Patwari A.U., Chowdhury N.A., "*Surface roughness characterization using digital image processing technique.*" Proceedings of the 13th Annual Paper Meet, Mechanical Engineering Department, Institute of Engineers, Bangladesh (2010).
67. User Guide of Digital Strain Display, Model- SM 1010, TQ Education and Training Ltd. (2007).
68. G. T. Smith, The Machinability and Surface Integrity of Engineering Components, Chapter 6 of Advanced Machining: The Handbook of Cutting Technology, IFS Publications Ltd., 1989
69. Md. Anayet U. Patwari, M.N. Mahmood, Shafi Noor, Md. Ziaul Haque Shovon, "*Investigation of machinability responses during magnetic field assisted turning process of preheated mild steel*" Submitted to 5th BSME-ICTE, Bangladesh (2012)
70. Dr. Anayet U. Patwari, M.N. Mahmood, Shafi Noor, Md. Ziaul Haque Shovon, S.M. Tawfiqullah, "*Study of the effect of external magnetic field on tool wear and surface roughness during turning operation of mild steel*" Submitted to International Conference on Mechanical, Industrial and Energy Engineering 2012, Khulna, Bangladesh

APPENDIX 1: GRAPHS OF TOOL WEAR:

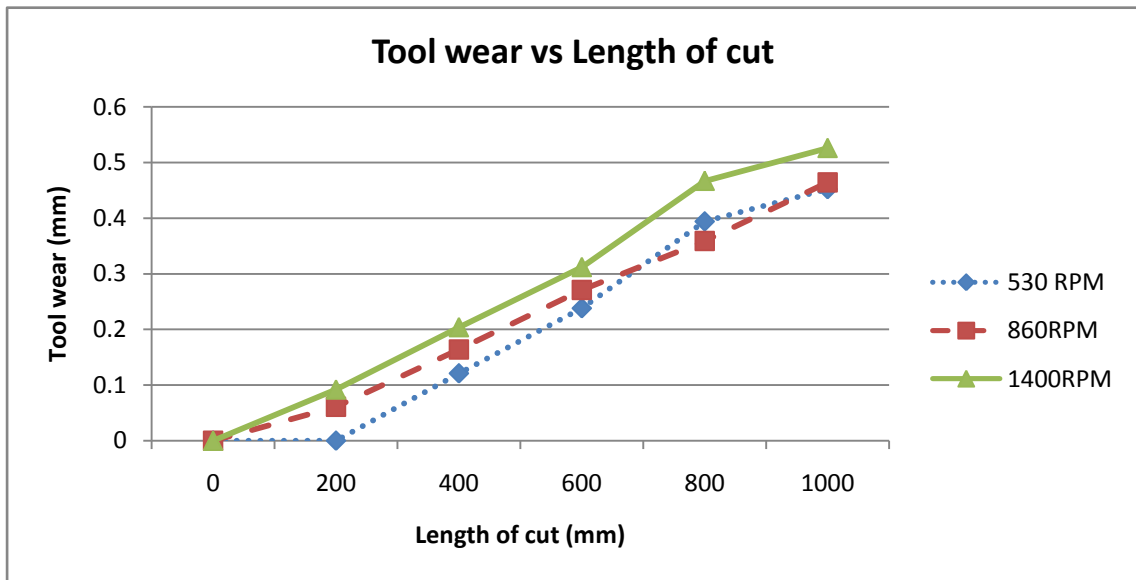


Fig. : Non magnetic cutting at 0.75 mm depth of cut

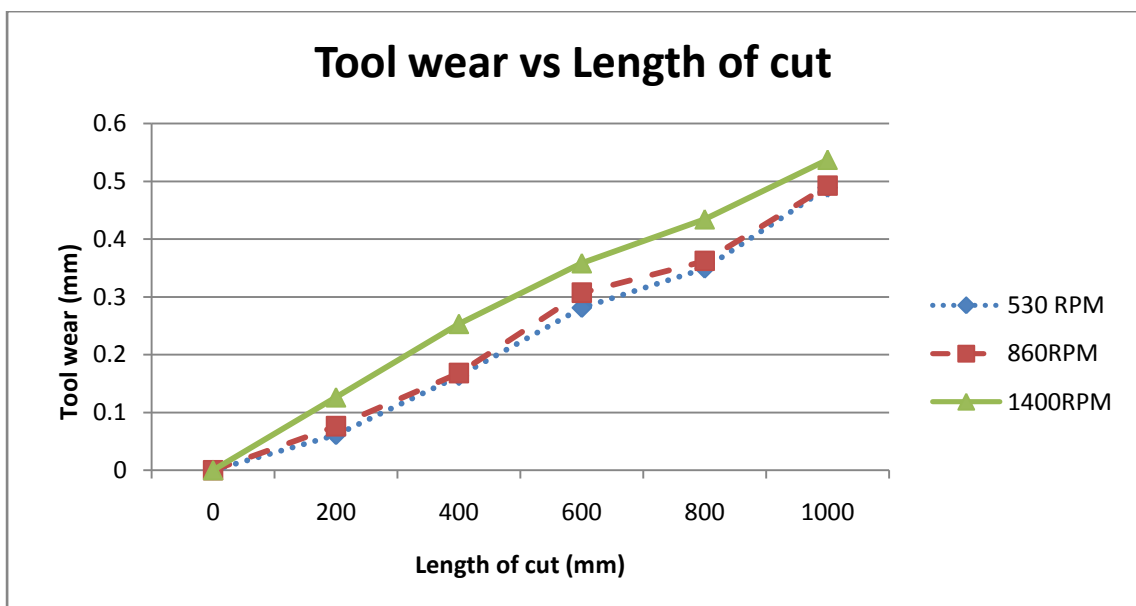


Fig. : Non magnetic cutting at 1.0 mm depth of cut

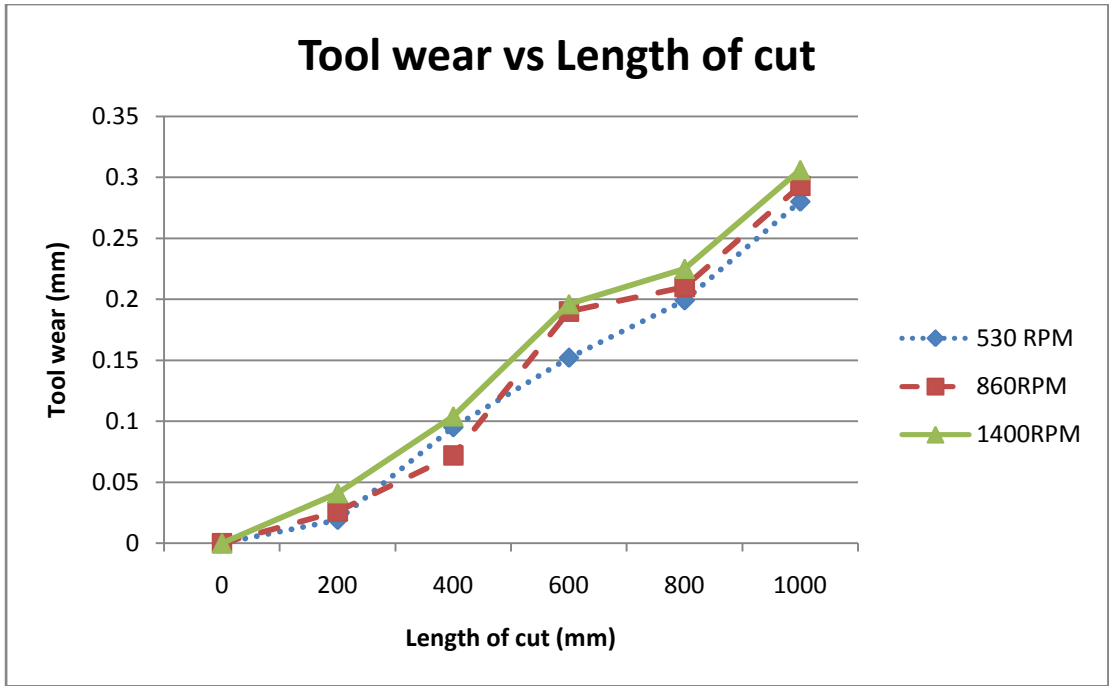


Fig. : Cutting with design 1 electromagnet at 0.75 mm depth of cut

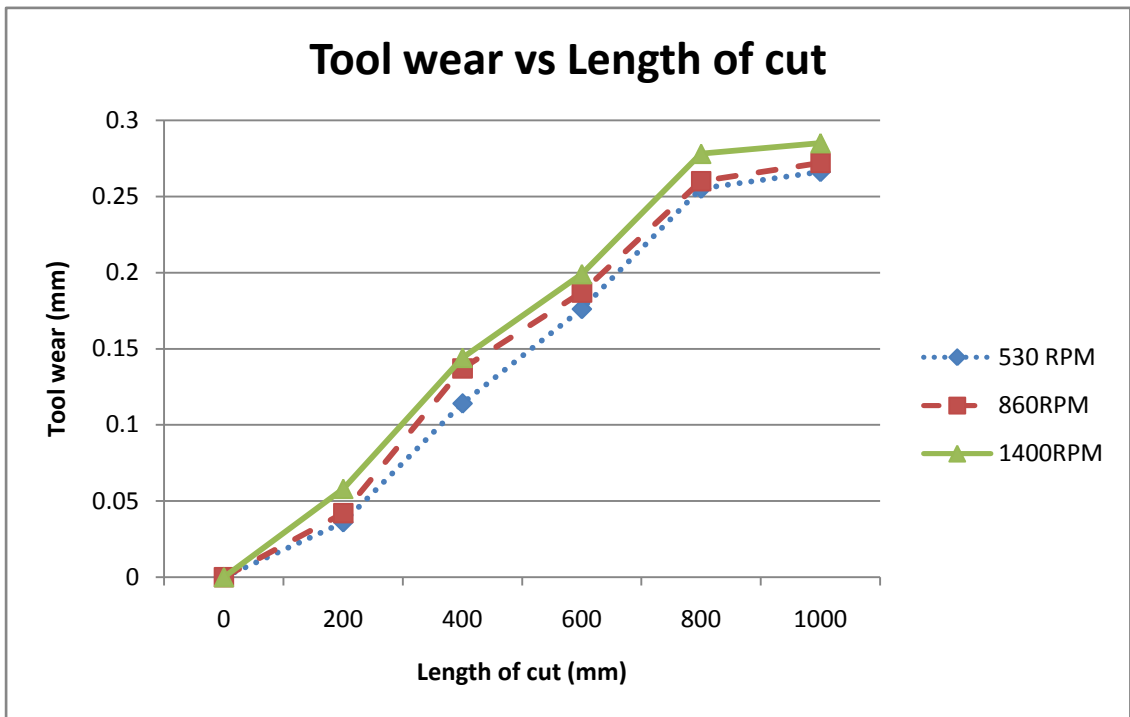


Fig. Cutting with design 1 electromagnet at 1.0 mm depth of cut

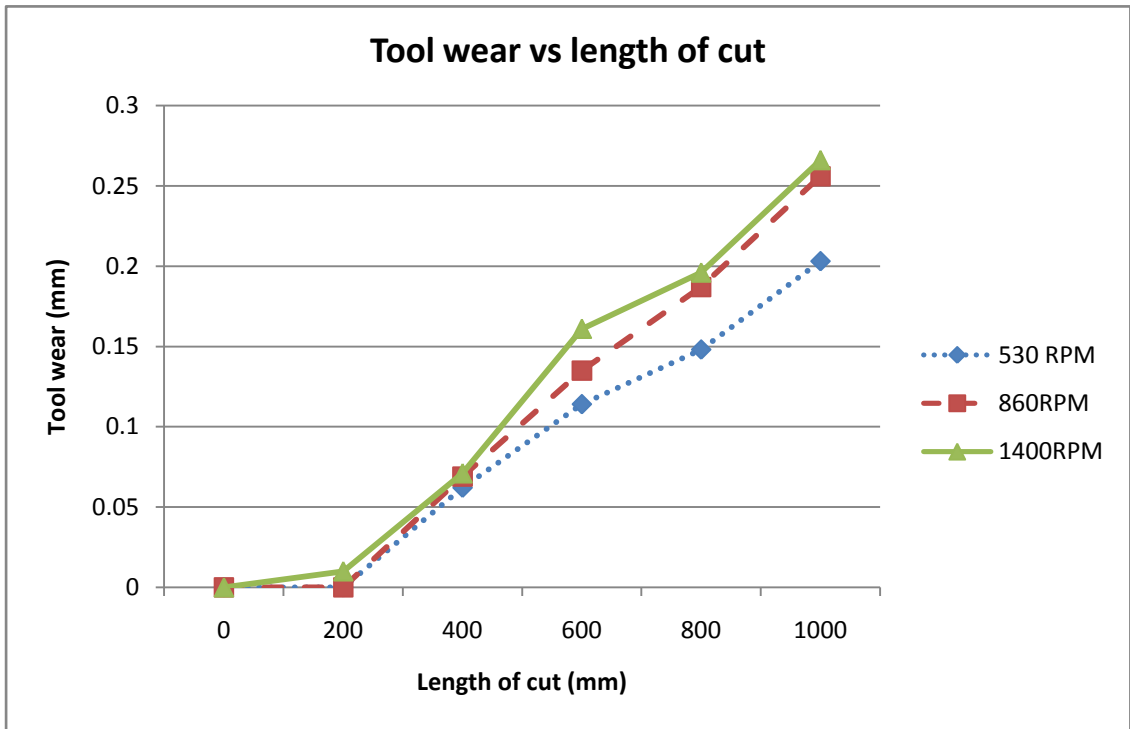


Fig. : Cutting with Design 2 electromagnet at 0.5 mm depth of cut

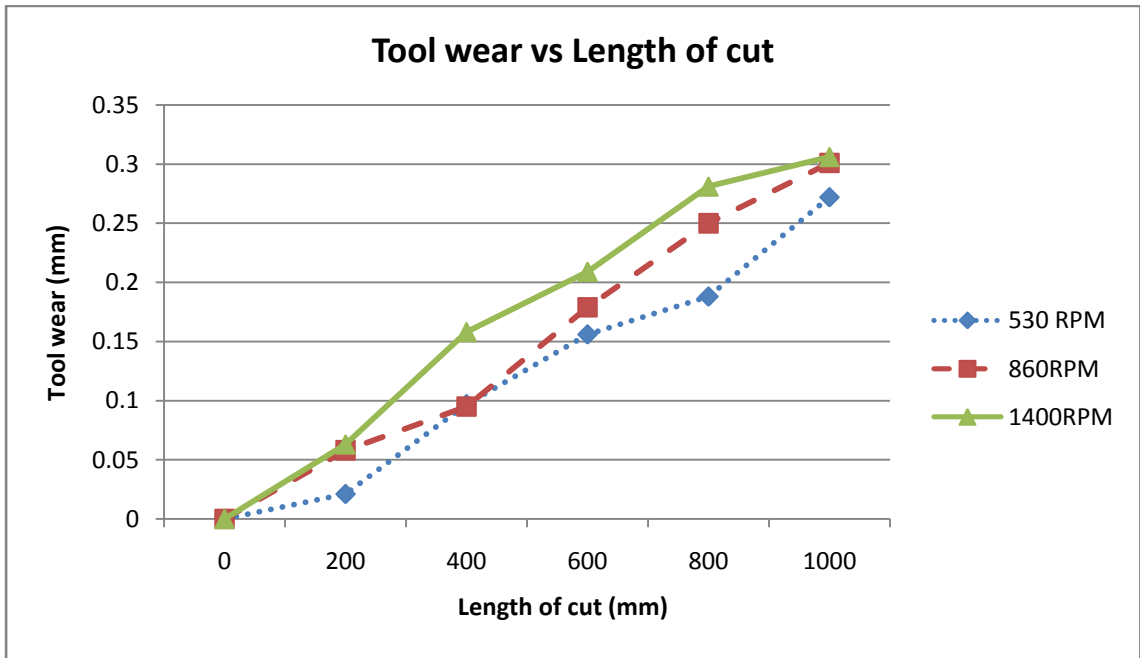


Fig. : cutting with design 2 electromagnet at 1.0 mm depth of cut

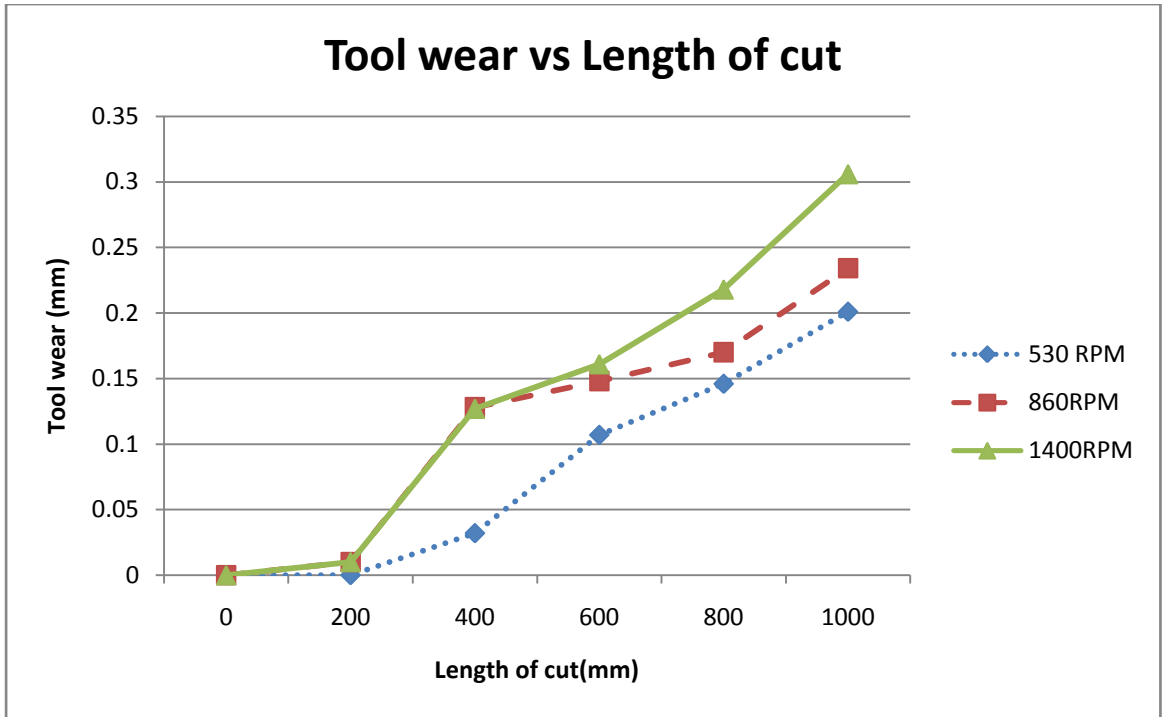


Fig. : Cutting with design 3 electromagnet at 0.5 mm depth of cut

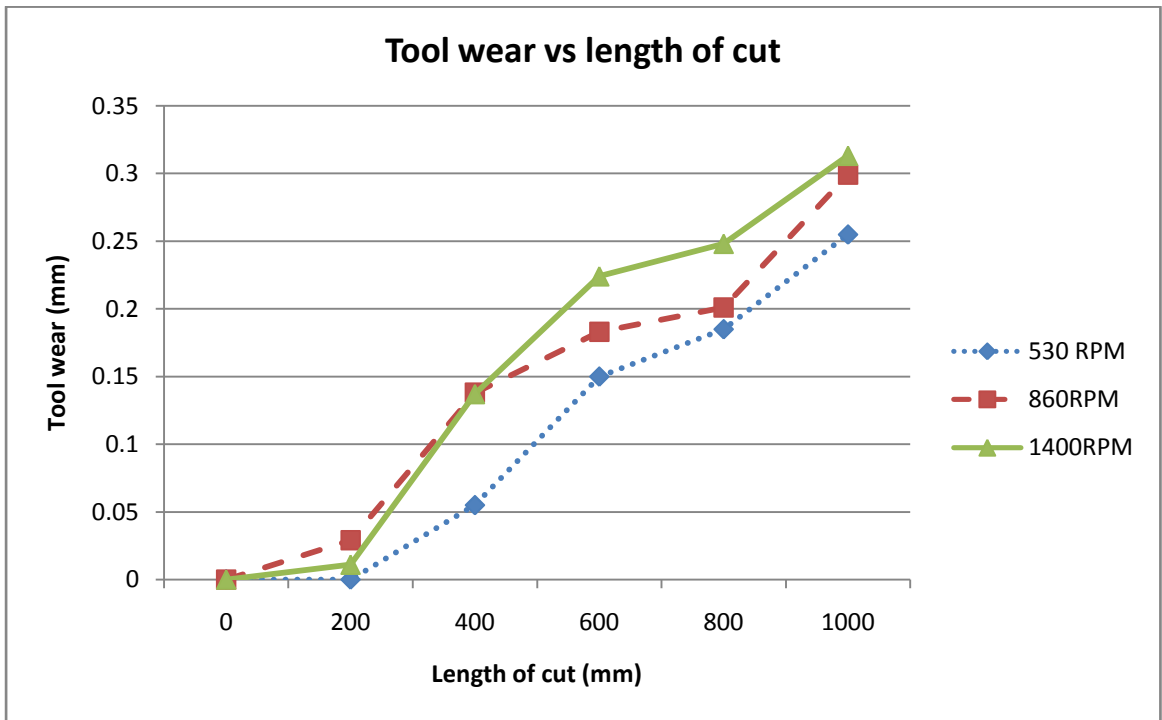


Fig. : Cutting with design 3 electromagnet at 0.75 mm depth of cut

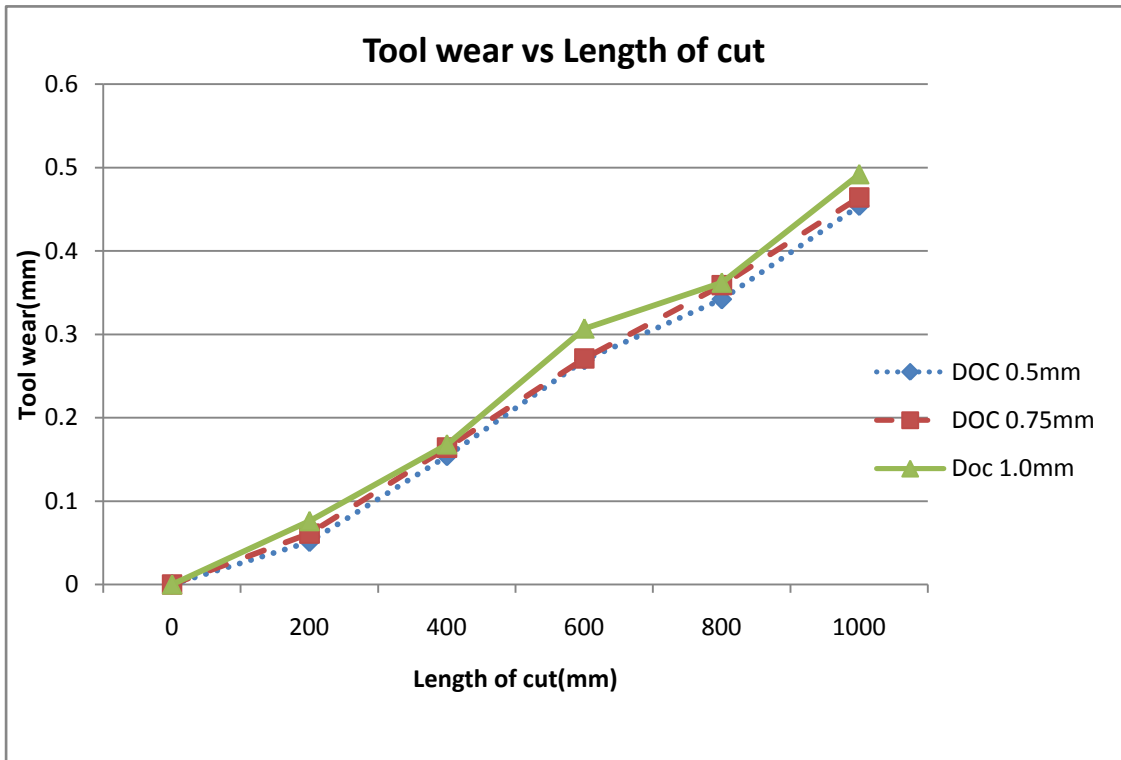


Fig. : Non magnetic cutting at a cutting speed of 860 rpm

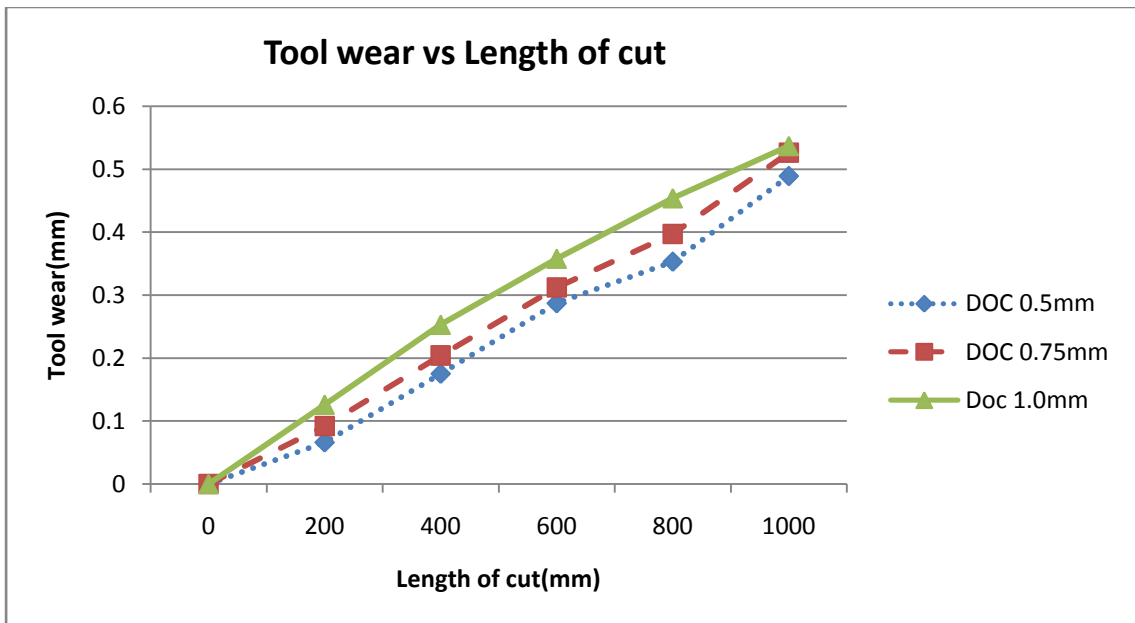


Fig. Non magnetic cutting at a cutting speed of 1400 rpm

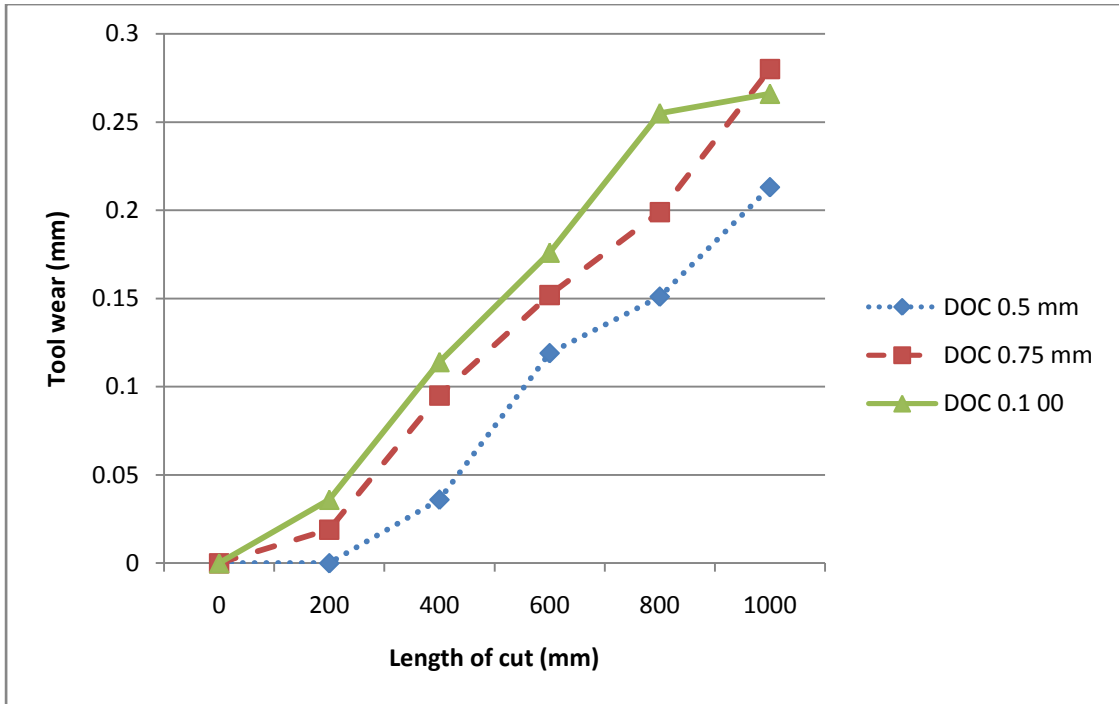


Fig. : Cutting with design 1 electromagnet at 530 rpm

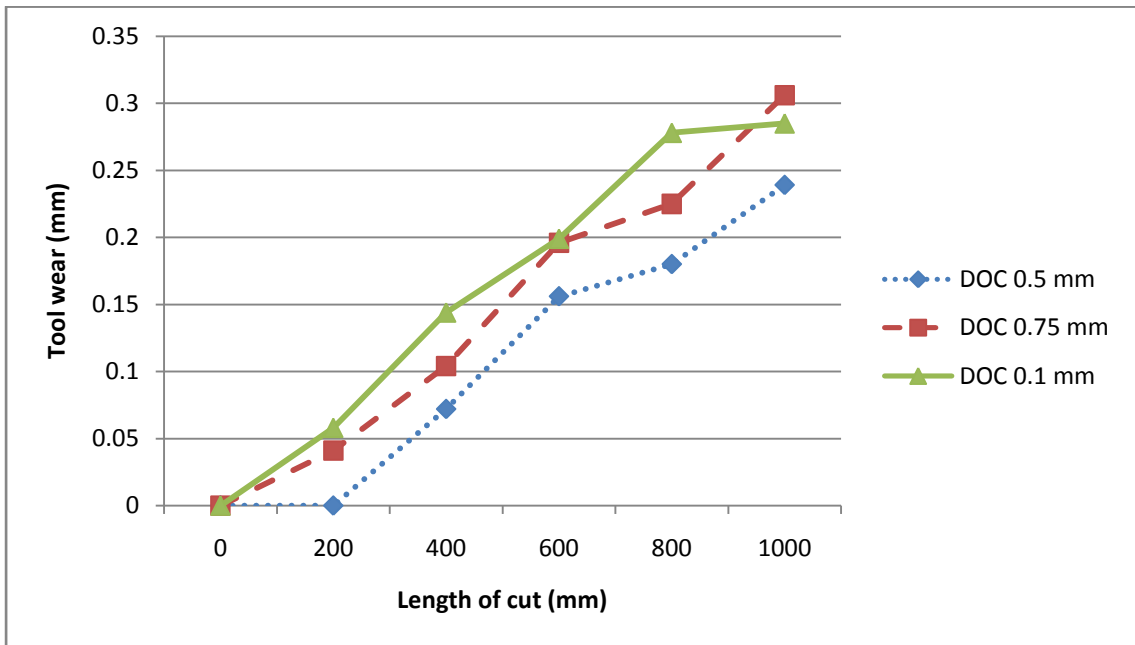


Fig. : Cutting with design 1 electromagnet at 1400 rpm

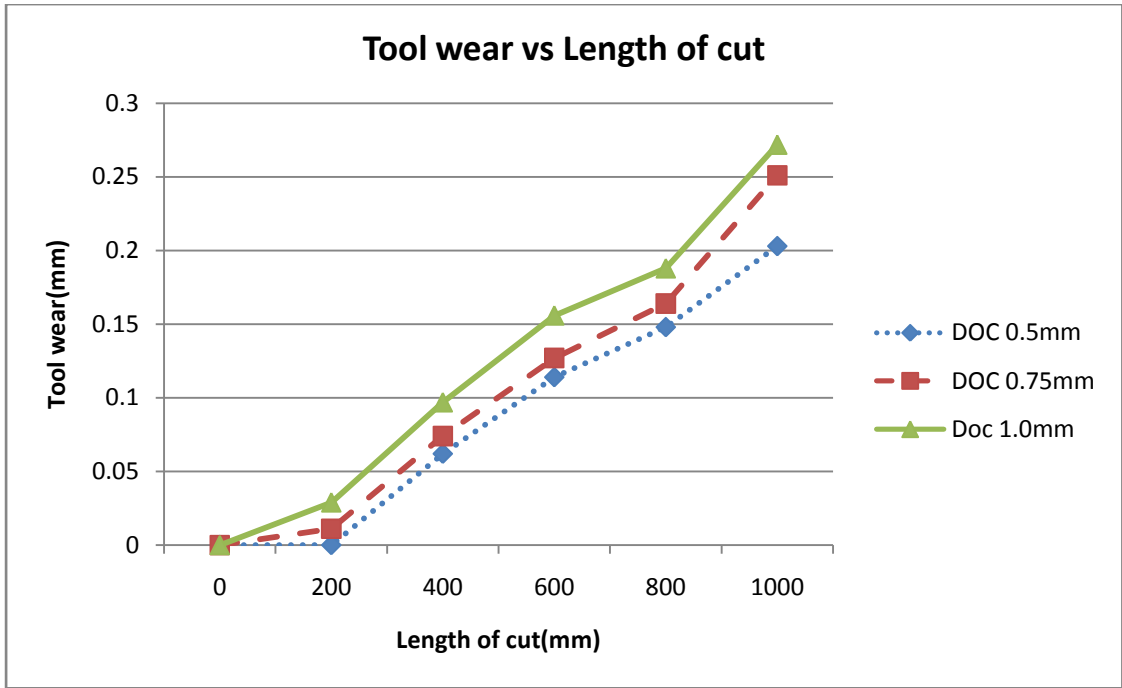


Fig. : Cutting with design 2 electromagnet at a cutting speed of 530 rpm

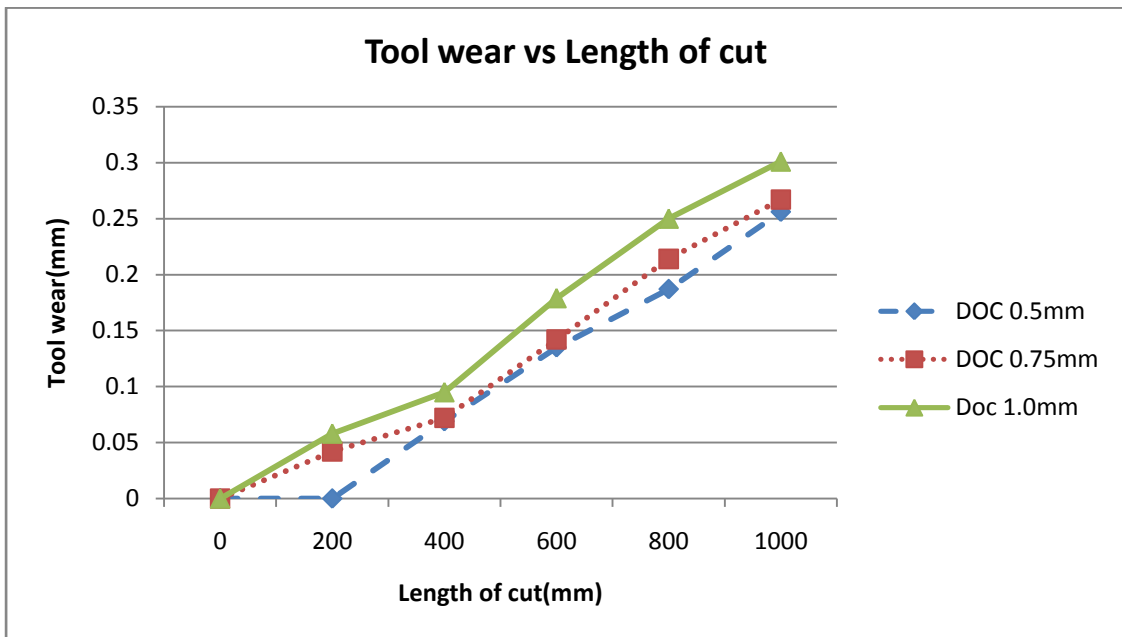


Fig. : Cutting with design 2 electromagnet at a cutting speed of 860 rpm

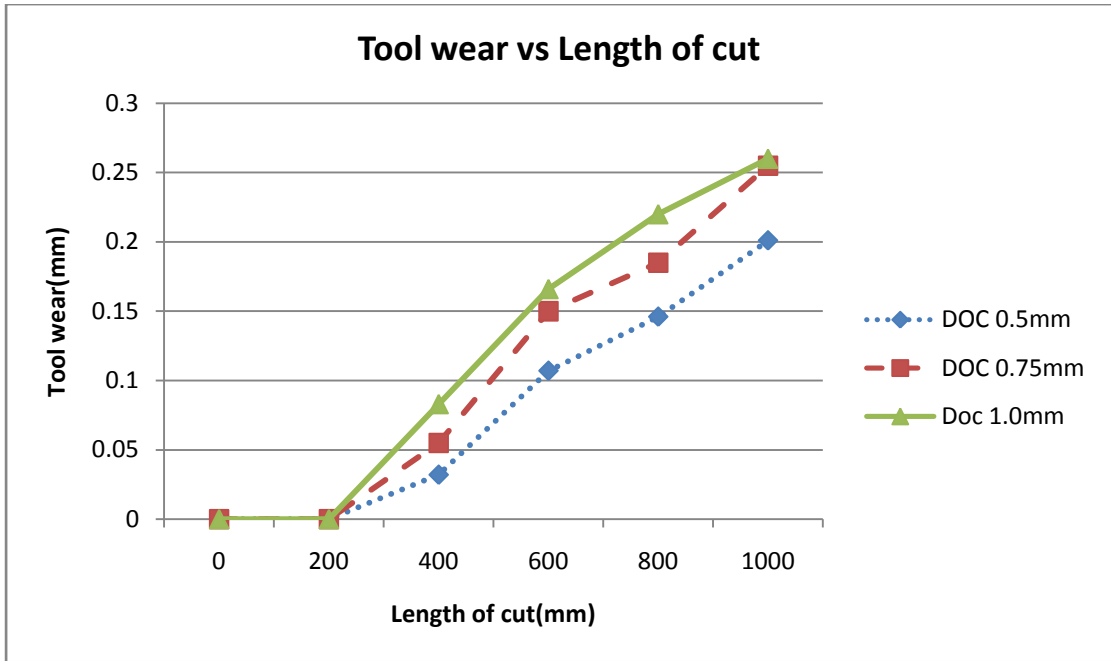


Fig. : Cutting with design 3 electromagnet at a cutting speed of 530 rpm

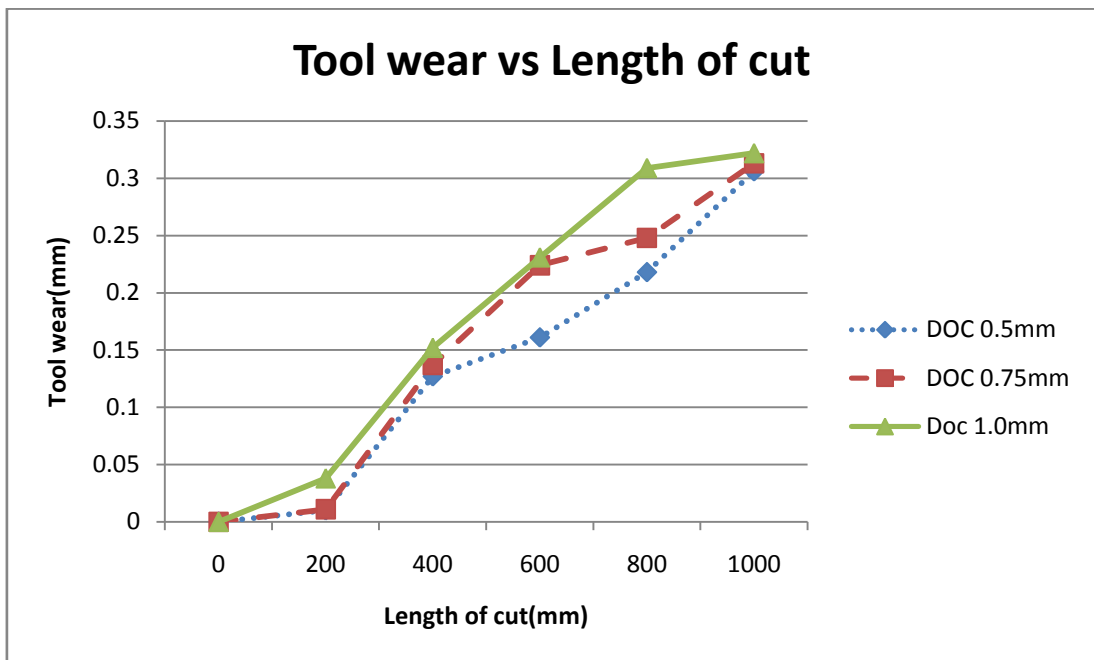


Fig. : Cutting with design 3 electromagnet at a cutting speed of 1400 rpm

APPENDIX 2: CHARTS OF SURFACE ROUGHNESS:

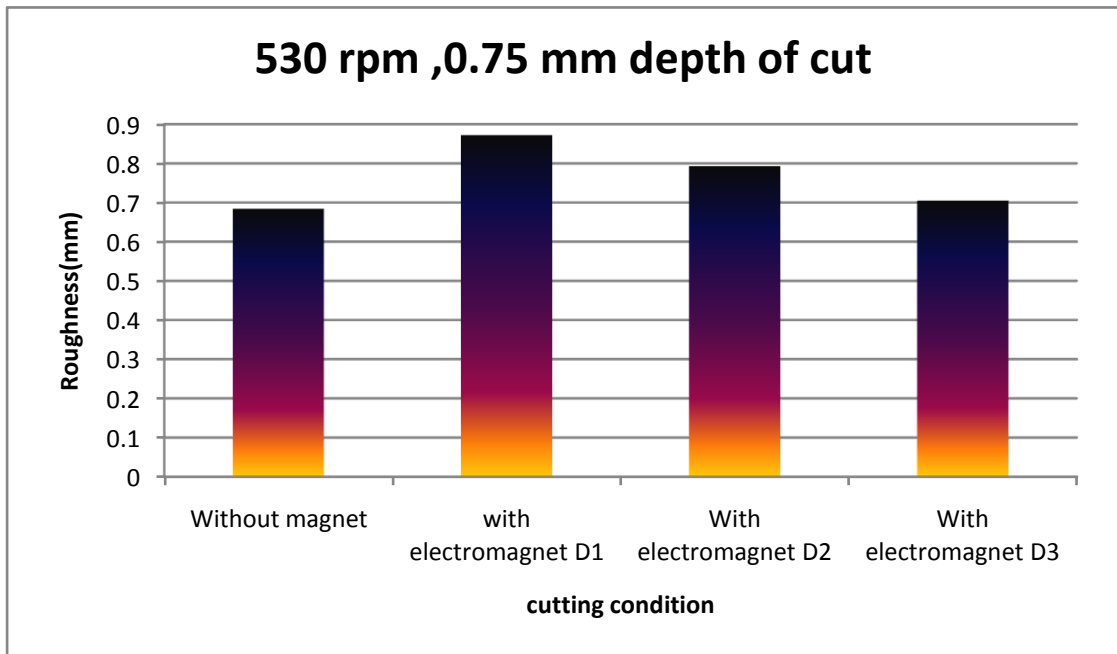


Fig. : Comparison of surface roughness at 530 rpm and 0.75 mm depth of cut\

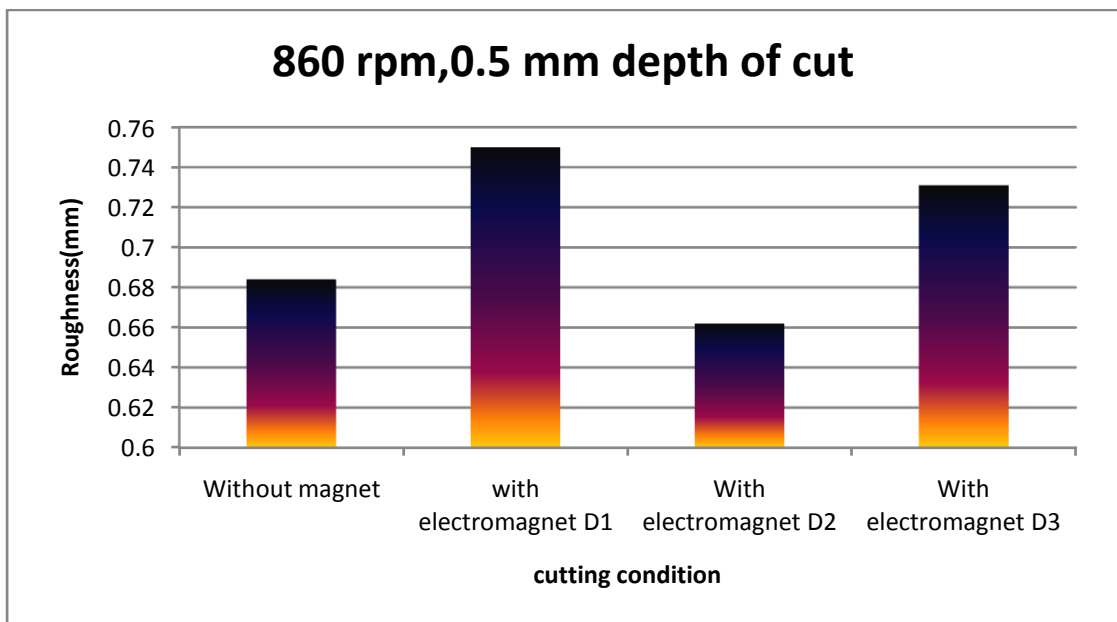


Fig. : Comparison of surface roughness at 860 rpm and 0.5 mm depth of cut

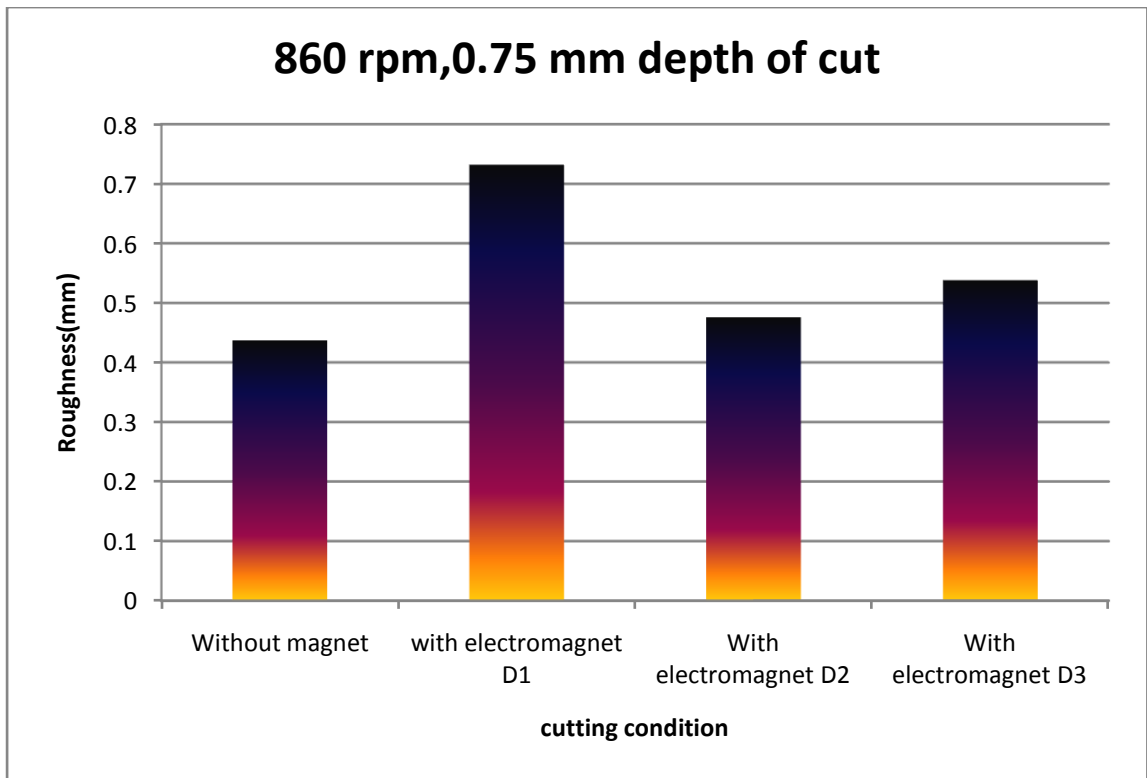


Fig. : Comparison of surface roughness at 860 rpm and 0.75 mm depth of cut

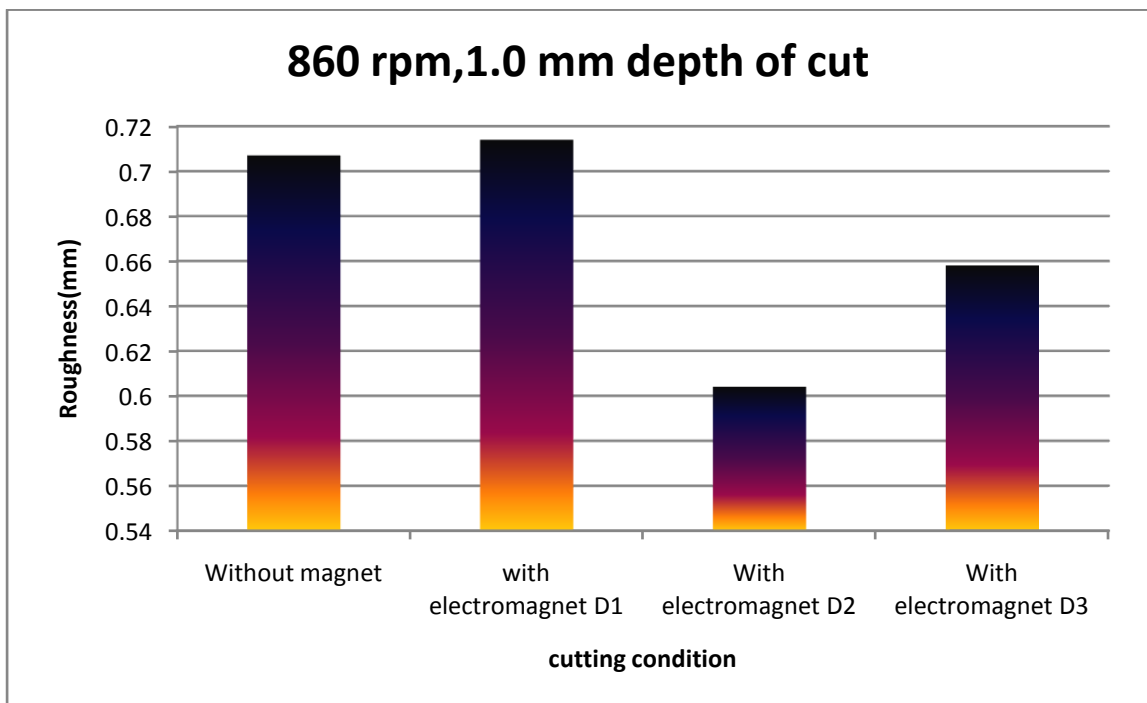


Fig. : Comparison of surface roughness at 860 rpm and 1.0 mm depth of cut

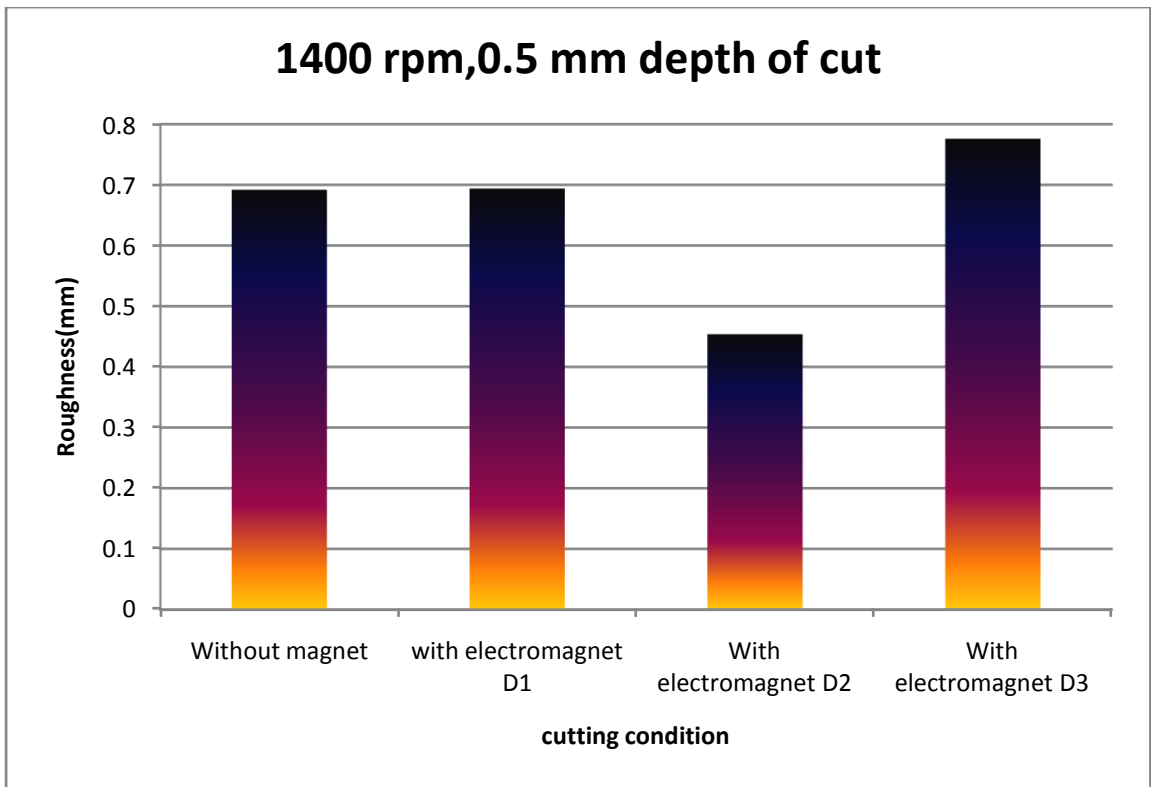


Fig. : Comparison of surface roughness at 1400 rpm and 0.5 mm depth of cut

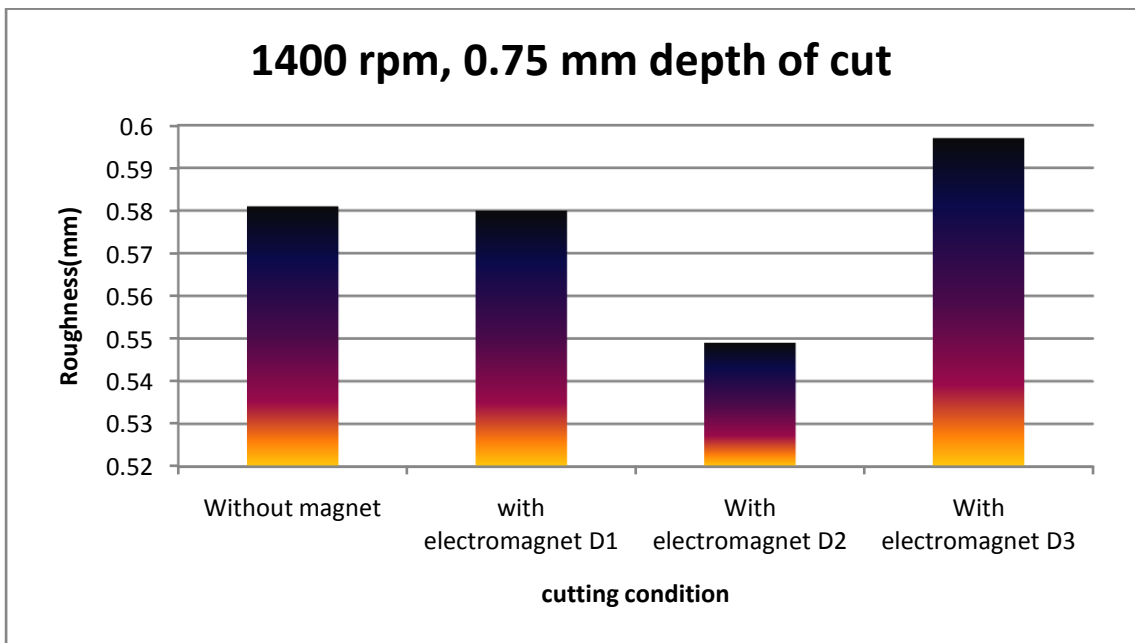


Fig. : Comparison of surface roughness at 1400 rpm and 0.75 mm depth of cut